CHARACTERIZATION OF HUMAN LYSOPHOSPHOLIPID ACYLTRANSFERASES IN THE REGULATION OF MEMBRANE TRAFFICKING

A Dissertation

Presented to the Faculty of the Graduate School

of Cornell University

in Partial Fulfillment of the Requirements for the Degree of

Doctor of Philosophy

by

Benjamin Alain Clarke

May 2014

CHARACTERIZATION OF HUMAN LYSOPHOSPHOLIPID ACYLTRANSFERASES IN THE REGULATION OF MEMBRANE TRAFFICKING

Benjamin Alain Clarke, Ph. D.

Cornell University 2014

Lysophospholipid acyltransferases (LPATs) catalyze the addition of an acyl chain to a lysophospholipid to form a phospholipid, dramatically altering lipid structure and behavior. These changes influence membrane curvature, the processes of vesicle and membrane tubule biogenesis, and the structure and trafficking dynamics of secretory organelles. At the beginning of my studies, I investigated the synergistic and antagonistic relationships between the activities of LPATs and phospholipases in regulating membrane trafficking. I went on to identify, by performing an overexpression screen, the human LPAT isoforms that are most important for regulating secretory membrane trafficking. I chose one of these enzymes for further characterization, the human membrane bound O-acyltransferase (MBOAT) gene family member lysophosphatidylcholine acyltransferase 3 (LPCAT3). Using selective membrane permeabilization immunostaining, I determined the topological orientation of LPCAT3's 11 transmembrane domains and luminal active site. I also found that a C-terminal K(x)KXX motif was necessary for LPCAT3 localization to the endoplasmic reticulum (ER). I observed the influence of LPCAT3 activity on the structure and dynamics of the early secretory system, through overexpression which reduced soluble protein secretion

to 22% of control and caused relocalization of COPI and COPII vesicle markers. Additionally, LPCAT3 knockdown had profound effects on retrograde trafficking from the Golgi and ER-Golgi intermediate complex (ERGIC) to the ER. Knockdown slowed trafficking of the p58 receptor (ERGIC-53) and Brefeldin A induced recycling of Golgi phosphoprotein of 130 kDa to the ER. Slowed retrograde transport was accompanied by increased membrane tubulation. These effects of knockdown were reflected in the localization of ERGIC-53 and markers of COPII and COPI vesicles, which were mislocalized in knockdown cells. However, the alteration of LPCAT3 expression levels, through knockdown or overexpression, did not disrupt the morphology of the Golgi complex, *trans*-Golgi network (TGN), adaptor protein 1 (AP-1)/clathrin-coated vesicles, or endosomes. These results suggest that LPCAT3 activity is important for efficient COPI vesiculation, the production of retrograde membrane tubules, and the fusion of retrograde membrane tubules with the ER. These findings support a novel role for LPAT activity in the regulation of COPI function, membrane tubulation, and retrograde trafficking to the ER.

BIOGRAPHICAL SKETCH

Benjamin Alain Clarke was born to Allan and Lenore Clarke at Strong Memorial Hospital of Rochester New York at 9:27 AM, eleven minutes preceding the birth of monozygotic twin brother Jeremy and four years preceding brother Peter. He was raised in the western suburbs of Philadelphia, where he attended Downingtown High School, graduating in 2001. In 2005, Ben earned his B.S. in Biochemistry and Molecular Biology from the Pennsylvania University in State College Pennsylvania. As an undergraduate, he was a singer in a cappella group *The Pennharmonics* and researcher in the laboratory of X-ray crystallographer Professor Song Tan. After college, Ben worked with biotechnology startup Locus Pharmaceuticals. During which time, he sang with a cappella group Project Philadelphia, therein meeting alto and future wife Leslie Hibbard. Ben matriculated to Cornell University Graduate School in August 2006 and soon joined the laboratory of Professor William Brown. When not pursuing science, Ben can be found enjoying the company of his wife, his daughter Maura, his two Labradors, and his homebrewing equipment.

ACKNOWLEDGMENTS

First, I want to thank Professor Bill Brown for his steadfast support, remarkable scientific insight, eloquence, and good humor, because of which I remember my graduate studies fondly. Also, thanks to my committee members Holger Sondermann and Gerald Feigenson for freely sharing their advice and considerable expertise. Additionally, I would like to thank Volker Vogt for his helpful suggestions and illuminating anecdotes.

To lab members, Sricharan Murugesan, Danielle Kalkofen, Kevin Ha, Marie Bechler, John Schmidt, Elysa Goldberg, Ed Cluett, and Amy Antosh, thank you for everything you have taught me, about science and otherwise.

The financial support for this research was provided by the NIH.

Finally, I would like to thank my family and friends for their boundless love and support. Most of all, love, thanks, and kisses to my wife and daughter.

TABLE OF CONTENTS

LIST OF FIGURES

LIST OF TABLES

LIST OF ABBREVIATIONS

AA	arachidonic acid
AGPAT	1-acylglycerol-3-phosphate O-acyltransferase
ALPS	ArfGAP1 lipid packing sensor
AP	adaptor protein
Arf	ADP-ribosylation factor
ArfGAP	ADP-ribosylation factor GTPase-activating protein
AWAT2	Acyl-CoA wax alcohol acyltransferase 2
BARS	Brefeldin-A ADP ribosylated substrate
BEL	bromoenol lactone
BFA	Brefeldin A
BTRD	transformed bovine testicular cells
CDP-DAG	cytidine diphospho-DAG
CGL	congenital generalized lipodystrophy
CI-976	2,2-methyl-N-(2,4,6,-trimethoxyphenyl) dodecanamide
CO_2	carbon dioxide
COP	coat protein complex
$cPLA_2$	cytosolic Ca^{2+} dependent PLA_2
DAG	diacylglycerol
DGAT2	diacylglycerol acyltransferase 2

eIF2α	eukaryotic initiation factor of translation
ER	endoplasmic reticulum
ERAD	ER associated degradation
ERES	ER exit site
ERGIC	ER-Golgi intermediate compartment
ERGIC-53	p58 lecithin receptor
FBS	fetal bovine serum
GAP	GTPase-activating protein
GBF1	Golgi Brefeldin A-resistance factor 1
GEF	guanine nucleotide exchange factor
GPAM	GPAT mitochondrial
GPAT	glycerol-3-phosphate acyltransferase
GPP130	Golgi phosphoprotein of 130 kDa
HRP/ssHRP	soluble secreted horseradish peroxidase
IF	immunofluorescence
$iPLA_2$	cytosolic Ca^{2+} independent PLA_2
LCLAT1	lysocardiolipin acyltransferase 1
L_d	liquid-disordered phase
LPA	lysophosphatidic acid
LPAAT	lysophosphatidic acid acyltransferase

LPAT	lysophospholipid acyltransferase
LPC	lysophosphatidylcholine
LPCAT	lysophosphatidylcholine acyltransferase
LPE	lysophosphatidylethanolamine
LPG	lysophosphatidylglycerol
LPGAT1	LPG acyl transferase 1
LPI	lysophosphatidylinositol
LPS	lysophosphatidylserine
MAG	monoacylglycerol
MBOAT	membrane bound O-acyltransferase
MEM	minimum essential medium
MOGAT	monoacylglycerol O-acyltransferase
ONO	ONO-RS-082
PA	phosphatidic acid
PAF	platelet activating factor
PAFAH	platelet-activating factor acetylhydrolase
PBS	phosphate buffered saline
PC	phosphatidylcholine
PE	phosphatidylethanolamine
PEI	polyethylenimine

PI	phosphatidylinositol
PIP	phosphatidylinositol phosphate
PIP2	phosphatidylinositol-4,5-bisphosphate
PLA	phospholipase A
PLA_1	phospholipase A_1
PLA_2	phospholipase A_2
PLB	phospholipase B
PLC	phospholipase C
PLD	phospholipase D
PM	plasma membrane
PORCN	porcupine
PS	phosphatidylserine
PSS	phosphatidylserine synthase
RER	rough endoplasmic reticulum
ROI	region of interest
SOAT	sterol O-acyltransferase
$sPLA_2$	secretory PLA_2
SRP	signal recognition particle
TAG	triacylglycerol
TAZ	tafazzin

TGN	*trans*-Golgi network
UPR	unfolded protein response
VSV-G	vesicular stomatitis virus glycoprotein

CHAPTER ONE: General introduction

Overview of the endomembrane system

When students are first introduced to the internal components of the mammalian cell, organelles are often explained metaphorically. Though the organelle names may be difficult to remember, even the most casual student instantly understands the function and importance of a cellular trash can (lysosome), power plant (mitochondria), factory (endoplasmic reticulum), or post office (*trans*-Golgi network). Locomotives on a railroad are a common metaphor for the movement of actin and microtubule motors as they transport vesicles (railcars); membrane bound small GTPases are the postal codes and addresses to which vesicles are delivered.

While these concepts are facile and not grossly misleading, they fail to capture the tremendous complexity of the mammalian cell. They do not speak of the density with which the cell is packed full of disparate molecules, to the fidelity and specificity of protein function, or to the importance of the membrane enclosed compartments that segregate intracellular space. To make these concepts clear, it is first necessary to briefly introduce the concept of enzyme kinetics.

Leonor Michaelis and Maud Menten first described the mathematical principles of enzyme catalyzed reaction[1]. They showed that reaction speed is proportional to the concentration of enzyme and substrate, so that the reaction accelerates in response to increases in either concentration. This is a powerful relationship that forms the basis for the evolution of the eukaryotic endomembrane system. Take for instance the lysosome, which has evolved to recycle damaged or unneeded macromolecules and to reduce

them into their basic components. It is enriched with macromolecule degrading hydrolases by the cell's targeted transport systems. Macromolecules are likewise labeled for recycling, transported by cellular trafficking systems, and concentrated at lysosomes. The high local concentration of hydrolytic enzymes and substrates to be hydrolyzed, allows remarkably efficient enzymatic reactions. These efficiencies would not be possible without the specific transport, segregation, and concentration mechanisms of the eukaryotic cell's extensive endomembrane system.

Given the efficiency of specialized organelles, one may ask why cellular compartments are not further specialized. Why do lysosomes possess all classes of hydrolase instead of being specialized to breakdown a single type of macromolecule? Could not further efficiencies be found in a class of lysosome specialized to breakdown proteins, another for lipids, and a third for nucleic acids?

One reason we do not see greater specialization is that the maintenance of high enzyme and substrate concentrations places significant demands on intracellular trafficking systems. Rapid transport mechanisms must continuously renew an organelle's supply of enzymes and substrates while simultaneously removing enzyme products. These demands are compounded by the need for trafficking machinery to differentiate between organelles to ensure the fidelity and specificity of transport mechanisms. For instance, the delivery of lysosomal nucleic acid hydrolases to the nucleus would have disastrous consequences for genomic integrity.

Ensuring the rapidity and specificity of membrane trafficking requires significant energy expenditure and machinery with incredible complexity. The complexity of

eukaryotic endomembrane systems is substantial enough to involve as much as half of the genome in the direct and indirect processes of membrane upkeep and trafficking.[2] Eukaryotic membrane trafficking is, arguably, the most complex of biological systems. Increased compartmentalization and specialization of organelles would yield energy savings from increased enzymatic efficiency; however this gain must be balanced against the increased demand of a further elaborated membrane trafficking system.

The organelles of the endomembrane system are responsible for the synthesis of all transmembrane proteins, secreted proteins, glycosylated proteins and most cellular lipids. They were first delineated by George Palade through groundbreaking electron microscopy and cell fractionation experiments. Palade characterized their structure, function, localization, variety, and ubiquity in eukaryotic life[3]. His discoveries formed the foundation of modern cell biology and his striking electron micrographs (Figure 1-1) still inspire students of cell biology.

A simplified model of the endomembrane system depicts a series of membrane bounded compartments through which secretory cargos are sequentially transported (Figure 1-2). The rough endoplasmic reticulum (RER), by virtue of membrane bound ribosomes, is the site at which secretory cargo is synthesized.[4,5] From the endoplasmic reticulum (ER), secretory cargo proceeds via coat protein complex II (COPII) coated vesicles to the ER-Golgi intermediate complex (ERGIC) and Golgi complex, where they fuse and release their cargo.[6] The ERGIC is thought to serve as an intermediate

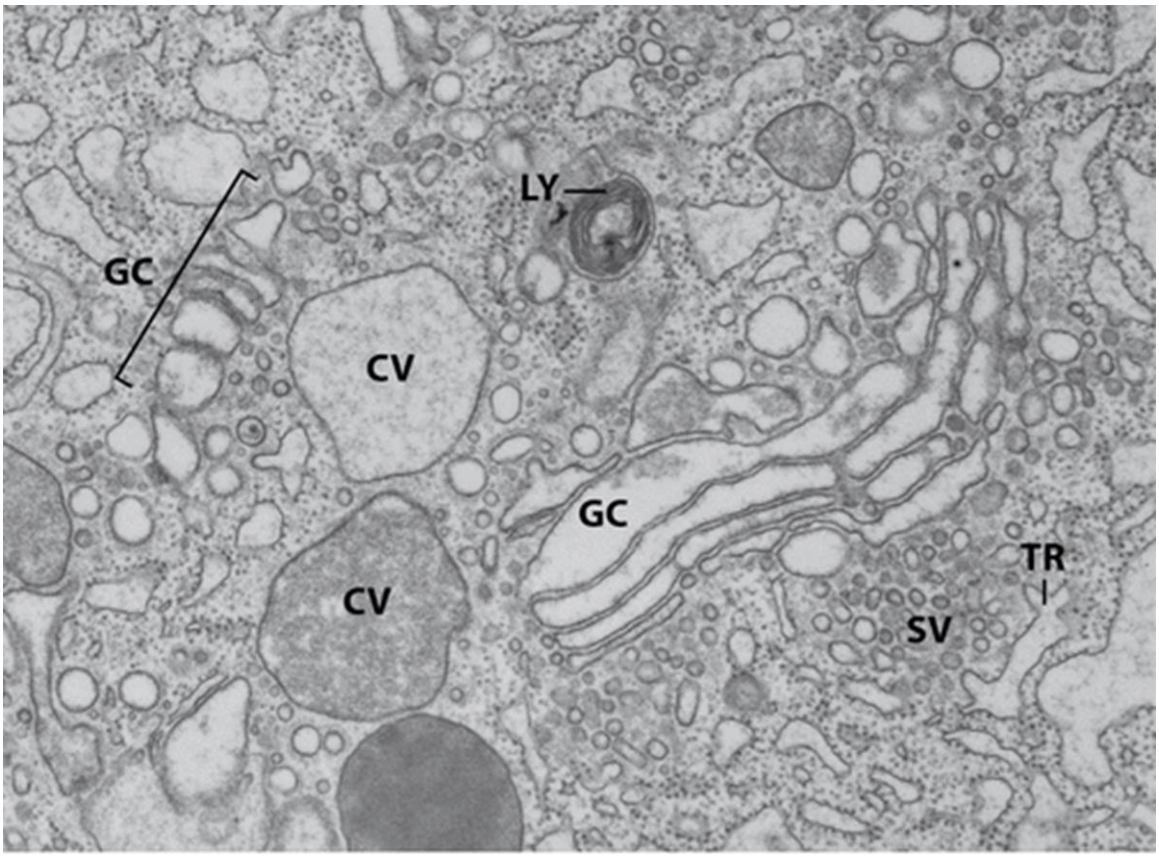

Figure 1-1: Electron micrograph from Palade depicting organelles of the endomembrane system

Abbreviations: CV: condensing vacuoles; GC: Golgi cisternae; SV: small peripheral ER-Golgi transport vesicles; TR: transitional elements; LY: lysosome. Reproduced from Palade *et al*[4].

trafficking and sorting station between the ER and Golgi complex. The Golgi complex is composed of a set of flattened, stacked cisternae at which secretory proteins are post-translationally modified (glycosylated, sulfated, etc.) and subsequently transported by vesicle and tubule carriers to a variety of endocytic compartments, the plasma membrane (PM), and the extracellular space.[7,8] These processes are collectively called anterograde membrane trafficking or secretion.

Intermingling with and parallel to the secretion system, the retrograde membrane trafficking system, also called the endocytic system, operates to retrieve proteins from anterograde compartments. The endocytic system is also responsible for internalizing extracellular materials to serve as nutrients, for membrane turnover, or receptor downregulation. The secretory and endocytic systems are not separate, independent systems but instead are interconnected pathways by which a single endomembrane system achieves homeostasis.

Transport of secretory and endocytic cargo between organelles takes place through membrane enclosed vesicular and tubular intermediates. Vesicles are, very generally speaking, spheres of 70-100 nm in diameter that form through a budding reaction catalyzed by organelle specific coat proteins[9]. The major classes of coat proteins are the ER-derived COPII coated vesicle, the ERGIC- and Golgi-derived COPI coated vesicles and the AP/clathrin coated vesicles which originate from the *trans*-Golgi network (TGN), endosomes, and PM. After shedding their coat proteins, vesicles are stable until triggered to fuse with a target membrane and can be stored or transported

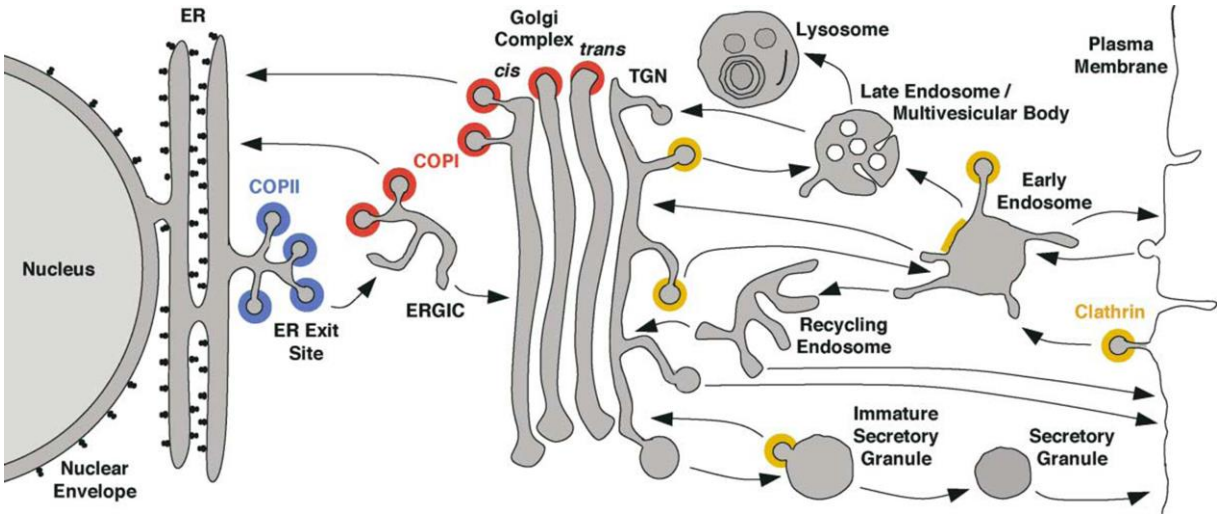

Figure 1-2: Simplified diagram of the mammalian endomembrane system

Reproduced from Bonifacino and Lippincott-Schwartz[10].

long distances. Membrane tubules on the other hand are ephemeral cylindrical membrane projections of 60-80 nm in diameter and a highly variable length.[10]

Our understanding of the details of the eukaryotic secretory and endocytic systems has grown since the discoveries of Palade and his colleagues. Tremendous progress has been made to elucidate many of the molecular mechanisms of membrane trafficking. This has culminated in the 2013 Nobel Prize for Physiology or Medicine being awarded to James Rothman, Randy Schekman, and Thomas Südhof for "their discoveries of machinery regulating vesicle traffic". Though, as we continue to learn and refine our techniques, we uncover new mysteries that force us to conclude that our understanding is not yet complete.

Organelles and trafficking mechanisms of the mammalian endomembrane system

The mammalian ER is a network of flattened membrane sheets, tubules, and budding vesicles that extend through the cytoplasm and are continuous with the nuclear envelope[11]. The ER is the site at which all transmembrane and luminal proteins of the endomembrane system are synthesized and because of this is often thought of as the 'beginning' of the secretory system. To synthesize a transmembrane or luminal protein, the protein's mRNA transcript is first partially translated in the cytoplasm. If the mRNA encodes an N-terminal ER signal sequence or a stretch of hydrophobic residues that can form a transmembrane domain, after these motifs are translated, they will be recognized by signal recognition particle (SRP) and further translation is halted. SRP then binds to the rough ER through interaction with the SRP receptor and begins the

translocation of the nascent protein across the translocon (Sec61 complex)[12]. Tightly associated with the ER, the complex of ribosome, mRNA, nascent protein, and translocon cotranslationally translocates the protein across the ER membrane. During translation and protein maturation, a signal peptidase removes the N-terminal signal sequence if present, oligosaccharyl transferase complexes glycosylate the protein, and luminal chaperones assist protein folding[4]. Failure of the protein to reach a stably folded state stimulates the process of ER associated degradation (ERAD) by which the protein is translocated to the cytoplasm and targeted for destruction by protein hydrolases[13].

The ER synthesizes the bulk of cellular lipids in a region called the smooth ER, so named because of the low density of attached ribosomes. These lipids include sphingolipids, ceramide, triglycerides, cholesterol, and phospholipids. Phospholipid synthesis begins by glycerol-3-phosphate acyltransferase (GPAT) mediated acylation of the sn-1 position of glycerol-3-phosphate followed by lysophospholipid acyltransferase (LPAT) mediated acylation of the *sn*-2 position to form phosphatidic acid (PA). PA is generally short-lived in the ER as it is quickly dephosphorylated by the enzyme phosphatidic acid phosphatase to create diacylglycerol (DAG)[14]. DAG is then remodeled through CDP:choline or CDP:ethanolamine phosphotransferase into phosphatidylcholine (PC) and phosphatidylethanolamine (PE), respectively[15]. Phosphatidylserine (PS) is created through head-group exchange from PC and PE through the enzymes phosphatidylserine synthase 1 (PSS1) and PSS2, respectively[16]. Phosphatidylinositol (PI) is synthesized by phosphatidylinositol synthase from CDP-diacylglycerol and *myo*-inositol[17].

Transport of proteins and lipids out of the ER is accomplished by COPII transport vesicles which form at specialized export areas of the ER known as ER exit sites (ERES)[18]. COPII vesicles form when the Sec12 guanine nucleotide exchange factor (GEF) activates the small GTPase Sar1 on the ER membrane and recruits a Sec23/Sec24 dimer, which in turn recruits a Sec13/Sec31 dimer[19]. These components assemble into an oligomeric lattice that coats the budding vesicle[20]. The Sec12 dependent activation of Sar1 is stimulated by Sar1 interaction with COPII cargo, leading to concentration of cargo in COPII vesicles[21]. Sec23 is a Sar1 GTPase-activating protein (GAP) and, in conjunction with Sec12, facilitates cargo recruitment by cycling Sar1 GTP/GDP state[22]. Sec24 possesses cargo binding sites and will retain COPII cargo irrespective of Sar1 GTP/GDP state[23]. The recruitment of Sec13/31 leads to the formation of positive membrane curvature and the stimulation of Sec23 GAP activity[24]. Sec13/31 is the final COPII component and its assembly is then sufficient to conclude the vesiculation process, as has been demonstrated with liposomes and *in vitro* reconstituted ER membranes[20].

Most secreted proteins undergo COPII mediated transport and thus COPII cargo is diverse in structure and composition. This diversity necessitates the formation of COPII vesicles with heterogeneous size and shape. Diameters of ~70 nm are most common but some mammalian cell types, such as cells from the intestinal epithelium, will regularly generate 400 nm coated vesicles, indicating a great deal of plasticity in COPII coat structure[25,26]. The recruitment of specific cargo proteins into COPII vesicles is known to be mediated by many mechanisms. Certain ‘privileged’ cargo molecules that cycle between the ER and Golgi complex, such as the SNARE protein Bet1p,

interact directly with Sar1 and Sec23/24 via a cytoplasmic domain[27]. The well-studied viral glycoprotein VSV-G is efficiently sorted into COPII vesicles by an EXD signal in its cytosolic carboxyl-terminus, that also interacts with Sar1 and Sec23/24[28]. Specific sorting of soluble cargo is thought to occur, at least in part, through binding of glycoproteins to the p58 receptor (ERGIC-53)[29]. These and other mechanisms assist ER export of specific cargo proteins, but these mechanisms are not necessary for all ER export, as secretion is the default trafficking pathway for ER synthesized proteins. Non-specific ER export, has been called the 'default', 'bulk flow', or 'constitutive' secretory pathway[30].

The capacity of the ER to produce proteins and lipids is controlled by an autoregulatory system called the ER stress response or unfolded protein response (UPR). UPR is used to dramatic effect in the maturation of a quiescent B-cell to an actively secreting plasma cell, which is accompanied by a dramatic ER expansion (Figure 1-3)[31]. The UPR system senses protein misfolding and lipid imbalance through ER localized sensor proteins PERK, ATF6, and IRE1. PERK is often the first sensor activated due to its sensitivity, followed by ATF6, and finally IRE1 in response to long-term or abundant unfolded proteins[32–35]. A multitude of pathways are activated by each sensor. Collectively, these include the transcriptional upregulation of protein folding chaperones, antioxidative enzymes, lipid metabolism enzymes, and the attenuation of translation through the phosphorylation of eukaryotic initiation factor of translation (eIF2α)[36]. If none of these steps are successful in restoring ER homeostasis, apopotosis is triggered through the PERK-ATF4-CHOP pathway and/or the IRE1-TRAF2-ASK1 pathway[37].

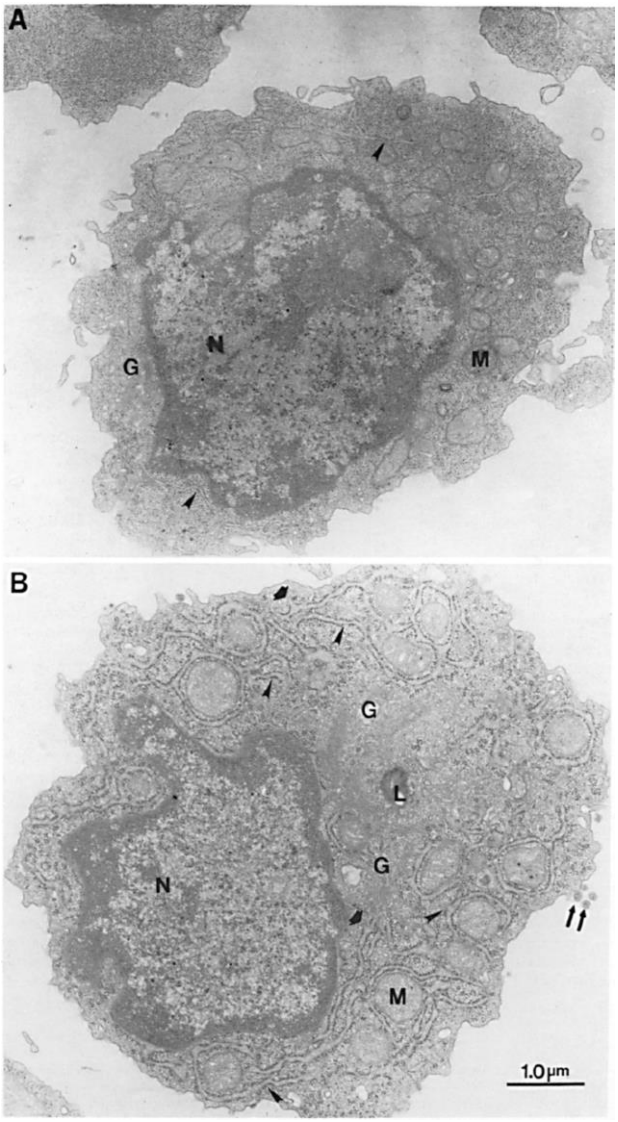

Figure 1-3. Electron micrograph depicting intracellular membrane remodeling

Proliferation of the ER during the differentiation of CH12 cells (murine B-cell lymphoma) from A) a quiescent state to B) a stimulated plasma cell in response to incubation with lipopolysaccharide. Differentiation is accompanied by a 12-fold increase in IgM secretion. N, nucleus; M, mitochondrion; L, lysosome; G, Golgi complex; arrowhead, RER; thin arrows, type C retroviruses; broad arrows, transitional elements of the ER. Reproduced from Wiest *et al*[31].

The ERGIC, once known as the vesicular tubular cluster, is a highly dynamic structure that is positioned between the ER and the *cis*-Golgi. The morphology of the ERGIC varies greatly based on cell fixation method. The classic tubulovesicular structure is observed in chemically fixed cells, while flash freezing reveals a highly budded pleiomorphic structure[38]. It is most often a single interconnected mass but can also be found as a collection of independent juxtanuclear clusters that intermittently exchange vesicles and membrane tubules[39]. The ERGIC receives COPII cargo from the ER and then sorts and repackages escaped ER proteins into COPI coated carriers for retrograde transport. From the ERGIC, COPI coated vesicles travel, often assisted by microtubule motors, to either the *cis*-Golgi or the ER (discussed further below)[40].

ERGIC-53 is a *cis*-Golgi, ERGIC, and ER resident transport protein that was experimentally important in helping to define the structure of the ERGIC. It is a single pass transmembrane protein with a short cytoplasmic sequence and a large luminal domain that directs its binding to mannosyl containing proteoglycans to facilitate their anterograde transport[41]. Its continuous cycling between compartments by COPII and COPI machinery requires the recognition of signals in its luminal, transmembrane, and cytosolic domains. The cytosolic domain contains a terminal di-phenylalanine motif that interacts with COPII and is required for efficient ER export[42]. The transmembrane and luminal domains are important for ER-ERGIC-Golgi cycling, though the underlying mechanism is not well understood[43]. Retrieval of ERGIC-53 to the ER is accomplished through specific interaction between COPI machinery and ERGIC-53's cytoplasmic C-terminal K(x)KXX motif[42,44].

The COPI coated vesicle was the first non-clathrin-coated vesicle to be identified and was thought to mediate anterograde transport through the Golgi complex[45]. It is now known that COPI coated vesicles primarily mediate retrograde trafficking between Golgi cisternae, from the Golgi to the ER, and from the ERGIC to the ER. It has also been found that COPI mediates ERGIC to Golgi anterograde trafficking[40]. The assembly of COPI coat proteins is initiated by small GTPases of the ADP-ribosylation factor (Arf) family. There are six mammalian isoforms (Arf1-Arf6) of which Arf1 is the best studied. When cytosolic Arf1 is activated by the GEF activity of a Sec7 family transmembrane protein such as GBF1 (Golgi Brefeldin A-resistance factor 1), it specifically associates with the Golgi and ERGIC[46]. The specificity of Arf1 localization is mediated by interaction with localized membrane proteins (e.g. the p24 family tethering proteins)[47]. Activated, membrane bound Arf1 promotes membrane curvature formation by intercalation of an amphipathic, myristoylated α-helix into the membrane bilayer. Subsequently, Arf1 recruits COPI coatomer subunits to the membrane[48,49]. The coatomer is composed of seven subunits that are organized into a trimeric subcomplex of α-COP, β´-COP, and ε-COP, and a tetramer of β-COP, γ-COP, δ-COP, and ζ-COP[50–52]. The interactions of p24 family members and the KDEL receptor with COPI coatomer help to recruit coatomer and ensure strong membrane binding. The p24 family of tethers interacts with the γ subunit of coatomer through a cytosolic di-phenylalanine di-basic motif, FFXX(K/R)(K/R)[51,53]. Similarly, the KDEL receptor has a dibasic motif, KKXSXXX, that binds coatomer when the serine residue is phosphorylated[54]. The luminal domain of the KDEL receptor binds luminal proteins that possess a KDEL motif and transports these proteins during COPI retrograde trafficking to the ER[55,56].

Transmembrane proteins, other than p24 and KDEL receptor, can be recruited to COPI vesicles if they possess a dilysine motif, K(x)KXX, in their carboxyl terminus. These dilysine motifs differ from the dibasic motifs of p24 and the KDEL receptor; they are recognized by α-COP or β-COP[57,58]. The recruitment of cargo proteins into COPI vesicles requires GTP hydrolysis. The requirement of GTP hydrolysis was experimentally determined using the poorly hydrolyzable GTP analogue GTPγS and Arf mutants that are locked into a GTP loaded state. Both of these conditions efficiently form COPI vesicles with normal concentrations of p24 and KDEL receptor, but are completely devoid of cargo proteins[59–66].

The only components that are necessary for COPI scission in an *in vitro* system using synthetic liposomes are Arf1 and the COPI coat components[67]. Scission occurs due to the confluence of Arf1-GTP's intrinsic membrane deformation activity and the activity of COPI to form curved membrane coat structures[68]. In the absence of coatomer, Arf1-GTP forms membrane tubule structures that never undergo scission[69]. Scission is regulated and made more efficient by accessory proteins, including p24, Brefeldin-A ADP ribosylated substrate (BARS), endophilin, Arf GTPase activating protein 1 (ArfGAP1), PLD2, and 1-acylglycerol-3-phosphate O-acyltransferase 3 (AGPAT3)[70–73].

The scission of COPI buds into vesicles is followed by an uncoating process in which coatomer proteins dissociate from the vesicle. Uncoating is dependent on ArfGAP activated hydrolysis of Arf1-GTP. ArfGAP is a stoichiometric component of the COPI coat that is regulated by membrane curvature and interacts directly with cargo

proteins[70,74–76]. Uncoated vesicles are then transported to their destination in the ER, ERGIC, or Golgi by microtubule motors and fuse with the destination compartment. While the details of the bidirectionality of COPI transport are still unclear and controversial, the differentiation of anterograde from retrograde COPI vesicles is dependent on vesicle composition[39]. Notable determinants are the cargo proteins and the isoforms of the p24 cargo receptors, Rabs, Arfs, tethering proteins and COPI coatomer subunits that make up the vesicle[65,77–83].

The Golgi apparatus is the final site at which proteins are processed and sorted before being transported to their destination[84]. Between cells, the number of cisternae and stacks (independent sets of cisternae) varies greatly, but cisternae are invariable described as *cis, medial*, and *trans.* The *trans*-Golgi should not be confused with the similarly named *trans*-Golgi network (TGN). The *cis*, *medial*, and *trans*-Golgi form a continuous interconnected network, while the TGN is adjacent to the *trans*-Golgi but is not continuous with it. Despite these distinctions, the TGN is often thought of as the final compartment of the Golgi complex[85].

The nomenclature that classifies the subcompartments of the Golgi complex underscores the sequential nature of cargo progression[86]. The biological imperative for the sequential passage of secretory cargo through the Golgi is likely due to protein glycosylation. Glycosylation sites on protein cargoes are modified by the ordered action of a series of glycosyltransferases with polarized localization across the cisternae[87].

Analysis of the movement of secretory cargo through the Golgi cisternae has sparked a great deal of controversy and the proposal of a succession of mechanistic

models. The first of these was the ‘stable compartment’ model, which was followed by the ‘cisternal maturation’ model, then the ‘rapid partition’ model, and most recently the ‘rim progression’ model. The stable compartment model posited that Golgi cisternae maintain a constant position while cargo proteins are transported by COPI vesicles between adjacent cisternae[88]. ‘Cisternal maturation’ instead proposes that cisternae progress in a *cis* to *trans* manner through the Golgi stack, retaining their maturing cargo, and exchanging cisternae specific Golgi resident enzymes through COPI trafficking.

Some of the first evidence against the stable compartment model came from the characterization of the cargo proteins contained in COPI vesicles, which are primarily Golgi and ER resident proteins and not secretory cargo proteins[89,90]. A second piece of evidence was found by studying large secretory proteins such as algae scales and procollagen aggregates, which due to their size could not possibly be transported by COPI vesicles and thus must move in concert with maturing cisternae[91,92]. The live imaging of yeast Golgi cisternae exchanging, in sequence, fluorescently-labeled *cis*-, *medial*-, and *trans*-Golgi enzymes is perhaps the most satisfying testament to the cisternal maturation model[93,94].

The ‘rapid partitioning’ model was a response to live cell fluorescent microscopy measurements of stochastic and exponential cargo export kinetics, which could not be explained by cisternal maturation. It postulates that the Golgi is subdivided into ‘phases’ that segregate processing enzymes from export machinery. Phase separation of the Golgi and the rapid partitioning of cargo proteins between phases would explain the kinetics of cargo secretion[95].

The most recently proposed model of Golgi structure-function, called 'rim progression,' was proposed by Rothman and colleagues[96]. Their experimental system was based on a reversibly aggregating FKBP mutant fused to a transmembrane cargo protein, which they called membrane 'staples' due to their distinctive appearance by electron microscopy, and an analogous soluble cargo. They found that aggregated membrane staples remained fixed within the center of immobile and non-maturing Golgi cisternae for at least 5-6 h (the longest observation period), during which time, anterograde trafficking of aggregated soluble cargo proceeded normally. The term 'rim progression' was derived from the localization of aggregated soluble cargo to cisternal rims during trafficking.

In a separate report, Luini and colleagues used a very similar model system to defend cisternal maturation[97]. They fused a transmembrane *cis*-Golgi resident protein with the FKBP mutant to form 'MANI-FM'. Disaggregated MANI-FM was retained in the cis-Golgi by COPI mediated retrograde trafficking. Aggregated MANI-FM was prevented from entering vesicles or membrane tubules. Over the course of 20 minutes, aggregated MANI-FM relocalized from the cis-Golgi to the *trans*-Golgi.

Luini's defense of the cisternal maturation model can be reconciled with the rim progression model. Rothman observed that large cargo molecules (soluble aggregates) traffic by the progression of cisternal rims. Membrane staples did not participate in rim progression because they were strictly localized to the center of cisternae and effectively excluded from rim progression. Luini's aggregated MANI-FM was distributed throughout cisternae, allowing trafficking by 'rim progression.'

The cisternae and stacks of cisternae of the mammalian Golgi are interconnected by membrane tubules[98,99]. Membrane tubules between Golgi stacks maintain organelle integrity and prevent fragmentation into many separate "mini-stacks[100]." Membrane tubules between adjacent cisternae may be important for the accelerated maturation and secretion of some cargo proteins such as the non-glycosylated albumin and proinsulin proteins[101].

Due to the ephemeral nature of membrane tubules, their physiological significance has been met with occasional skepticism. There is agreement that certain organelles, particularly the ERGIC and TGN, exhibit significant tubulation activity under normal cellular conditions, which can be visualized with GFP-tagged membrane proteins in live cells[102,103]. Perhaps the greatest source of controversy, and also one of the field's most important experimental systems, is the massive tubulation of the ERGIC, Golgi, TGN, and endosomal compartments that can be stimulated by perturbation of Arf GTP cycling. The most common method is by incubation with the fungal metabolite Brefeldin A (BFA), a specific inhibitor of Arf GEF, which prevents COPI and AP-1 coat proteins from binding[104–106]. Specific siRNA knockdown of Arfs or their GEFs will also replicate most aspects of the BFA phenotype [78,107,108].

The transport of membrane tubules is often assisted by the activity of microtubule motors [108–112]. The relocalization of Golgi markers to the ER in response to BFA treatment is inhibited by simultaneous treatment with microtubule depolymerizing drugs[113].

The relationship between vesicles and tubules is currently unclear. Studies of vesicle formation have shown that coat proteins are necessary *in vivo* and sufficient *in vitro* for vesicle formation[114]. The role of coat proteins in membrane tubulation is more subtle. Electron microscopy studies have shown that coat proteins decorate membrane tubules, where they induce the formation of bulges[115–117]. One model proposes that membrane tubulation sites are initiated by coat protein binding and membrane deformation[73]. However, this theory discounts the numerous observations of spontaneous membrane tubulation in *in vitro* systems that do not contain coat proteins[118–120]. It also does not adequately explain why BFA treatment stimulates membrane tubulation (i.e. when coat proteins cannot bind). Additionally, transport via membrane tubules of VSV-G from the TGN to the PM is not dependent on coat proteins[121,122].

A competing model for the genesis of membrane tubules deemphasizes the role of coat proteins. It theorizes that coat proteins are one of many mechanisms by which membrane curvature can be promoted and tubules can be formed. Membrane curvature is regulated by a combination of several mechanisms.

Membrane curvature

Membrane curvature can be induced by protein intercalation into the lipid bilayer which disrupts the packing of adjacent lipids, as in the case of Arf1. Its short, hydrophobic α-helix, called an ArfGAP1 Lipid Packing Sensor (ALPS) motif, directly induces membrane curvature by intercalation into a membrane[123].

Similarly, proteins are able to bend membranes by penetrating a single layer of the membrane with an amphipathic domain. The result is a small difference between the surface areas of each side of the membrane, an effect called bilayer-coupling[124]. Since the effect of changing the membrane surface area is proportional to the original surface area, small vesicles are most affected by bilayer coupling while large membranes are nearly unaffected[125].

Another mechanism by which protein-membrane interactions can induce membrane curvature is through the formation of a curvature stabilizing protein scaffold. The BAR domain, an anti-parallel dimer of curved α-helices, is one example of membrane stabilizing protein scaffold. Interactions of BAR domain containing proteins with the surface of the membrane stabilizes or promotes membrane bending to fit the BAR domain's natural curvature [126]. Many BAR domain containing proteins, such as amphiphysin, endophilin, BRAP and nadrin have been shown to create membrane tubules *in vitro*[126–129].

Lipids also affect the curvature of membranes. Studies of artificial membrane systems make it clear that certain combinations of lipid species exhibit large spontaneous curvatures[125]. Curvature is generated roughly in proportion to the ratio between the cross-sectional area of the hydrophilic head group and hydrophobic side chains. For example, the PS head group is much larger than the head group of PA, and hence PS would favor positive membrane curvature and PA would not. Similarly, phospholipids, having two acyl chains, contribute more negative curvature than lysophospholipids, which have a single acyl chain[130–132].

Lipids can also indirectly influence membrane curvature by recruiting lipid binding proteins to deform the membrane. Epsin is an example of a membrane deforming protein that is recruited by the phospholipid phosphatidylinositol-4,5-bisphosphate (PIP2). It deforms membranes by the insertion of an amphipathic helix region[133,134]. This and similar lipid specific protein recruitment events are an indispensable mechanism by which lipid remodeling can be linked to localized, transient changes in membrane curvature.

It is important to note that in live cells, membrane curvature is rarely affected by only one force in isolation. It is sometimes the case that all of the above mechanisms are involved at a single tubulation or vesiculation site.

Phospholipid remodeling

The enzyme classes that remodel phospholipid acyl chain composition are called phospholipase As (PLAs) and LPATs. PLAs remove acyl chains through a hydrolysis reaction and LPATs re-esterify acyl chains. The balance of activity between these two enzyme classes creates a dynamic and continuous process of acyl chain turnover called phospholipid remodeling.

The work of William Lands and colleagues in the 1960s first characterized phospholipid remodeling processes, and they are sometimes referred to as the “Lands cycle” in his honor. This dissertation will focus on how the acyl chain composition of phospholipids and their remodeling influences intracellular membrane trafficking and the biogenesis of membrane vesicles and tubules. However, phospholipid remodeling plays an important role in several other processes, whose discussion is beyond the

scope of this work. They include the incorporation and release of arachidonic acid (AA) for the production of eicosanoids and prostaglandins[135], production of platelet activating factor (PAF)[136–138], the regulation of lipid droplet morphology[139], triglyceride secretion via lipoprotein synthesis in the liver[140], and the incorporation of host-derived fatty acids into membrane phospholipids in *Giardia* and other intracellular parasites[141].

Phospholipases

Phospholipases are a diverse class of soluble enzymes. They are found in all life forms and cell types due to the essential utility of phospholipids in membranes. Phospholipases also have many specialized roles, such as in digestion, intracellular and extracellular signaling, as an active ingredient in many types of venom, and as an essential part of the defense and immune responses of plants and animals.

Phospholipases are differentiated into super families based on their preferred substrate and hydrolysis site. These super families are phospholipase A_1 (PLA_1) and A_2 (PLA_2), phospholipase B (PLB), phospholipase C (PLC), and phospholipase D (PLD) (Figure 1-4). PLA_1 and PLA_2 produce lysophospholipids by hydrolyzing the *sn*-1 and *sn*-2 acyl chain of phospholipids, respectively. Enzymes classified as PLB have PLA_1 and PLA_2 activity and will hydrolyze both acyls chain of a phospholipid[142]. PLC produces DAG by hydrolyzing the phosphodiester linkage between glycerol and the head group. PLD produces PA by hydrolyzing the bond between the head group and glycerophospholipid[143–147]. A single super family is assigned to each phospholipase, however, many phospholipases have broad specificity that can overlap multiple super families or include non-phospholipid substrates[148]. For example, pancreatic lipase

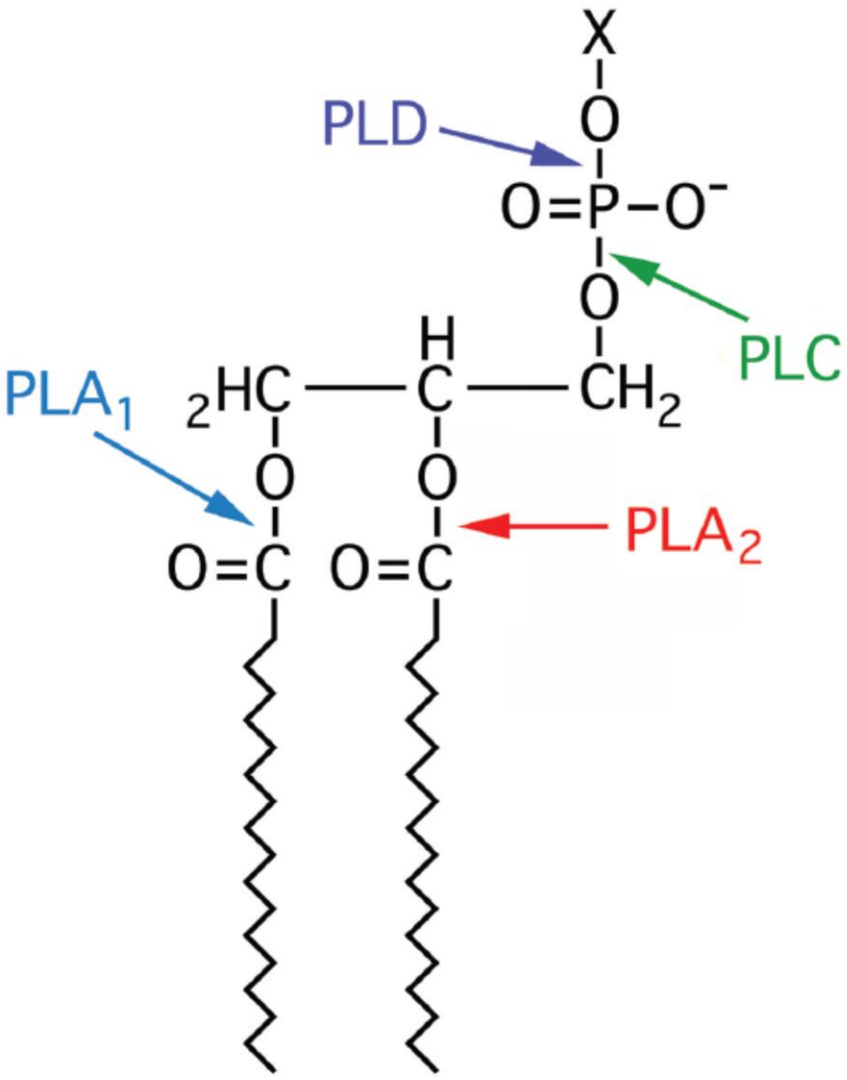

Figure 1-4. Hydrolysis preference of phospholipase groups

R represents acyl chains and X represents head groups (choline, ethanolamine, inositol, etc.) Reproduced from Brown et al[150].

related protein 2, a PLA_2, hydrolyzes phospholipids, galactolipids, vitamin esters, and triglycerides[149].

The PLA_2 superfamily is divided into 15 groups but are more commonly referenced based on the classifications: secretory ($sPLA_2$), cytosolic Ca^{2+} dependent ($cPLA_2$), cytosolic Ca^{2+} independent ($iPLA_2$), platelet-activating factor acetylhydrolases (PAFAH) and lysosomal[150,151]. Of these, the classes $cPLA_2$, $iPLA_2$, and PAFAH are most relevant to intracellular membrane trafficking and together include four enzymes that are known to regulate membrane tubulation, $cPLA_2\alpha$, PAFAH Ib, $iPLA_2$-β, and $iPLA_1\gamma$.

The $cPLA_2$ family, also known as Group IV, has six members, $cPLA_2$ α, β, γ, δ, ε, and ζ. These enzymes have a conserved active site dyad of serine and aspartic acid (S228/E529 in $cPLA_2\alpha$). All but $cPLA_2\gamma$ contain an N-terminal α/β sandwich "C2 domain" that binds Ca^{2+}, regulates lipase activity, enables membrane translocation, and interfacial activation[152]. Of the $cPLA_2$ enzymes, $cPLA_2\alpha$ is the most studied, due to its early discovery, ubiquitous expression, and importance in regulating eicosanoid signaling. $cPLA_2\alpha$ has a strong preference for *sn*-2 arachidonyl acyl chains, which are shunted into the production of the eicosanoids prostaglandins, thromboxanes, and leukotrienes. Eicosanoids are local signaling molecules with many important roles, among them the regulation of the inflammatory response, immunity, and the nervous system[153].

The role of $cPLA_2\alpha$ in membrane trafficking was first suggested when increased cytoplasmic Ca^{2+} was shown to recruit $cPLA_2\alpha$ to the Golgi complex[154]. It has also been

shown that cPLA$_2$α is recruited to endothelial cells upon reaching confluence, where its activity is necessary for efficient transport of membrane proteins such as VE-cadherin, occluding, and claudin-5 to junction complexes[155,156]. A bolus of secretory cargo has been shown to stimulate a transient increase in cytosolic Ca^{2+}, translocation of cPLA$_2$α to the Golgi complex, and cPLA$_2$α mediated formation of intercisternal tubular connections to accelerate anterograde trafficking. Conversely, blocking cPLA$_2$α activity suppresses the formation of Golgi membrane tubules. These effects are independent of changes in eicosanoid pathway throughput and are unaffected by arachidonic acid supplementation[101].

The biological relevance of cPLA$_2$α has yet to be convincingly established in a whole organism, as the growth and viability of the cPLA$_2$α knockout mouse is phenotypically normal[157]. However, there is one documented case of a human patient possessing two loss-of-function alleles for cPLA$_2$α. This patient exhibits decreased eicosanoid production, intestinal ulcers, and platelet dysfunction[158,159]. While cPLA$_2$α activity does not appear to be essential for efficient membrane trafficking, a siRNA screen of other PLA$_2$s in a cPLA$_2$α deficient cell line indicated that PAFAH Ib α1 may have a redundant role in supporting anterograde secretory transport[101].

PAFAH Ib is an enzyme complex consisting of a dimer of two Ca^{2+}-independent, Group VIII phospholipases of the PAFAH category and a dimer of Lis1 (gene name PAFAH Ib 1), a dynein regulator and a lissencephaly associated gene. The catalytic complex can be either a homo- or hetero-dimer of PAFAH Ib α1 and α2 (gene names PAFAH Ib 2 and 3), paralogues with 63% amino acid identity, partially overlapping

substrate specificity, and slightly different expression pattern[160–162]. The enzyme category, PAFAH, is derived from the ability of purified enzymes to hydrolyze the *sn*-2 acetyl group from the extracellular lipid PAF[163,164]. The physiological relevance of this activity for PAFAH Ib is dubious as it is a cytoplasmic enzyme complex. Also, subsequent studies have shown that PAFAH Ib is not involved in organism-wide PAF signaling[138].

The formation of membrane tubules and the maintenance of Golgi structure is influenced by PAFAH Ib activity, which was first shown using a chromatographically fractionated preparation of bovine brain cytosol. The fraction containing PAFAH Ib was capable of stimulating Golgi membrane tubulation in an *in vitro* tubulation assay[165]. Later studies showed that tubulation activity is dependent on PAFAH Ib α1 and/or α2 catalytic activity and that Lis1 is dispensable. In cells however, α1, α2, and Lis1 are all important for regulating Golgi structure and function. Knockdown of any of these enzymes causes the Golgi to fragment into mini-stacks[110].

The iPLA$_2$ enzyme family includes one member, iPLA$_2$-β, a Group VI-2 PLA$_2$, also known as PLA2G6 and PNPLA9, which has been shown to regulate ERGIC membrane trafficking[135,166]. Double knockdown of Arf1 and Arf4 generates ERGIC membrane tubules and tubulation is dependent on iPLA$_2$-β activity. iPLA$_2$-β-dependent tubulation is important for the transport of GFP-ERGIC-53 between ERGIC clusters. iPLA$_2$-β also controls ERGIC tubulation and GFP-ERGIC-53 transport in wild-type cells without Arf knockdown. Cells incubated at 16°C for 3 h accumulate GFP-ERGIC-53 in the ERGIC and can then be warmed to 37°C to stimulate tubulation. Upon warming,

iPLA$_2$-β translocated from the cytoplasm to GFP-ERGIC-53 labeled membrane tubules where its activity was necessary for tubulation[166].

The final phospholipase that has been reported to be involved in membrane trafficking is iPLA$_1$γ (gene name DDH2 or KIAA0725p), a Golgi and ERGIC localized protein. Overexpression of iPLA$_1$γ causes disorder of the Golgi and ERGIC as well as dispersion of Golgi associated tethering proteins[167]. Two conflicting studies have been published, the first showing that iPLA$_1$γ knockdown disrupts COPI- and Rab6-independent Golgi-to-ER retrograde trafficking (such as BFA mediated Golgi recycling, but not COPI- and Rab6-dependent retrograde transport such as ERGIC-53 recycling). Also, knockdown did not affect VSV-ts045-GFP anterograde trafficking[168]. The second study noted that the siRNA used in the first study had an unintended off-target effect that decreased Rab6 expression. They went on to examine BFA induced retrograde trafficking with three other specific siRNAs and found no effects on retrograde trafficking, though VSV-ts045-GFP anterograde trafficking to the plasma membrane was slowed[169].

Our understanding of phospholipases owes a great deal to the discovery and development of small molecule inhibitors[170]. A pioneering study of small molecule PLA$_2$ inhibitors uncovered the PLA$_2$ dependency of tubule-mediated retrograde trafficking and maintenance of the architecture of the Golgi complex[171]. This study showed that treatment of mammalian cells with PLA$_2$ inhibitors leads to fragmentation of the Golgi complex and suppresses BFA stimulated Golgi membrane tubulation. Among the inhibitors tested was the irreversible membrane permeant small molecule bromoenol

lactone (BEL), which is a substrate analogue with 1000-fold selectivity to $iPLA_2$s over $cPLA_2$s. BEL inhibits BFA mediated Golgi recycling with an IC_{50} of 4 μM and TGN tubulation at 20 μM. It has become an indispensable reagent for testing phospholipase dependence in membrane trafficking studies. Another important inhibitor is ONO-RS-082 (ONO), which has reversible binding and an IC_{50} for BFA stimulated tubulation of the Golgi and TGN of 4 and 7 μM, respectively. Since its discovery as an inhibitor of membrane trafficking, ONO has become a fixture of "wash-out" studies due to its reversible binding. Fifteen years later, these two inhibitors and a handful of others, have been pivotal in demonstrating the importance and ubiquity of phospholipases in regulating membrane tubulation and the structure and function of the endomembrane system.

Lysophospholipid acyltransferases

The opposing enzymatic activity to that of PLA_1 and PLA_2 enzymes is provided by a diverse group of enzymes that are collectively called LPATs. Enzymes are classified as LPATs if they possess the ability to transfer an acyl chain to a lysophospholipid. They were first described in the 1950s by the researchers Kennedy, Weiss, and Lands who uncovered two major systems for phospholipid synthesis and remodeling[172–174]. The *de novo* process of phospholipid synthesis from glycerol-3-phosphate and fatty acids is named the Kennedy pathway and the LPAT mediated remodeling of phospholipids has become known as the Lands cycle[175,176].

The acyltransferases of the Kennedy pathway produce PA with saturated acyl chains at both the *sn*-1 and *sn*-2 position. PA is then converted to other phospholipids

through the intermediates DAG and cytidine diphospho-DAG (CDP-DAG)[177]. However, bulk cellular phospholipids contain nearly equal portions of saturated and unsaturated acyl chains. Saturated acyl chains are predominantly in the *sn*-1 position and unsaturated acyl chains are nearly exclusive to the *sn*-2 position. The Lands cycle maintains the asymmetry of acyl chain saturation in phospholipids through continuous PLA_2 dependent hydrolysis of the *sn*-2 acyl chain and LPAT dependent reacylation[172].

While the importance of the Kennedy pathway for bulk lipid synthesis has long been understood, the significance of the Lands cycle is still being discovered. The most studied aspect of the Lands' cycle is its role in the potentiation of the inflammatory response through polyunsaturated fatty acid derived signaling molecules[178,179]. It is also important in the production of surfactant in the lungs, embryogenesis and development, and the production of apolipoproteins. Finally, there is a growing understanding that the Land's cycle is important for regulating intracellular membrane trafficking.

The first solid indication that LPATs were involved in membrane trafficking emerged from studies that utilized a powerful new tool, the small molecule inhibitor CI-976 (2,2-methyl-N-(2,4,6,-trimethoxyphenyl) dodecanamide). This molecule is a fatty acid anilide derivative designed to mimic fatty acyl-CoA and to inhibit acyl-CoA:cholesterol acyltransferase in the treatment of heart disease[180]. However, CI-976 possesses only weak inhibitory activity against acyl-CoA:cholesterol acyltransferases, but is a strong inhibitor of LPATs. The utility of this hydrophobic, membrane permeant LPAT inhibitor was first discovered during a 2003 screen for the inhibition of Golgi associated LPAT activity; CI-976 showed strong inhibition of lysophosphatidylcholine

(LPC) and lysophosphatidylethanolamine (LPE) acyltransferase activities[181]. Treatment of mammalian cells with CI-976 stimulated a remarkable enhancement of Golgi membrane tubulation and retrograde trafficking. This tubulation activity was phenotypically similar to BFA induced tubulation, although comparatively delayed. Additionally, CI-976-induced Golgi tubulation was inhibited by concomitant PLA_2 inhibition, indicating for the first time that PLA_2s and LPATs work in concert to regulate the dynamic structure of the Golgi complex[182].

Like PLA_2 enzymes, LPATs are involved in membrane trafficking at the ER and endosomes. For example, CI-976 reversibly inhibited a very late step in COPII vesicle budding, resulting in the accumulation of secretory cargo at ERESs[183]. Interestingly, ERESs exhibited Sar1p-dependent membrane tubulation in the presence of CI-976, suggesting the involvement of LPAT activity in the fission of COPII budding elements *in vivo*. CI-976 was also found to stimulate membrane tubule genesis from endosomes and to inhibit the recycling of transferrin and transferrin receptors from the endocytic recycling compartment, suggesting a role for LPATs in the budding of vesicles from endosome tubules[184]. The LPAT isoforms inhibited by CI-976 and their roles in regulating membrane trafficking are not yet known.

The identification and characterization of the human LPATs began in earnest about 40 years after Kennedy and Lands seminal work. This work was pioneered by Takao Shimizu and colleagues, who have assayed the substrate specificity of nearly every LPAT enzyme, laying the groundwork for a modern understanding of human

LPAT biology and the relationships that exist between LPAT enzymes[185]. In excess of fifteen mammalian LPATs have been identified; they are distributed across the AGPAT,

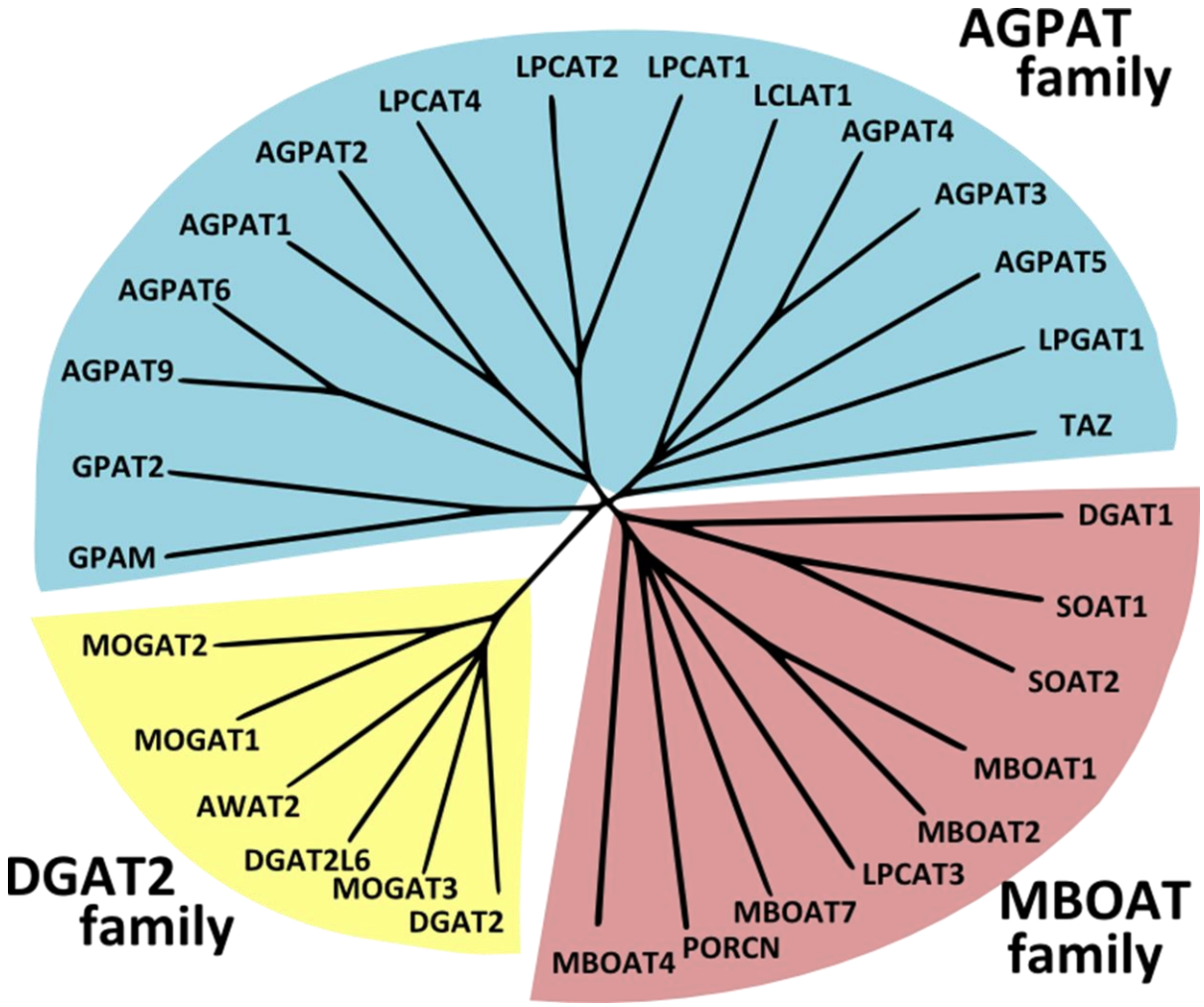

Figure 1-5. A partial phylogenetic tree of human acyltransferase enzymes

Adapted from Hishikawa et al[211].

diacylglycerol acyltransferase 2 (DGAT2), and membrane bound O-acyltransferase (MBOAT) gene families (Figure 1-5).

Naming conventions for LPATs are a subject of ongoing disagreements, partly because of multiple, nearly simultaneous 'discoveries' and differences in naming conventions between interspecies orthologs. Complicating matters further, efforts have been made to rename LPATs based on their substrate specificity. Empirical determinations of LPAT specificity vary dramatically depending on the assay type, experimental conditions, and the LPAT ortholog's species of origin. In order to avoid potential confusion, herein the naming convention of the NCBI for human genes will be followed.

Of the three LPAT gene families, the smallest is the DGAT2 family. DGAT2s are specific for primarily diacylglycerol and monoacylglycerol acceptors and have lesser activity for lysophospholipid acceptors. The founding member of the family, DGAT2, is a 40-44 kDa integral membrane protein of the ER, with one or two transmembrane spans and an active site histidine that primarily synthesizes triacylglycerol (TAG) from DAG and acyl-CoA[186,187]. It is highly conserved from yeast to humans and is thought to be responsible for the bulk of TAG synthesis in most, if not all, tissues. There is also evidence that DGAT2 is inextricably linked to *de novo* glycerolipid synthesis and the sequestration of free fatty acids[188,189]. The monoacylglycerol O-acyltransferase 1 (MOGAT1) and MOGAT2 enzymes synthesize DAG from monoacylglycerol (MAG) and acyl-CoA, a key step toward the synthesis of TAG and an activity that is concentrated in the small intestine, stomach, kidney, adipose, and liver[190,191]. Acyl-CoA wax alcohol

acyltransferase 2 (AWAT2) is involved in the synthesis of long chain alcohols (waxes) of the skin[192]. Little is known about the remaining two DGAT2 family members DGAT2-like 6 (DGAT2L6) and MOGAT3.

The MBOAT family consists of multipass, usually ER-localized enzymes. The family has a very wide range of acyl chain acceptor specificities. The enzymes DGAT1 and the sterol O-acyltransferase (SOAT1) and SOAT2 paralogs catalyze the formation of TAG from DAG and acyl-CoA and sterol esters from free cholesterol and acyl-CoA. They are very important enzymes for the synthesis of neutral lipids destined for lipid droplets or apolipoproteins[186,193–196]. Despite the similar name and substrate specificity, DGAT1 and DGAT2 are not evolutionarily related[197]. In a study of hepatic DGAT1 and DGAT2 function, DGAT2 was shown to mediate TAG synthesis from glycerol and endogenous (saturated) fatty acids, whereas DGAT1 mediated the incorporation of exogenous oleic acid into TAG[198]. MBOAT1 prefers acylating lysophosphatidylserine (LPS) with oleoyl-CoA, MBOAT2 prefers lysophosphatidic acid (LPA) and LPE acceptors and oleoyl-CoA donors, LPCAT3 prefers LPC and unsaturated and polyunsaturated acyl donors, and MBOAT7 is a lysophosphatidylinositol (LPI) acyltransferase with incredible specificity to arachidonoyl acyl donors[199]. MBOAT7 has been studied by two groups in a mouse knockout model and has been shown to be very important for brain development[200,201]. MBOAT4 octanoylates the ghrelin peptide and is crucial for regulating feeding urges, adiposity, and insulin secretion[202]. Porcupine (PORCN) palmitoylates Wnt family proteins and is essential for Wnt trafficking to the extracellular environment[203].

The large AGPAT family has been alternatively known as the LPAAT (lysophosphatidic acid acyltransferase) family, though most family members are not specific to LPA[204,205]. AGPATs are characterized by a conserved amino terminal NHX_4D motif and a less conserved central EGTR motif, both of which play a role in enzymatic activity[206,207]. All members are integral membrane proteins; the transmembrane topological orientation of AGPAT1 and AGPAT3 isoforms has been mapped[208,207]. The crystal structure of a chloroplast localized AGPAT from squash indicates that acyl chain specificity may be determined by the length and amino acid composition of a semi-conserved hydrophobic 'tunnel'[209,210].

The AGPAT family contains four enzymes with primarily glycerol-3-phosphate acyltransferase (GPAT) activity: GPAT mitochondrial (GPAM), GPAT2, AGPAT9, and AGPAT6[211]. GPAM is localized to the mitochondrial outer membrane and is transcriptionally regulated through insulin and glucose signaling. Overexpression of GPAM results in the net redirection of exogenous oleic acid to TAG in preference to phospholipids, suggesting a role in TAG anabolism[212,213]. GPAT2 is another mitochondrial GPAT but, unlike GPAM, does not seem to be under metabolic transcriptional control and is most highly expressed in testis, liver, and brown adipose[214,215]. AGPAT9 is ER localized, widely expressed, and influenced by PPARγ agonists[216–218]. AGPAT6 is a widely expressed, ER localized GPAT. AGPAT6 knock-out models show that it is essential for lactation and the formation of subcutaneous fat stores[218–222].

AGPAT1 is an ER localized LPA acyltransferase with broad acyl-CoA specificity[223]. AGPAT2 is an ER localized LPA acyltransferase that is best known for being the gene that is mutated in congenital generalized lipodystrophy (CGL) type 1, also known as Berardinelli-Seip Congenital Lipodystrophy. CGL individuals have a remarkable absence of subcutaneous adipose tissue, as well as hyperglycemia and hepatic steatosis[224–226]. LPCAT4 is an ER localized LPE specific acyltransferase that is most highly expressed in the brain. It prefers long chain saturated and mono-unsaturated acyl donors, and has broad specificity for lysophospholipid acceptors that, as its name suggests, includes LPC but also LPA, lysoPAF, and LPS[227]. LPCAT2 is an ER and lipid droplet localized LPAT that has dual enzymatic activities for the synthesis of PAF from lysoPAF and acetyl-CoA in response to inflammatory signaling and for the synthesis of PC from LPC and arachidonoyl-CoA[136,228]. LPCAT1 is an ER localized LPC acyltransferase with specificity to saturated acyl donors; it plays a crucial role in the production of lung surfactant[228–233]. Lysocardiolipin acyltransferase 1 (LCLAT1) is a mitochondrial enzyme that is responsible for the production of cardiolipid and, to a lesser extent, PI[234–237]. AGPAT4 is highly expressed in the brain and also in the gut, lung, spleen, leukocytes, and adipose; it prefers to acylate LPA[238–240]. AGPAT5 is an ER and mitochondria localized LPAT with specificity to LPA and LPE; it is most highly expressed in the testis[237–239]. Lysophosphatidylglycerol (LPG) acyl transferase 1 (LPGAT1) is ER localized and has a preference for LPG acceptors and saturated, long chain acyl-CoA donors[241]. TAZ (tafazzin) is a lysocardiolipin specific acyltransferase that is localized to the mitochondria. Mutations in TAZ cause the human disease Barth

syndrome, which is characterized by cardiomyopathy, exercise intolerance, and neutropenia[242–244].

AGPAT3 is a LPA and LPI acyltransferase with strong preference for arachidonoyl-CoA[239,245,246]. It colocalizes with *cis*-Golgi, ER, and nuclear envelope markers[239,245]. Expression is very broad but highest in the testis, liver, and kidney[238,246]. The protein likely contains two transmembrane domains, the first of which bisects cytoplasmic NHX_4D and luminal EGTR catalytic motifs[207]. Its enzymatic activity is important for the regulation of Golgi complex structure and function, including membrane tubule formation. When AGPAT3 is overexpressed, the formation of Golgi membrane tubules is inhibited. Knockdown of AGPAT3 accelerates both anterograde and retrograde protein trafficking and leads to Golgi fragmentation[245].

Overexpression of AGPAT3 counteracts the tubule-inducing effects CI-976, suggesting that AGPAT3 is a target of the drug. However, it is possible that another LPAT also contributes to Golgi membrane remodeling because CI-976 has been shown to inhibit Golgi localized LPC and LPE acyltransferase activity. Alternatively, Golgi localized LPC and LPE acyltransferase activity could be the consequence of the remodeling of AGPAT3 generated PA into DAG by PA phosphatase, followed by conversion to PC and PE by Golgi localized cholinephosphotransferase and phosphoethanolamine transferase (Figure 1-6)[245,247,248].

The LPAT antagonist CI-976 has been shown to inhibit COPI vesicle formation, a process whose molecular mechanism is the focus of a recent study by Hsu and colleagues[71]. A model incorporating their findings, together with the findings from other

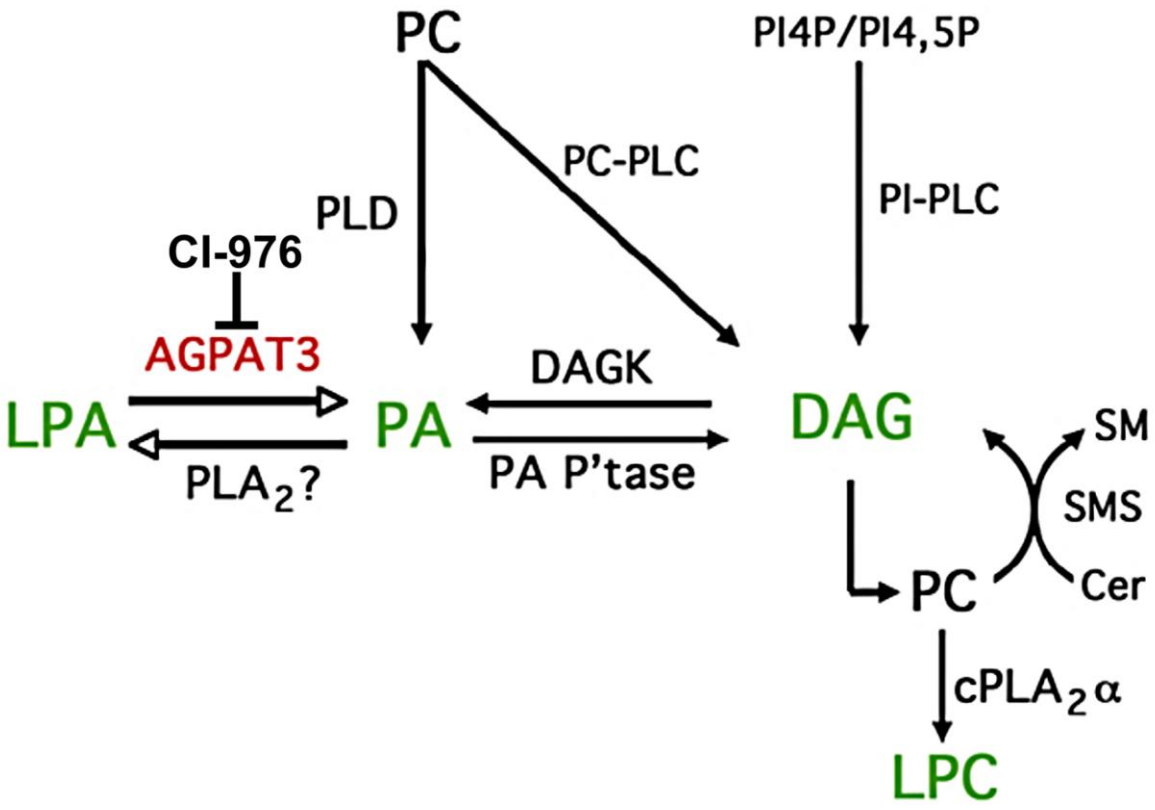

Figure 1-6. Pathways of lipid remodeling

Enzymatic pathways which lead to the modification and interconversion of lipid species. Sphingomyelin (SM); ceramide (Cer); PI 4-phosphate (PI4P); PI-4,5-phosphate (PI4,5P); DAG kinase (DAGK); PA phosphatase (PA P'tase); PC specific phospholipase C (PC-PLC); PI specific PLC (PI-PLC); SM synthase (SMS). Adapted from Ha *et al*[248].

labs, is shown in Figure 1-7. In an *in vitro* COPI budding assay using purified Golgi membranes and cytosol, COPI coatomer subunits and Arf1 are required for both vesicle and membrane tubule formation. Ablation of AGPAT3 activity by addition of CI-976 or AGPAT3 specific antibody decreased COPI budding and concomitantly increased membrane tubule formation. The addition of pharmacological PLA_2 inhibitors or anti-$cPLA_2\alpha$ antibody increased vesicle formation and decreased tubule formation. The opposite effect was observed when purified $cPLA_2\alpha$ was added to the assay.

Examination of endogenous $cPLA_2\alpha$ and AGPAT3 by immunofluorescence microscopy shows colocalization with endogenous coatomer proteins. The α-COP coatomer subunit was shown by immuno-EM to localize to the base and tip, but not the length, of membrane tubules. They propose that Arf1 and COPI coatomer recruitment initiates bud formation and that buds mature into either vesicles or membrane tubules, depending on the balance of $cPLA_2\alpha$ and AGPAT3 activity.

AGPAT3 generates PA, a negative membrane curvature inducing phospholipid, a recruiter of COPI coatomer subunits, and a recruiter of BARS, which mediates COPI vesicle fission[125,131]. Through these mechanisms, AGPAT3 is thought to stimulate COPI vesicle budding and scission. $cPLA_2\alpha$ generates LPC, a positive membrane curvature inducing phospholipid that stabilizes budding vesicles and membrane tubules. Thus $cPLA_2\alpha$ activity is important for both vesicle and membrane tubule biogenesis, but unbalanced $cPLA_2\alpha$ activity primarily leads to increased membrane tubulation. The final step of COPI vesicle fission requires the conversion of PC to PA by PLD2[73].

Hsu and colleagues also assert that the biogenesis of all Golgi membrane tubules is initiated as COPI buds, however they do not attempt to reconcile this assertion with the mechanisms of COPI independent membrane tubulation. The model presented in Figure 1-7G argues that COPI independent membrane tubulation is the product of phospholipase activity. In the absence of COPI vesicle formation, which normally acts to consume membrane extensions, $cPLA_2\alpha$ activity maintains long, stable, membrane tubules.

The above studies demonstrate that a complex relationship exists between vesicle coat components, phospholipases, LPATs, and the myriad accessory proteins that regulate the formation of membrane vesicles and tubules. This dissertation addresses these issues by focusing on how lipid remodeling by phospholipases and LPATs affects membrane trafficking. I will examine the relationship between phospholipases and AGPAT3 in Chapter 2, the importance of LPATs in secretion in Chapter 3, the transmembrane topology of LPCAT3 in Chapter 4, and the importance of LPCAT3 activity for the regulation of membrane trafficking in Chapter 5.

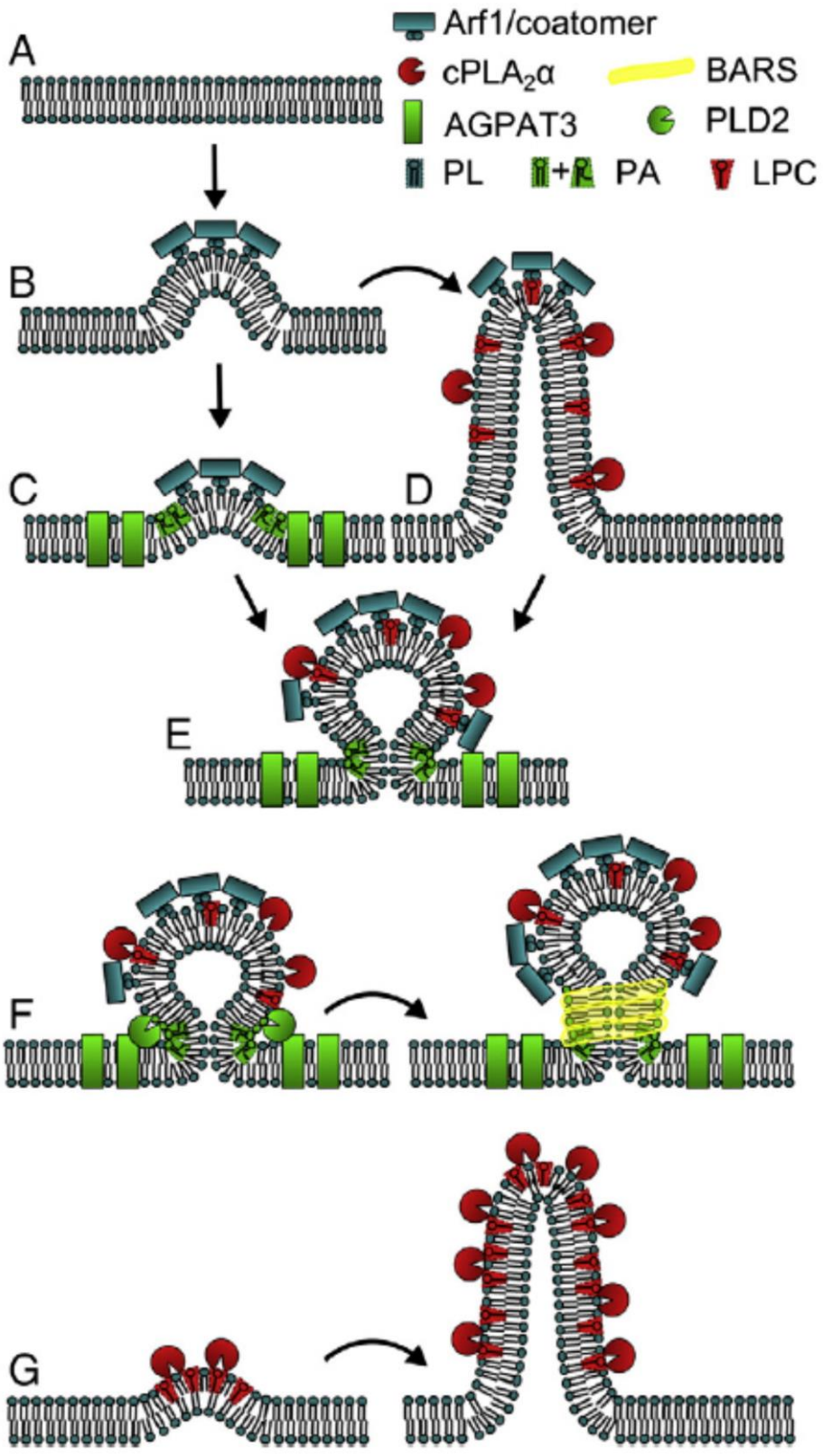
Arf1/coatomer
cPLA2α
BARS
AGPAT3
PLD2
PL
+
PA
LPC
A
B
C
D
E
F
G

Figure 1-7. Mechanisms of cPLA$_2$α and AGPAT3 mediated membrane deformation

Models of cPLA$_2$α and AGPAT3 activity as it contributes to COPI vesicle and Golgi membrane tubule formation. (A) Flat membrane that will be modified by curvature inducing proteins; (B) Arf1 and coatomer binding deforms membranes, initiating the first steps of vesiculation or tubulation; (B to C) AGPAT3 activity produces unsaturated PA, a lipid that resists positive curvature; (B to D) cPLA$_2$α activity produces LPC, a positive curvature and membrane tubule stabilizing lipid; (C and D to E) LPC stabilizes positive curvature of the bud and unsaturated PA stabilizes negative curvature at the bud neck; (F) The concerted PA production activities of AGPAT3 and PLD2 at the bud neck help to recruit BARS and aid vesicle fission; (G) PLA$_2$ activity can produce membrane curvature and tubulation in the absence of Arf1 and coatomer. Reproduced from Ha *et al*[248].

CHAPTER TWO: Regulation of Golgi function by AGPAT3 and PLA enzymes

Introduction

The membrane dynamics and structure of the Golgi complex are regulated, in part, by the activity of LPATs and phospholipases[171,183,184,249,250]. The strongest evidence for the involvement of LPATs in Golgi membrane trafficking comes from studies which show that the LPAT inhibitor CI-976 induces Golgi membrane tubulation and recycling to the ER[181]. Also, studies of the LPAT enzyme AGPAT3 show that overexpression or knockdown affects Golgi morphology and membrane dynamics[245].

A great deal of evidence has been collected to support the role of phospholipases in regulating Golgi membrane dynamics. PLA_2 inhibitors (e.g. BEL, ONO-RS-082) and agonists (e.g. melittin) have profound effects on membrane trafficking[148]. The phospholipase PAFAH IB induces Golgi membrane tubule formation in an *in vitro* reconstitution system and when overexpressed in mammalian cells; its knockdown induces Golgi fragmentation[110]. The phospholipase $iPLA_1\gamma$ mediates retrograde transport from the Golgi complex and its knockdown delays BFA-mediated Golgi recycling and cholera toxin B retrograde trafficking[168]. The phospholipase $cPLA_2\alpha$ hydrolyzes arachidonic acid from Golgi phospholipids and induces the formation of membrane tubules in response to secretory load[101,251,252]. Overexpression of $cPLA_2\alpha$ can lead to Golgi fragmentation and decreases the rate of anterograde transport[253].

While the roles of LPATs and PLA_2s have been studied in isolation, there has been little progress toward an integrated model of LPAT and phospholipase activity as

they affect Golgi membrane structure and dynamics. It is likely that there are unappreciated antagonistic and/or synergistic relationships between these classes of enzymes because their activities are, broadly speaking, opposite. The mechanisms and prevalence of LPAT-PLA_2 functional relationships will vary depending on the relevant enzyme isoforms, tissue/cell-type, and experimental conditions.

The mechanisms of AGPAT3 and phospholipase enzyme localization and substrate availability will be the primary focus of these experiments. The trafficking of a bolus of secretory cargo is known to stimulate membrane binding of phospholipases and stimulate their activity, often in combination with transiently increased Ca^{2+} concentrations[101,166]. AGPAT3 is limited by substrate availability, but other transient regulatory mechanisms have yet to be discovered. Production of PA by AGPAT3 activity is thought to help recruit COPI coatomer[248]. It is possible that AGPAT3 localization and activity is also regulated in response to membrane trafficking events.

AGPAT3 and phospholipases may have an antagonistic relationship if they are colocalized and have complementary substrate and product specificities, as their net activities would not be expected to alter total PA or LPA concentration. Antagonism might also be seen with phospholipases that hydrolyze other phospholipids. All lysophospholipids induce positive membrane curvature to a much greater extent than their corresponding phospholipids, which would counteract negative curvature induced by AGPAT3 derived PA.

Synergy between colocalizing AGPAT3 and phospholipases could occur if their lipid products influence two independent aspects of the same process, for instance

lysophospholipid stabilization of the positive curvature of a budding COPI vesicle and PA stabilization of the negative curvature at the bud neck in COPI budding (Figure 1-7 E, F). By this mechanism, even phospholipases that hydrolyze PA could be synergistic with AGPAT3 as their complimentary activities would resupply their substrates.

In this chapter, I present an investigation of these topics in the context of mammalian overexpression and co-overexpression of AGPAT3 and three PLA enzymes.

Materials and methods

Plasmids

GFP-tagged AGPAT3 and HA-tagged PAFAH IB expression plasmids were constructed as previously described[110,245]. The GFP-tagged cPLA$_2$α expression plasmid was a kind gift from Victor Hsu. FLAG-tagged iPLA$_1$γ expression plasmid was a kind gift from Hiroki Inoue.[167]

Cell culture

HeLa cells and transformed bovine testicular cells (BTRD) were grown and maintained in minimal essential medium (MEM) supplemented with 10% Fetal Bovine Serum (FBS) and 1% penicillin/streptomycin at 37°C in 95% humidity and 5% carbon dioxide (CO_2).

Immunofluorescence

Cells were transfected in 35 mm^2 culture dishes using polyethylenimine (PEI) from Polysciences Inc. or Lipofectamine 2000 (Invitrogen, Carlsbad, CA) according to manufacturer's instructions. Transfection was performed using 1 µg DNA and 5 µg PEI/2.5 µl Lipofectamine for the 24 h prior to experiments. Cells were grown on glass

coverslips and fixed with 3.7% formaldehyde in phosphate buffered saline (PBS), washed 3 times in PBS, and permeabilized with 0.1% Triton X-100 in PBS. Cells were incubated with primary antibodies for 1 h at room temperature using the manufacturer's recommended dilution, washed 3 times, treated identically with secondary antibodies, and mounted on glass slides with VectaShield (Vector Laboratories). Cells were viewed and imaged using a Perkin-Elmer Ultraview spinning disk confocal microscope at 100X. Image analysis was performed using the ImageJ software package (NIH, Bethesda, MD) or the FIJI distribution of ImageJ[254]. Rabbit anti-GPP130 (Covance), mouse anti-HA (Covance), and FITC/TRITC/Cy5 conjugated secondary antibodies (Jackson ImmunoResearch Laboratories and Invitrogen) were used for immunofluorescence (IF).

BFA and CI-976 assays

Cells were washed three times with 37°C MEM (without FBS) followed by incubation with 2.5 µg/ml Brefeldin A (Endo Life Sciences or Sigma-Aldrich) or 50 µM CI-976 (Tocris, Ellisville, MO) at 37°C. In BFA washout experiments, BFA was incubated with HeLa cells for 20 min and with BTRD cells for 15 min, cells were washed 3 times with 37°C MEM containing FBS and then returned to a 37°C incubator. Scoring for intact Golgi complexes was performed by visual inspection under a mercury lamp at 100X; cells were categorized as having 'intact' Golgi complexes only if GPP130 was not dispersed, fragmented, or partially ER localized. Error bars are SEM. Significance determined by paired Student's t-test.

Results

AGPAT3 or PLA overexpression does not disrupt the Golgi

Golgi morphology is established through vesicle and tubule dependent processes that balance anterograde and retrograde trafficking, maintain the integrity of the Golgi ribbon, and establish cisternal identity through the partitioning of resident enzymes. AGPAT3 and PLAs influence Golgi vesicle and tubule dynamics, therefore I began my investigation with an assessment of Golgi morphology in AGPAT3 and PLA overexpressing cells. The morphology of the Golgi complex was scored as 'intact' or 'not intact' by IF using anti-GPP130 as a Golgi marker. Increased peripheral staining was observed in PAFAH IB overexpressing cells, but Golgi morphology was not significantly disrupted under this or any other expression condition (Figure 2-1).

Golgi reformation following BFA washout is accelerated by AGPAT3, iPLA$_1$γ, and cPLA$_2$α overexpression

To investigate possible relationships between AGPAT3 and PLA enzymes in Golgi membrane dynamics, I examined the reassembly of the Golgi complex following BFA washout in HeLa cells overexpressing AGPAT3 and/or a PLA enzyme. Compared to control cells expressing GFP, all cells expressing AGPAT3 or a PLA enzyme showed accelerated Golgi complex reformation (Figure 2-2). The combination of AGPAT3 and PAFAH IB accelerated Golgi reformation by a rate that is intermediate to that of AGPAT3 or PAFAH IB alone. Co-overexpression of AGPAT3 and iPLA$_1$γ accelerated Golgi reformation to a greater extent than either enzyme individually.

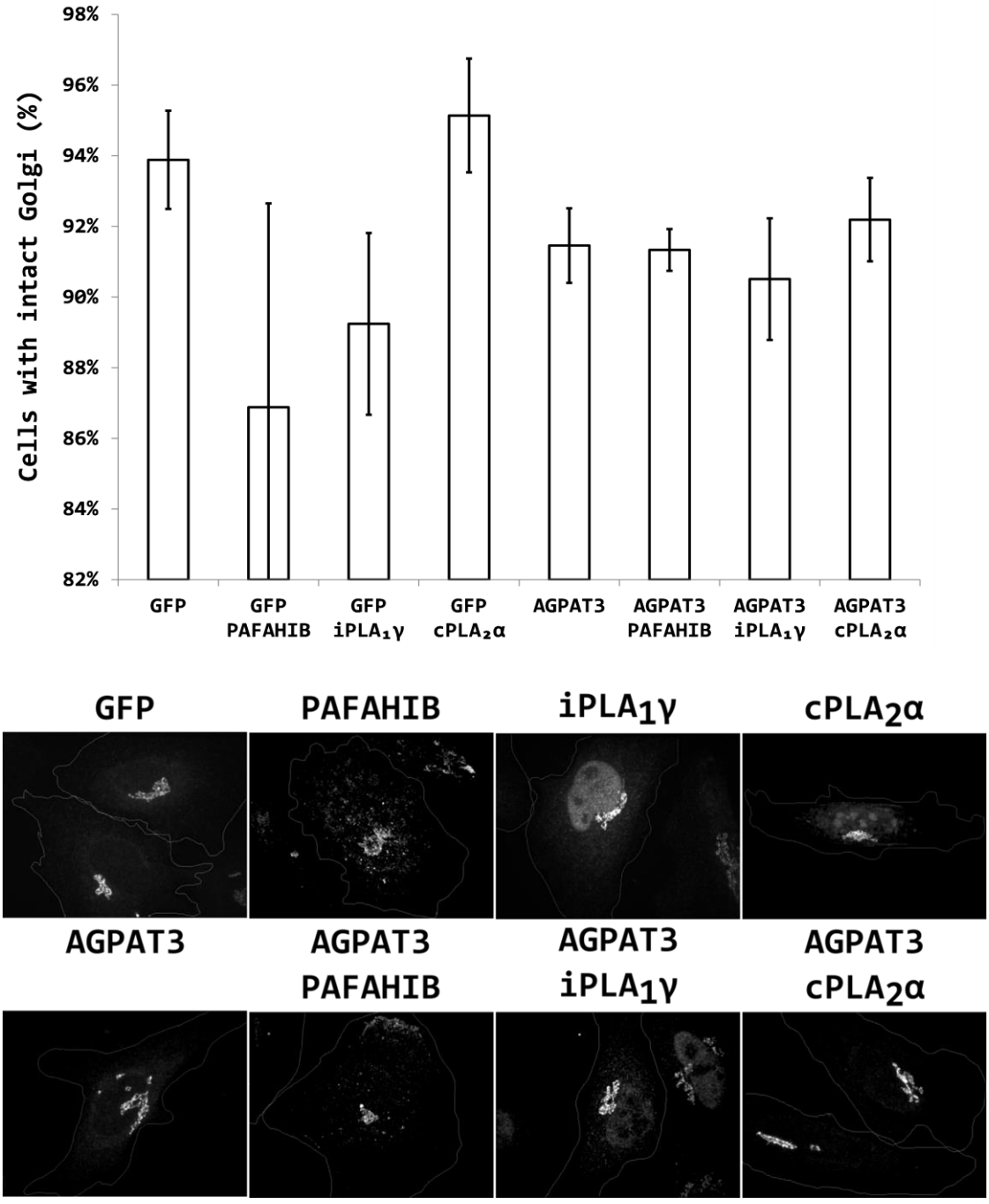

Figure 2-1. Steady state Golgi morphology

AGPAT3 and PLA overexpression did not significantly affect steady state Golgi morphology of HeLa cells. (n=3)

Co-overexpression of AGPAT3 and cPLA2α also accelerated Golgi reformation to a greater extent than does either enzyme alone.

A similar BFA washout experiment was performed in BTRD cells. BTRD cells, a bovine testicular cell line, were used due to their generally large and well-formed Golgi apparatus that undergoes dramatic tubulation events amenable to live cell microscopy. While the expression of AGPAT3 has not been experimentally confirmed for these cells, it should be noted that in one study of AGPAT3 expression in 18 tissues, the highest expression level was found in testicular tissue[239].

The Golgi reassembly experiment showed $cPLA_2\alpha$ was even more effective at accelerating Golgi reformation than it was in HeLa cells (Figure 2-3). AGPAT3 did not significantly accelerate Golgi reformation in BTRD cells, in contrast to the acceleration observed in HeLa cells. The combination of $cPLA_2\alpha$ and AGPAT3 had an intermediate phenotype to the individually expressed enzymes.

AGPAT3 and $cPLA_2\alpha$ do not "interact" in the regulation of Golgi recycling

Under normal conditions, the Golgi complex undergoes COPI vesicle and membrane tubule mediated retrograde trafficking, or recycling, to the ERGIC and ER. This process can be greatly exaggerated by treatment with BFA or CI-976, which allows for the measurement of recycling kinetics. AGPAT3 overexpressing HeLa cells have been shown to have slowed Golgi recycling to the ER[245]. It is possible that $cPLA_2\alpha$ could "interact" with AGPAT3 to perturb Golgi recycling. This possibility was tested in by inducing Golgi recycling using either BFA or CI-976 treatment of BTRD cells overexpressing AGPAT3 and $cPLA_2\alpha$.

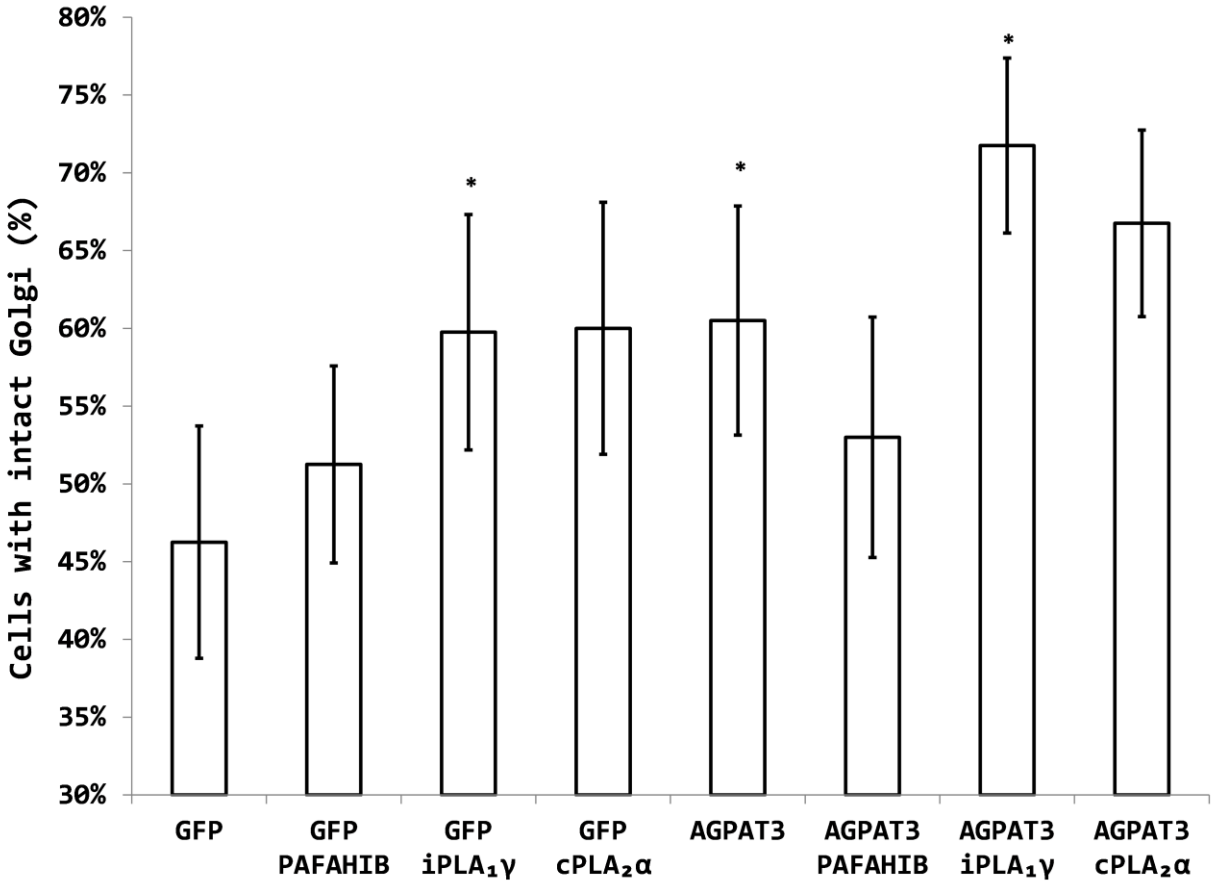

Figure 2-2. Golgi reassembly in HeLa cells during BFA washout

AGPAT3 and PLA overexpression accelerated Golgi reformation during BFA washout. HeLa cells were treated with BFA for 20 min, washed three times, fixed 1-2 h after washout, and stained for endogenous GPP130. GFP+iPLA$_1$γ, AGPAT3, and AGPAT3+iPLA$_1$γ have significantly more intact Golgi than control cells expressing GFP alone. (n=4, * $p<0.05$)

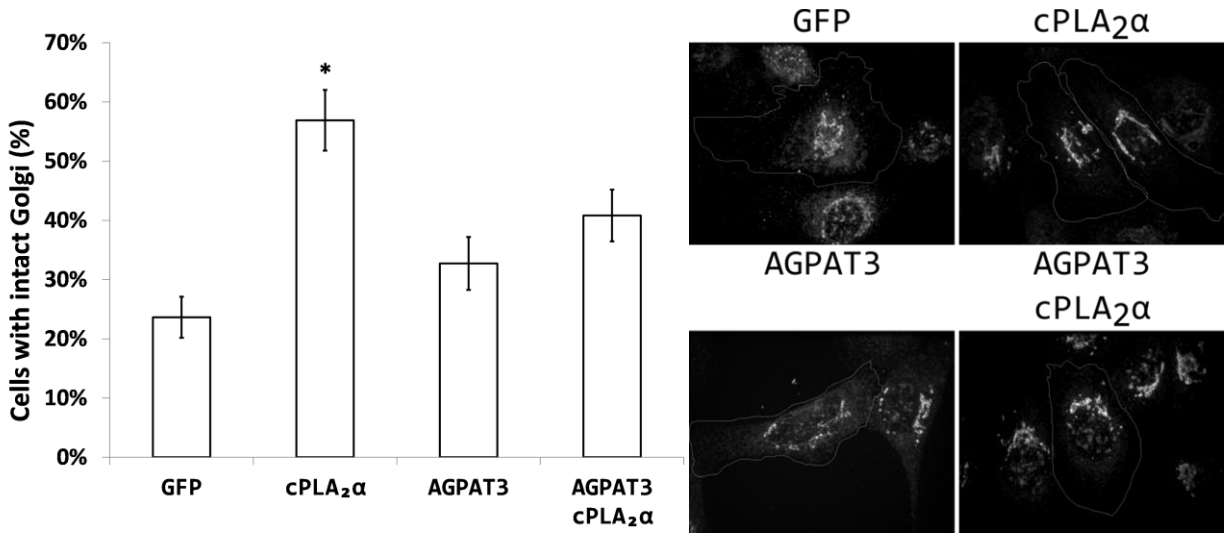

Figure 2-3. Golgi reassembly in BTRD cells during BFA washout

AGPAT3 and $cPLA_2\alpha$ overexpression accelerated Golgi reformation during BFA washout. BTRD cells were treated with BFA for 15 min, washed three times, and fixed 55 min after washout. The Golgi marker was endogenous GPP130. $cPLA_2\alpha$ significantly accelerated Golgi reformation. (n=5, * $p<0.05$)

BFA treatment of BTRD cells induced Golgi recycling to the ER over ~12 min (Figure 2-4). Golgi recycling kinetics were not significantly different in cells overexpressing AGPAT3, cPLA$_2$α, or both AGPAT3 and cPLA$_2$α.

CI-976 is a broad inhibitor of AGPAT activity that stimulates Golgi membrane tubulation and recycling to the ER[184]. Golgi recycling induced by CI-976 was slowed in cPLA$_2$α overexpressing cells (Figure 2-5). AGPAT3 overexpression did not affect CI-976 induced Golgi recycling rates and the co-overexpression of AGPAT3 and cPLA$_2$α had an intermediate phenotype.

Discussion

These experiments were performed in order to integrate AGPAT3 and PLA activity into a model of Golgi membrane dynamics and phospholipid remodeling. The results confirm that AGPAT3 and PLA activity is important for these processes and suggests synergy between AGPAT3 and iPLA$_1$γ to accelerate Golgi reformation. Evidence for antagonism between AGPAT3 and cPLA$_2$α activity was seen in Golgi reformation as well as Golgi recycling to the ER.

Steady state Golgi morphology

Golgi morphology was not grossly disrupted by the overexpression of AGPAT3 or the tested PLAs (Figure 2-1). Not surprisingly, co-overexpression of AGPAT3 and PLA enzymes also did not significantly alter Golgi morphology. The lack of effects could be due to various reasons including mechanisms to compensate for overexpression, inability to significantly change the lipid composition *in vivo*, or in the case of co-overexpression, compensatory increases in rivaling enzyme activities.

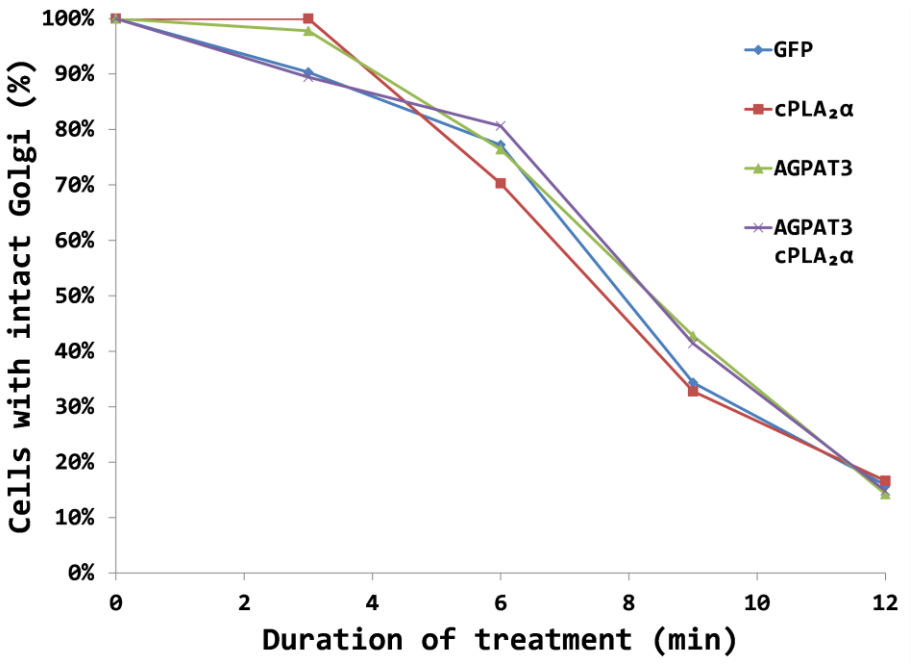

Figure 2-4. Golgi recycling during BFA treatment

BTRD cells were incubated with 2.5 µg/ml BFA and analyzed by anti-GPP130 IF for recycling to the ER. AGPAT3 and cPLA$_2$α overexpression did not affect Golgi recycling during BFA treatment. (n=3)

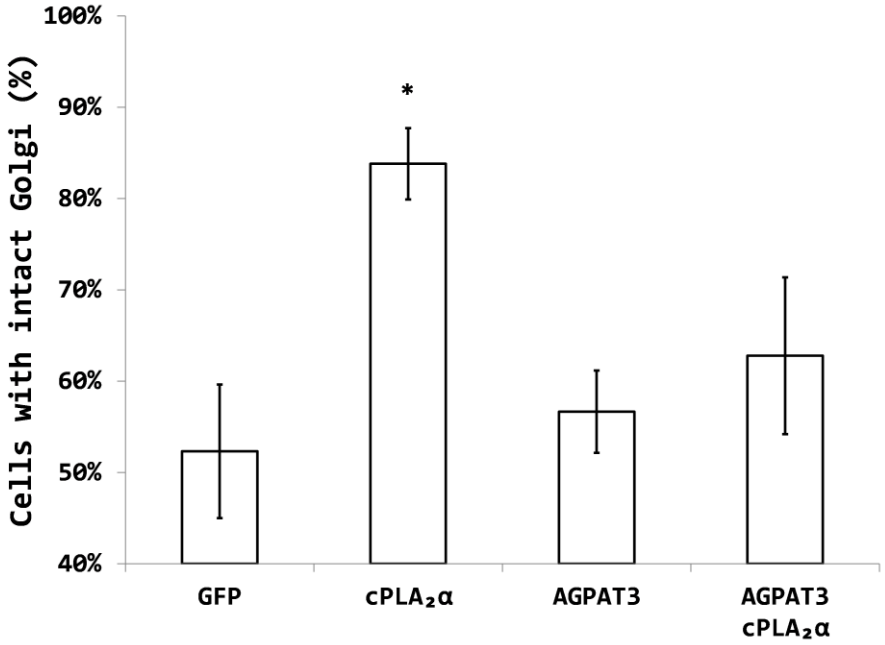

Figure 2-5. Golgi recycling during CI-976 treatment

BTRD cells were incubated with 50 μM CI-976 for 35-45 min and analyzed by anti-GPP130 IF for Golgi recycling to the ER. $cPLA_2\alpha$ overexpression significantly slows Golgi recycling. (n=3, * $p<0.05$)

Golgi reformation during BFA washout

Golgi reformation during BFA washout relies on COPII and COPI vesicle transport and membrane tubulation. During BFA treatment, COPI vesiculation is inhibited, which causes the Golgi complex to recycle to the ER and form a contiguous ER-ERGIC-Golgi membrane network. To a large extent, Golgi, ERGIC, and ER markers all partition within this membrane network. When BFA is washed out of the system, COPI budding is restored and membrane trafficking begins to return to normal. A combination of COPII and COPI budding from the ER-ERGIC-Golgi network eventually reestablishes independent Golgi, ERGIC, and ER compartments. The reforming Golgi is initially fragmented into 'mini-stacks' that then merge into a single network by the action of membrane tubule connections. Due to the influence of COPII, COPI, and membrane tubulation on Golgi reformation, this assay is excellent for identifying abnormalities in these processes. However, due to the confluence of processes in Golgi reformation, this assay is poorly suited to characterizing the molecular mechanisms of membrane trafficking.

AGPAT3 activity has been shown to promote COPI budding and decrease membrane tubule formation[73,245]. One would predict that AGPAT3 overexpression accelerates the COPI dependent formation of Golgi mini-stacks, but may slow the membrane tubule dependent interconnection of mini-stacks. $cPLA_2\alpha$ promotes Golgi membrane tubulation which is expected to be important for mini-stack interconnection. $iPLA_1\gamma$ overexpression has previously been shown to favor membrane tubulation, an activity that could accelerate the reconnection of Golgi mini-stacks[167].

The study of Golgi reformation following BFA washout in HeLa cells (Figure 2-2) showed that AGPAT3, iPLA$_1$γ, and cPLA$_2$α accelerated Golgi reformation. Co-overexpression of AGPAT3 with a PLA further accelerated Golgi reformation. These results are evidence that AGPAT3 and PLAs synergistically accelerate Golgi reformation.

When Golgi reassembly was examined in a different cell type, BTRD cells, cPLA$_2$α significantly accelerated Golgi reformation but AGPAT3 only very slightly accelerated reformation. In co-overexpressing cells, the phenotype was intermediate to that of separately overexpressing cells. BTRD cells are expected to have high AGPAT3 expression, therefore it is unclear what can be concluded from these results. One possible conclusion is that very high AGPAT3 activity is antagonistic of cPLA$_2$α activity during Golgi reformation.

To better understand the mechanisms that mediate synergistic and antagonistic relationships between AGPAT3 and PLA activity, more targeted assays are required. *In vitro* assays (COPI budding, COPII budding, Golgi tubulation) would be the most specific and are feasible using purified Golgi from overexpressing cells.

Golgi recycling to the ER

Golgi membranes recycle to the ER by COPI vesicles and membrane tubules. Treatment of cells with BFA or CI-976 induces extensive Golgi tubulation, decreases COPI vesiculation, and merges the Golgi with the ER.

To determine if AGPAT3 and cPLA$_2$α have synergistic or antagonistic effect on tubule mediated recycling of the Golgi to the ER, BTRD cells overexpressing these

enzymes were treated with either BFA or CI-976 and scored for Golgi disruption. No statistically significant differences were observed in BFA treated cells, contradicting a previously published report of slowed Golgi recycling in AGPAT3 overexpressing HeLa cells[245]. The small size of the BTRD data set my be preventing the observation of a weak inhibition of Golgi recycling, however it is possible that BTRD and HeLa cells have different characteristics in this assay.

The inhibition of LPAT activity by CI-976 treatment has a number of consequences on membrane trafficking, including halting COPII budding from the ER, COPI budding from the Golgi, and the induction of Golgi membrane tubulation, followed by eventual fusion of the Golgi with the ER.

It has been previously reported that cPLA$_2$α stabilized the Golgi by promoting the formation of intra-cisternal membrane tubules and that AGPAT3 increased Golgi stability by inhibiting the formation of CI-976 induced retrograde membrane tubules[73,245]. The CI-976 Golgi recycling experiment reported here supports these previous results. cPLA$_2$α stabilized the Golgi during CI-976 treatment and AGPAT3 overexpression slightly increased Golgi stability. Co-overexpression of AGPAT3 and cPLA$_2$α had an intermediate phenotype to separately overexpressing cells, indicating possible antagonism between their activities.

AGPAT3 and cPLA$_2$α activity was found to be antagonistic during CI-976 induced Golgi recycling and Golgi reformation following BFA washout. Immediately following the completion of these experiments, Victor Hsu and colleagues published a remarkably relevant report detailing antagonism between AGPAT3 and cPLA$_2$α activity[73]. They

showed that AGPAT3 and cPLA$_2$α colocalize at COPI budding sites, where AGPAT3 activity promotes vesiculation at the expense of membrane tubulation, while the opposite is true of cPLA$_2$α. Given this additional evidence, it is very likely that these enzymes have antagonistic activities that regulate Golgi membrane dynamics. One caveat to this model is that the experimental conditions under which antagonism is observed, expression/activity levels were altered. In untreated cells, balanced AGPAT3 and cPLA$_2$α activity could have a synergistic effect to promote efficient COPI vesiculation (Figure 1-7 E,F).

However, it has also been reported that cPLA$_2$α and AGPAT3 colocalize to COPI budding sites and where their activities may be either antagonistic or synergistic[73].

Further investigation of synergistic and antagonistic relationships between LPAT and phospholipase activity is likely to prove fruitful. However, there are a great number of possible combinations of LPATs and phospholipases; too large for an exhaustive screen. It may be better to search for interactions with a single LPAT (as done here) or phospholipase or to use broad specificity inhibitors.

CHAPTER THREE: Screening for the involvement of LPATs in membrane trafficking

Introduction

There are at least 15 enzymes from the AGPAT, MBOAT, and DGAT2 gene families that are suspected to have lysophospholipid acyltransferase activity[136,185]. Previous studies using chemical inhibitors (CI-976) have strongly suggested that multiple LPATs play roles in regulating intracellular membrane trafficking[181,183,255]. To determine which LPAT enzymes play a significant role in regulating membrane trafficking, I screened cells overexpressing a set of LPAT enzymes for changes in secretion. The secretion phenotype is an excellent measure of membrane trafficking disruption because secretory cargo transport starts in the ER and relies on the efficient function of several other organelles (ERGIC, Golgi, TGN) and trafficking intermediates (COPII, AP/clathrin coated vesicles). A defect at any of these steps would disrupt trafficking.

The screening assay measured the extracellular concentration of an overexpressed enzyme that was secreted by 'bulk flow', horseradish peroxidase (ssHRP/HRP) fused to the secretory signal sequence of human growth hormone. If the secretion of ssHRP was significantly altered by the co-overexpression of an LPAT enzyme, it suggests a significant alteration of the pathways responsible for the trafficking of soluble secreted cargo proteins. Due to the integrated nature of membrane trafficking, it is likely that disrupted secretion will be accompanied by the

alteration of other membrane trafficking pathways. One LPAT enzyme was selected for additional characterization, which will be the focus of Chapters 4 and 5.

Materials and methods

Plasmids

GFP-tagged AGPAT3 expression plasmid was constructed as previously described[245]. AGPAT4, AGPAT5, and AGPAT6 GFP tagged expression constructs were a kind gift from John Schmidt. AGPAT1, MBOAT1, MBOAT2, MBOAT7, LPCAT3, and LPCAT4 cDNAs were cloned into pEGFP-C2 (Clonetech) as described on Table 3-1.

Cell culture and HRP assay

HeLa cells were grown and maintained in MEM supplemented with 10% FBS and 1% penicillin/streptomycin at 37°C in 95% humidity and 5% CO_2. Cells were transfected in 35 mm^2 culture dishes using PEI from Polysciences Inc. according to the manufacturer's instructions. Transfection was performed using 2 µg DNA (1 µg of ssHRP and 1 µg of LPAT/GFP) and 5 µg PEI for the 24 h prior to experiments. To perform the HRP secretion assay, cells were washed three times in MEM without FBS and then incubated in MEM containing 3% FBS. Every hour for 5 h, 100 µl of media was removed and placed on ice. In a 96-well plate, 50 µl of TMB chromogenic reagent (Pierce) was added to duplicate 10 µl media samples, the reaction allowed to proceed until saturation, halted by the addition of 50 µl 1 M sulfuric acid, and absorbance measured at 450 nm. Error bars are SEM.

Table 3-1. Plasmid construction

Gene	Sequence	Supplier	Sense	Primer	Restriction Enzymes
AGPAT1	BC090849	Open Biosystems	5'	GGATGAATTCATGGATTTGTGGCCAGGG	EcoRI-KpnI
			3'	GGTAGGTACCTTATCCCCCAGGCTTCTTCAGA	
MBOAT1	BC150652	Life Technologies	5'	GGATAGATCTCGATGGCAGCAGAGCCAC	BglII-BamHI
			3'	CCTAGGATCCCTTAGTCGGTCTTCCTCTTGTTGATAG	
MBOAT2	BC016005	Open Biosystems	5'	GGATAGATCTCGATGGCCACCACCAGCA	BglII-KpnI
			3'	GGTAGGTACCTTACTGCTTTAGTGATGAATGTCTCGA	
MBOAT7	BC003164	Open Biosystems	5'	GGATGAATTCATGTCGCCTGAAGAATGGAC	EcoRI-BamHI
			3'	CCTAGGATCCCTTACTCCTCCCGGAGCTTCT	
LPCAT3	BC065194	Open Biosystems	5'	GGTAGGTACCGCATGGCGTCCTCAGCGG	KpnI-BamHI
			3'	CCTAGGATCCCTTATTCCATCTTCTTTAACTTCTCTTTCCTT	
LPCAT4	BC092463	Open Biosystems	5'	GGATGAATTCATGAGCCAGGGAAGTCCG	EcoRI-KpnI
			3'	GGTAGGTACCTTAGTCTCCCTTCTGCTTGGG	

Fluorescence microscopy

Cells were grown on glass coverslips and fixed with 3.7% formaldehyde in PBS, washed 3 times in PBS, and mounted on glass slides with VectaShield (Vector Laboratories). Cells were viewed and imaged using a Perkin-Elmer Ultraview spinning disk confocal microscope at 100X. Image analysis was performed using the ImageJ software package (NIH, Bethesda, MD) or the FIJI distribution of ImageJ[254].

Phylogenetic tree

Consensus coding sequences from NCBI's CCDS database were aligned using Clustal Omega with default parameters[256,257]. The resulting guide tree was plotted with the PHYLIP 3.67 drawgram tool[258].

Results

LPAT intracellular localization

The enzymes tested were taken from the AGPAT and MBOAT gene families so as to obtain at least one representative LPAT from each major branch of the AGPAT phylogenetic tree and all suspected MBOAT LPATs (Figure 3-1). N-terminal GFP fusion constructs were overexpressed in HeLa cells and analyzed by fluorescent microscopy to determine localization (Figure 3-2). All LPATs exhibited a similar, primarily ER localization; colocalization with ER markers was confirmed for LPCAT3 (Figure 3-3)[259]. AGPAT3 partially localized to the Golgi complex, as previously reported by Schmidt *et al.*[245]. In addition, AGPAT1, AGPAT6, MBOAT1, MBOAT7, and LPCAT3 showed a propensity to form large puncta or karmellae-like structures (Figure 3-2 and Figure 3-3). Karmellae are poorly understood ER structures consisting of closely

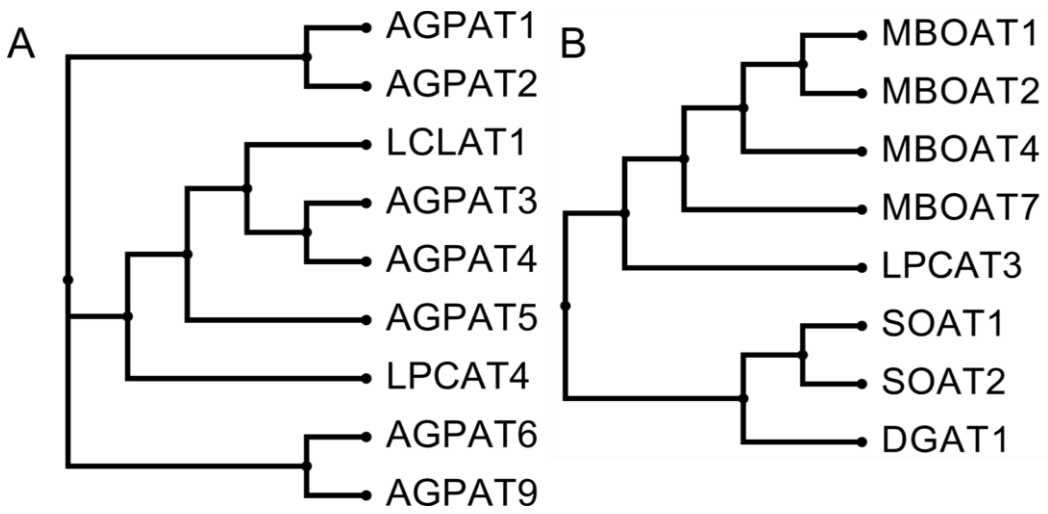

Figure 3-1. LPAT phylogenetic trees

A) Phylogenetic tree of selected human AGPAT family enzymes. B) Phylogenetic tree of human MBOAT family enzymes.

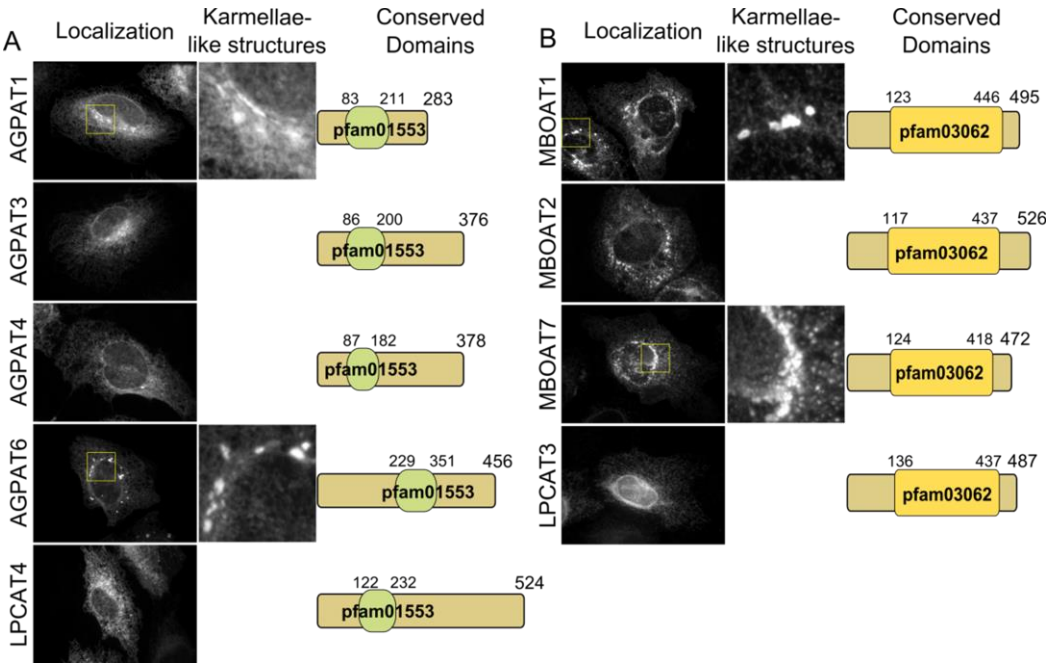

Figure 3-2. LPAT overexpression

A) Localization, karmellae-like structures, and conserved domains of tested AGPAT enzymes. The green box indicates the location of the conserved acyltransferase domain (pfam01553 as per the NCBI's Conserved Domain Database). B) Localization, karmellae-like structures, and conserved domains of tested MBOAT enzymes. The yellow box indicates the conserved MBOAT domain (pfam03062).

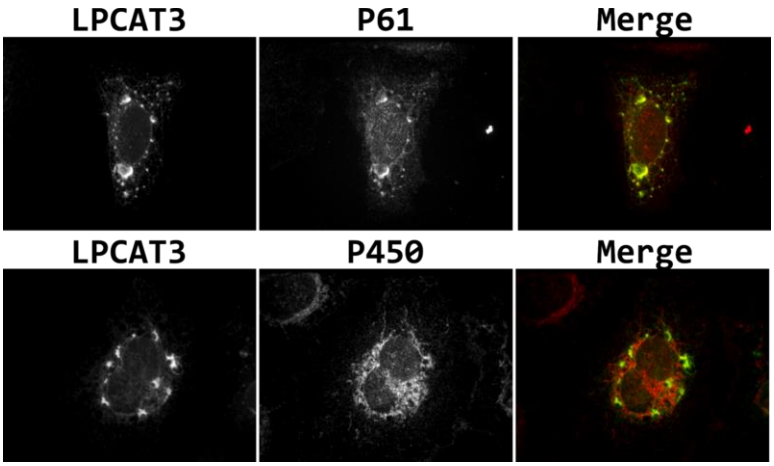

Figure 3-3. ER localization of LPCAT3

Overexpressed GFP-LPCAT3 colocalizes with endogenous p61 and P450. Note that p61, a chaperone that participates in disulfide bond formation[259], colocalizes with LPCAT3 in karmellae-like structures, while P450 does not.

opposed membrane stacks or whorls. Their biogenesis is not an uncommon response to the overexpression of transmembrane proteins and they are not inherently detrimental to the cell[260].

LPAT overexpression alters secretion

The effect of LPAT co-overexpression on ssHRP secretion varied widely between LPAT isoforms (Figure 3-4). The greatest reduction was seen in the MBOAT7 overexpression condition (7% of control). Overexpression of AGPAT1, AGPAT3, AGPAT4, MBOAT1, and LPCAT3 significantly reduced ssHRP secretion by very similar amounts, to between 20-30% of control. In notable contrast to these LPATs, overexpression of AGPAT5 significantly increased the amount of ssHRP secretion. Finally, overexpression of AGPAT6, MBOAT2, and LPCAT4 had no appreciable effect on ssHRP secretion. These changes were independent of expression levels, as determined by western blotting against GFP (data not shown).

Discussion

Except in one case, AGPAT5, it appears that LPAT overexpression slows ssHRP secretion. LPAT enzymes are generally ER localized and may regulate ER export directly. However, their phospholipid products are mobile and may disrupt secretion at any point along the secretory system. Mechanisms by which LPATs and lipid remodeling could inhibit secretion are discussed in the following contexts: perturbation of lipid homeostasis, disruption of COPII function, and induction of the UPR.

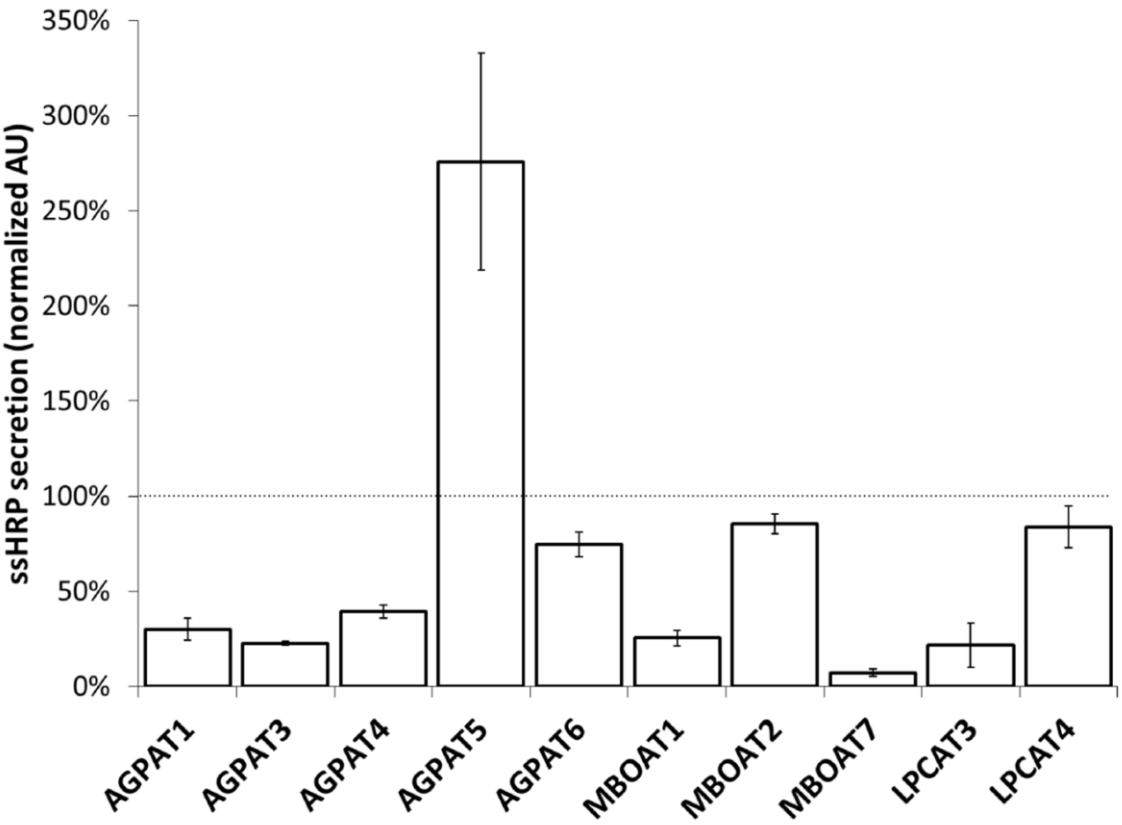

Figure 3-4. HRP secretion as affected by LPAT co-overexpression

ssHRP and an LPAT were co-overexpressed for 5 h and the media tested for HRP activity. Values are normalized to an ssHRP and GFP co-overexpressing condition. (n=3)

Lipid imbalance

The primary function of LPAT enzymes is to remodel membrane lysophospholipids into phospholipids. To delineate the possible consequences of LPAT activity on ssHRP secretion, the substrate specificity of the tested enzymes will be discussed. For additional isoform specific details, please see the accompanying references.

First, consider the enzymes that acylate LPA to form PA. These are AGPAT1[223], AGPAT3[73,245,248], AGPAT4[238,239,261], and AGPAT5[238,239], which altered HRP secretion to 30%, 23%, 39%, and 276% of control, respectively. Due to PA's small head group, negative charge, and strong interactions with Ca^{2+}, it can induce dramatic changes in membrane structure that are important for some fission and fusion events[262–265]. PA can also recruit secondary effector proteins to facilitate membrane trafficking events[266–268]. However, it is possible that these PA-dependent membrane trafficking mechanisms are not important at the ER, at least under normal conditions. PA concentrations in the ER are kept very low due to rapid metabolism by enzymes of the Kennedy pathway to DAG, PC, and PE[177,269,270]. While overexpression of PA synthesizing LPATs may have elevated PA concentrations sufficiently to directly regulate membrane trafficking, it is just as likely that secretory defects were due to the increased synthesis of PA-derived lipids. Note that AGPAT5, unlike any other LPAT that was tested, is involved in mitochondrial lipid synthesis and localizes to a specialized ER domain called the mitochondrial-associated membrane[264,268,271,272]. The increased secretion of AGPAT5

overexpressing cells may be related to increased mitochondrial health and energy generation.

AGPAT6 is an ER localized GPAT that catalyzes the addition of saturated and unsaturated acyl-CoA to glycerol 3-phosphate to produce LPA. Its activity is important for triglyceride metabolism but has little effect on membrane phospholipid composition or membrane trafficking[218–222]. These previous reports are in agreement with the observation that APGAT6 overexpression did not dramatically alter HRP secretion (74% of control).

MBOAT1 strongly reduced HRP secretion. It is an ER localized LPAT that prefers acylating LPS and LPE with oleoyl-CoA[199,261]. As the most abundant anionic phospholipid in mammalian cells, PS has important roles in membrane trafficking[273]. PS localization is the most asymmetric of all phospholipids; it is present on the luminal side of the ER and Golgi as well as the cytosolic side of the *trans*-Golgi network, endosomes, and plasma membrane[274]. PS mediates the localization and activity of a variety of proteins, among them protein kinase C, synaptotagmin, Ras and Rho-family GTPases and Cdc42[16,275,276]. PS has been shown to be essential for retrograde trafficking through recycling endosomes/early endosomes[277]. It is possible that an overabundance of PS could disrupt the localization and activity of enzymes that interact with PS. For instance, there are two classes of TGN derived secretory vesicles 1) a clathrin-coated vesicle that is enriched in PS and 2) a vesicle that is poor in PS and clathrin. Increased PS concentrations could enrich the population of clathrin-coated vesicles at the expense of other anterograde vesicles[278].

MBOAT2 and LPCAT4 have very similar substrate specificities and effects on HRP secretion; both enzymes prefer to acylate LPE and decreased HRP secretion to 85% and 84% of control, respectively[199,227,261,279].

MBOAT7 overexpression decreased ssHRP secretion to a greater extent than did any other LPAT. MBOAT7 is a LPI acyltransferase with incredible specificity to AA acyl-CoA donors, though a mouse knockout model suggests MBOAT7 may also possess LPC and LPE acyltransferase activity[199,201,280]. In mammals, the majority of PI contains polyunsaturated acyl chains (AA, linoleic acid, etc.) at the *sn*-2 position and it is suspected that MBOAT7 is responsible for most of their synthesis[201,281]. PI is a precursor to the synthesis of phosphatidylinositol phosphates (PIPs), a class of lipids that are incredibly important for the regulation of membrane trafficking. It is likely that overexpression of MBOAT7 increases the concentration of PI, which may lead to increased synthesis of phosphatidylinositol phosphate (PIP) species. PIP regulated enzymes are too numerous to describe here, but their misregulation would invariably cause membrane trafficking defects. For a detailed discussion of the biology of PI, PIPs, and their acyl chains, please see D'Souza and Epand's recent review[282].

LPCAT3 overexpression strongly inhibited ssHRP secretion. A detailed discussion of LPCAT3 lipid remodeling and its effects on membrane trafficking is reserved for Chapter 5.

Disruption of COPII trafficking

ER export of soluble proteins, such as ssHRP, is dependent on efficient cargo loading, budding, and scission of COPII vesicles from ERES. LPAT enzyme

overexpression could, by direct interaction or through lipid remodeling, disrupt the localization of components that are critical for efficient COPII vesicle formation. For example, the LPAT inhibitor CI-976 inhibits a late stage in the formation of COPII coated vesicles[183]. LPAT overexpression sometimes leads to karmellae formation, though the mechanisms and physiological implications of karmellae formation are not well understood, their presence indicates abnormal ER membrane dynamics and possible disruption of COPII functions[283].

Unfolded protein response

The overexpression of transmembrane and soluble secreted proteins places increased biosynthetic load on the ER that can induce the UPR. The UPR copes with increased biosynthetic load by producing additional protein folding chaperones, increasing the degradation of misfolded proteins, and decreasing the rate of protein translation[284]. These three mechanisms all act in the short-term to decrease secretory throughput. Over longer periods of time (days to weeks), these and other slow responses to ER stress lead to cell adaption and increased tolerance to secretory load[285]. In the context of this secretory assay, UPR induction would dramatically decrease HRP synthesis and the rate of HRP's secretory processing.

The overexpression of any transmembrane protein can induce the UPR, but the LPAT enzymes used in this screen are multi-span and have non-native GFP fusions; this makes misfolding not unlikely. The UPR can also be induced by perturbation of membrane lipid composition due to LPAT activity[286]. It has been reported that LPCAT3

knockdown, in combination with other stressors, leads to lipid imbalance and UPR induction[287].

To determine if the UPR plays a role in LPAT mediated inhibition of secretion, it would be necessary to characterize the UPR state of LPAT overexpressing cells. If the UPR is activated by LPAT overexpression, future experiments should investigate lowering LPAT expression levels, expressing untagged LPAT enzymes that may have a lower tendency to misfold, treatment with UPR antagonists, and the selection of a cell line with more robust secretory activity.

In selecting a LPAT from this screen for further study, I considered several criteria. First, as a member of the AGPAT family had been extensively characterized by John Schmidt, a selection from the unstudied MBOAT family of enzymes was preferred. This left MBOAT1, MBOAT7, and LPCAT3 as potential candidates with strong inhibition of HRP secretion. MBOAT7 is a LPI specific acyl transferase and as the biology of PI and PIPs has been extensively studied in other contexts, MBOAT1 or LPCAT3 was preferred. The mechanism by which MBOAT proteins are localized to the ER was unknown. LPCAT3 possesses an unconfirmed but canonical ER retention motif in its C-terminus, while MBOAT1 does not. LPCAT3 is also reported to be involved in the fascinating Lands cycle process of maintaining the asymmetry of saturated and unsaturated acyl chains between the *sn*-1 and *sn*-2 positions of phospholipids[261]. Therefore, LPCAT3 was selected for further study. The characterization of LPCAT3's predicted ER retention motif and transmembrane topological orientation will be the topic

of Chapter 4. The role of LPCAT3 in regulating membrane trafficking will be the topic of Chapter 5.

CHAPTER FOUR: LPCAT3 transmembrane topology

Introduction

Human LPCAT3 is a multi-span transmembrane protein of 487 amino acids. LPCAT3 has a conserved MBOAT domain (pfam03062 in the NCBI's Conserved Domain Database)[288]. An accurate model for the topological orientation of MBOAT enzymes is important for understanding their function, particularly in regards to the availability of substrates at the active site and the location of enzymatic products. The transmembrane topologies of human MBOAT family members SOAT1, SOAT2, and DGAT1 have been extensively investigated, likely due to the importance of these enzymes in cardiovascular disease [289–293]. However, these enzymes are not LPATs and are evolutionarily divergent from the human MBOAT LPATs (MBOAT1, MBOAT2, MBOAT7, and LPCAT3).

The only LPAT with an MBOAT domain that has had its transmembrane topology experimentally determined is the yeast protein Ale1[294]. Pagac *et al.* examined the Ale1 active site topology by constructing Ale1-SUC2-HIS4C chimeras. Chimeras were constructed by C-terminal truncation and fusion to a dual topology reporter, SUC2-HIS4C. These studies determined that the active site histidine residue is oriented toward the lumen (Figure 4-1).

LPCAT3 has a C-terminal amino acid sequence, KKME, that matches the K(x)KXX dilysine motif, an ER localization signal[261,295]. This C-terminal amino acid conservation within the human MBOAT gene family is highlighted in Figure 4-2. In some cases, substitution of positively charged (arginine or histidine) residues

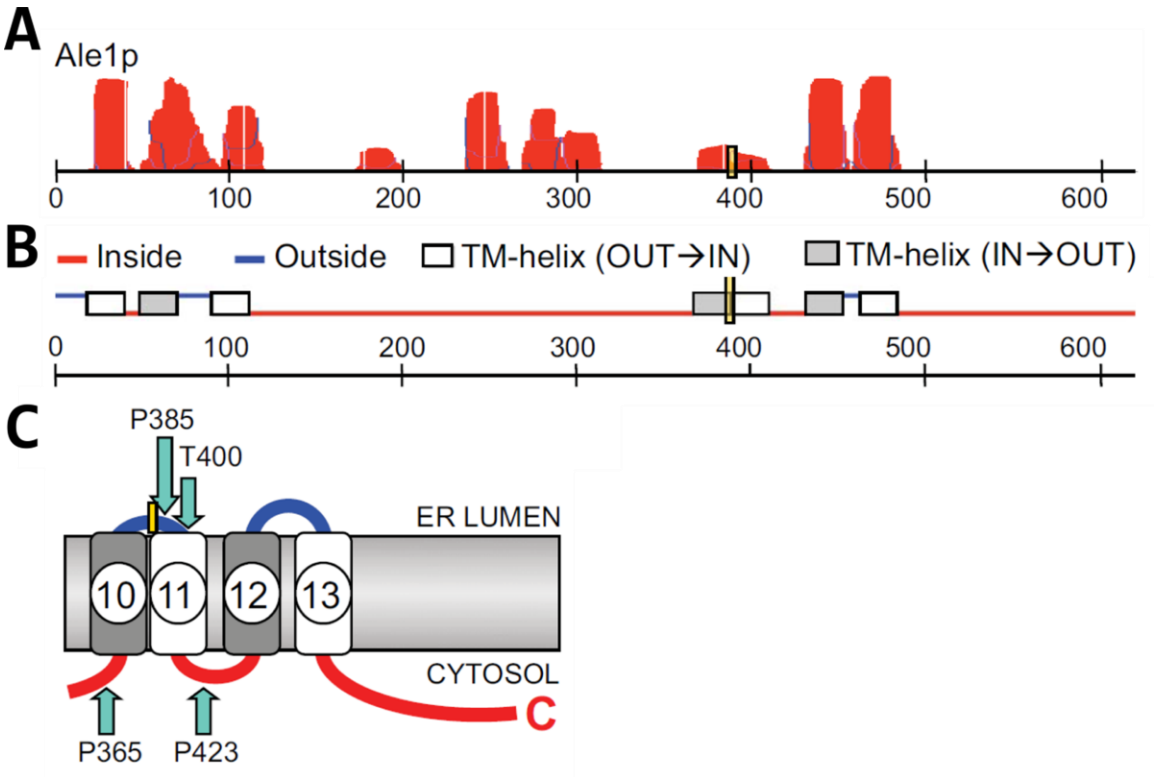

Figure 4-1. Topology of the yeast MBOAT Ale1

A) Transmembrane domain probability as predicted by TMHMM, B) transmembrane domains predicted by TOPCONS global alignment algorithm, and C) active site topology as inferred by EndoH band shift and histidine auxotrophy of yeast expressing four Ale1-SUC2-HIS4C variants. Arrows indicate sites of C-terminal truncation and SUC2-HIS4C fusion. Adapted from Pagac *et al*[294].

LPCAT3	Leu **Lys** **Lys** Met Glu
MBOAT1	**Lys** Arg **Lys** Tyr Asp
MBOAT2	His Ser Ser Leu Lys
MBOAT4	**Lys** His **Lys** Cys Asn
MBOAT7	**Lys** Leu **Arg** Glu Glu

Figure 4-2. C-terminal sequence of MBOAT family LPATs

LPCAT3, MBOAT1, and MBOAT4 have two lysines in their C-terminus conforming to the K(x)KXX ER localization motif. The C-terminus of MBOAT7 contains a lysine and a positively charged arginine.

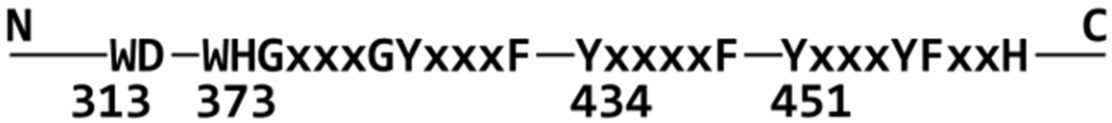

Figure 4-3. MBOAT motifs essential for activity

The residues of LPCAT3 that are essential for enzymatic activity, as shown by alanine replacement mutagenesis, Chinese hamster ovary cell overexpression, microsomal purification and *in vitro* lipase assay. Adapted from Shindou *et al*[298].

for lysine is a conservative mutation that maintains the ER localization activity of K(x)KXX motifs[296,297].

Mutagenesis studies of LPCAT3 by Shindou *et al* have identified several residues (motifs) that are important for LPCAT3 enzymatic activity[298]. Histidine 374 is very likely the catalytic amino acid as it is the best conserved amino acid of the MBOAT domain and its mutation abolishes catalytic activity in LPCAT3 and other MBOAT LPATs[281,290,298–303]. Other important LPCAT3 motifs have been identified by Shindou *et al.* and are diagramed in Figure 4-3. Depending on their topology, the motifs at amino acids 313, 434, and 451 could mediate LPCAT3 interaction with cytosolic acyl-CoA and alignment into the active site.

Materials and methods

Plasmids

cDNA for LPCAT3 was obtained from OpenBiosystems (BC065194). N-terminal HA, internal HA, and C-terminal myc tags were added to LPCAT3 by PCR extension and the coding sequence inserted into a pEGFP-N1 (Clontech) vector from which the EGFP coding sequence had been excised. PCR extension of all LPCAT3 variants with internal HA epitopes used GGTAGGTACCGACCATGGCGTCCTCAGCGG as the forward primer and GGAAAGAGAAGTTAAAGAAGATGGAATAAGGATCCAAAG as the reverse primer. Additional primers for the construction of HA epitope tagged LPCAT3 are detailed in Table 4-1. HA-LPCAT3(AAME) was constructed with the following reverse primer:

TGGTGCCAAGGAAAGAGAAGTTAGCAGCAATGGAATAAGGATCCGGCG.

Table 4-1. Oligonucleotide primer sequences

HA epitope site	Priming Direction	Primer sequence (sense)
N-terminus	Forward	CCGTATGATGTGCCAGATTATGCGATGGCGTCCTCAGCGG
		AACTCGAGAACCATGTATCCGTATGATGTGCCAGATTATG
		GAAACTCGAGAACCATGTATCCG
	Reverse	GGAAAGAGAAGTTAAAGAAGATGGAATAAGGATCCAAAG
135	Forward	CCTTATGATGTGCCAGATTATGCAAACTACGATATCAAGTGGACAATG
	Reverse	TATTACACTGCCACCGGCTATCCTTATGATGTGCCAGATTATGCA
167	Forward	TATCCTTATGATGTGCCAGATTATGCATCCTTGTCCTCTGAGCAACA
	Reverse	TGACGGAGGGAAAGATCAGAATTATCCTTATGATGTGCCAGATTATGCA
218	Forward	GTGCCAGATTATGCAATACCAGGAAAGATACCAAACAGC
		TATCCTTATGATGTGCCAGATTATGCAATACCAGG
	Reverse	GCAGGGAGAGCTGATTGACTATCCTTATGATGTGCCAGATTATGCA
260	Forward	TATCCTTATGATGTGCCAGATTATGCATATGACAACCACCCCTTCTGG
	Reverse	AGAAGACTATCTCCTCACTGAAGACTATCCTTATGAT
		CTCCTCACTGAAGACTATCCTTATGATGTGCCAGATTATGCA
303	Forward	TATCCTTATGATGTGCCAGATTATGCAGGCTTTGAAGAAAAGGGCAAG
	Reverse	GGGCCTGGGCTTCAATTATCCTTATGATGTGCCAGATTATGCA
358	Forward	CATATCCGTATGATGTGCCACTGCTCAGCCCCCACA
	Reverse	TCTACCTAGTGGGCTACACATATCCGTATGATGTGCCACT
375	Forward	TATCCGTATGATGTGCCAGATTATGCGGGCCTGCACTCAGGAT
	Reverse	CCTGGCCCTCTGGCACTATCCGTATGATGTGCCAGATTATGCG
402	Forward	TATCCTTATGATGTGCCAGATTATGCAGAGAGCCCCACCCTGA
	Reverse	GCTGCCAGGCTCATTCAATATCCTTATGATGTGCCAGATTATGCA
445	Forward	CCAGATTATGCAAAATGGCTTAAGGTGTATAAATCCATCT
		TATCCTTATGATGTGCCAGATTATGCAAAATGGCTTAAGG
	Reverse	GCCTCTTCACGTGGGACTATCCTTATGATGTGCCAGATTATGCA

LPCAT3-myc was constructed with the following reverse primers: TCGCTGATGAGTTTTTGTTCTTCCATCTTCTTTAACTTCTCTTTCCTTG and CAAAGCGGCCGCTTATAAATCTTCTTCGCTGATGAGTTTTTGTTCTTCC.

Cell culture

HeLa cells were grown and maintained in MEM supplemented with 10% FBS and 1% penicillin/streptomycin at 37°C in 95% humidity and 5% CO_2 environment. Cells were transfected in 35 mm^2 culture dishes using PEI from Polysciences Inc. according to the manufacturer's instructions. DNA transfection was performed using 1 µg DNA/5 µg PEI for the 24 h prior to experiments.

IF microscopy

Cells were grown on glass coverslips and fixed with 3.7% formaldehyde in PBS, washed 3 times in PBS, and permeabilized with 0.1% Triton X-100 in PBS or digitonin solution (3 µg/ml digitonin, 0.3 M sucrose, 5 mM $MgCl_2$, 120 mM KCl, 0.14 mM $CaCl_2$, 2 mM EGTA, 25 mM HEPES pH to 7.6 with KOH). Cells were incubated with primary antibodies for 1 h at room temperature using the manufacturer's recommended dilution, washed 3 times, treated identically with secondary antibodies, and mounted on glass slides with VectaShield (Vector Laboratories). Cells were viewed and imaged using a Perkin-Elmer Ultraview spinning disk confocal microscope at 100X. Image analysis was performed using the ImageJ software package (NIH, Bethesda, MD) or the FIJI distribution of ImageJ[254]. To calculate Pearson's correlation coefficient for K(x)KXX colocalization experiments, a threshold was applied to the GPP130 channel, the mask smoothed, enlarged by 2 pixels, and converted to a selection. Selection was applied as

a region of interest (ROI) for Pearson's correlation calculation using the "Colocalization Threshold" tool. Error bars are SEM. Significance determined by paired Student's t-test.

Computational methods

The TMHMM Server v. 2.0 (http://www.cbs.dtu.dk/services/TMHMM/) and TOPCONS server (http://topcons.cbr.su.se/) with the default settings were used to predict LPCAT3 membrane topology[304,305]. The second prediction provided by the TOPCONS server (Figure 4-8) was performed with the following restrainment parameters: "1-1-o;487-487-i;135-135-o;167-167-i;218-218-i;260-260-o;303-303-i;402-402-i;445-445-o;". Amino acid conservation, protein sequence alignment, and phylogenetic relationships were determined using the Conserved Domain Database, Clustal Omega, and the PHYLIP package[257,258,288]. Glycosylation prediction performed by the NetNGlyc (http://www.cbs.dtu.dk/services/NetNGlyc/) and NetOGlyc (http://www.cbs.dtu.dk/services/netoglyc/) servers[306,307].

Results

Computational prediction of LPCAT3 transmembrane domain orientation and glycosylation

TMHMM is a transmembrane prediction algorithm that models helix length, hydrophobicity, charge bias, and the alternation of cytoplasmic and luminal loops. It has been shown to correctly predict the transmembrane topology of approximately 77% of membrane proteins and has been applied to the identification of membrane proteins in a large collection of genomes[304]. It predicted that LPCAT3 has seven transmembrane

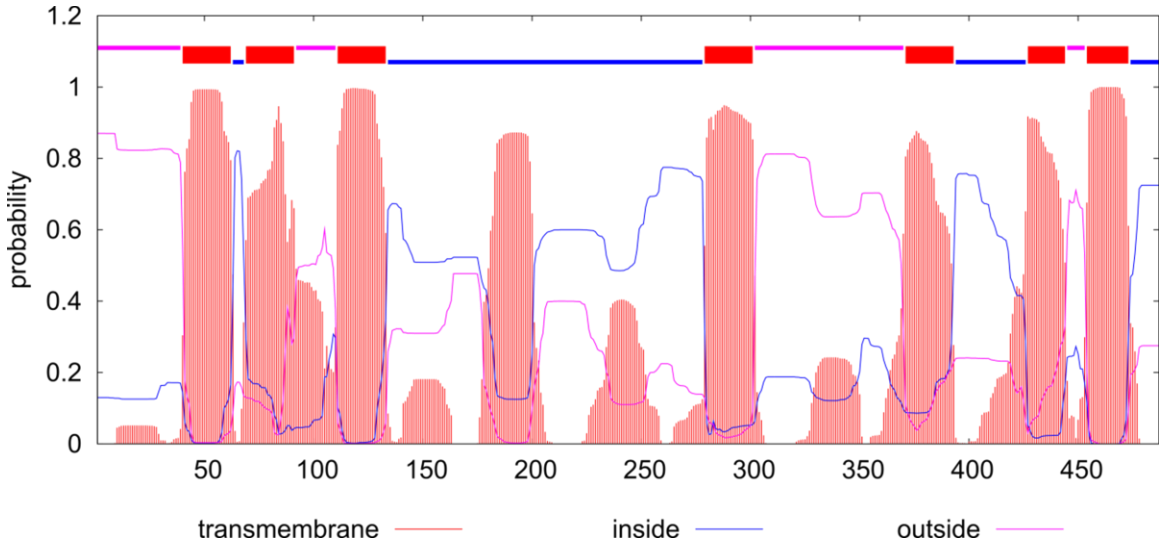

Figure 4-4. TMHMM predicted transmembrane domains of LPCAT3

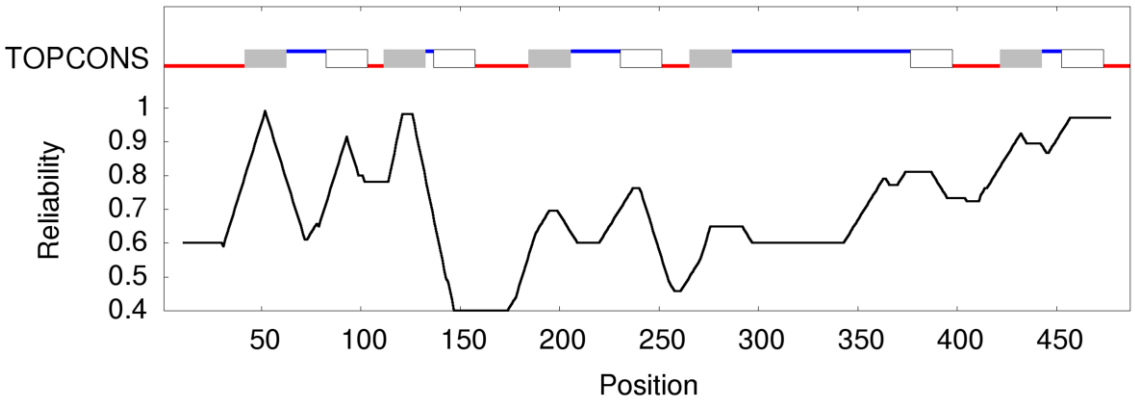

Figure 4-5. TOPCONS predicted transmembrane domains of LPCAT3

Blue: lumen, red: cytoplasm.

domains, a luminal N-terminus, a cytoplasmic C-terminus, and a luminal active site (Figure 4-4).

The TOPCONS topology prediction server combines the predictions of five topology prediction algorithms into a consensus prediction and quantifies the reliability of the prediction based on the degree of consensus. The prediction can also be restrained by experimentally determined cytoplasmic and luminal loops. A naïve prediction by the TOPCONS server showed 10 transmembrane domains, a luminal N-terminus, luminal active site and cytoplasmic C-terminus (Figure 4-5).

O-linked glycosylation takes place at serine and threonine sites in regions that are enriched in serine, threonine, proline, and alanine[308]. N-terminal glycosylation is known to be important for the proper function and membrane trafficking of some transmembrane proteins. For instance, a mutation within the human potassium ion channel subunit KCNE1 that eliminates N-terminal glycosylation has been identified as causing long QT syndrome, a form of congenital heart disease[309]. Glycosylation can only happen within the lumen of the ER and would stabilize the topological orientation of the glycosylation site within the ER. The NetNGlyc and NetOGlyc glycosylation site prediction servers identified serine 3 and serine 4 as potential LPCAT3 N-linked glycosylation sites (no O-linked glycosylation sites were predicted)[306,307]. Mammalian LPCAT3 homologues have a conserved serine/threonine residue in an alanine rich region of the N-terminus (Figure 4-6). If these sites are glycosylated in the lumen of the ER, it would stabilize the topological orientation of their N-termini.

H. sapiens	Met Ala **Ser Ser** Ala Glu
M. musculus	Met Ala **Ser Thr** Ala Asp
B. taurus	Met Ala **Ser** Ala Ala Glu
C. lupus	Met Ala **Ser** Ala Ala Glu

Figure 4-6. N-terminal sequences of mammalian LPCAT3 homologues show conservation of potential O-linked glycosylation site

LPCAT3 from humans, mouse, cow, and dog have a conserved serine/threonine within an alanine rich region. This motif is predicted to be an O-linked glycosylation site.

Selective permeabilization reveals topological orientation of LPCAT3

The topology model of Ale1 reported by Pagac *et al.* predicts a catalytic histidine in the lumen of the ER but provides no information concerning the topology of most extra-membrane loops[294]. To more completely map LPCAT3 transmembrane domain topology, HA epitope tags were inserted by mutagenesis into 10 predicted loop regions. The selection of epitope tag insertion sites was guided by a previously published predicted topology, the Ale1 topology studies of Pagac *et al*., the computer generated topology predictions shown above, and amino acid conservation estimates[294,310]. Epitopes were inserted into predicted extra membrane loops with preference to regions of low amino acid conservation.

The topological orientation of each epitope was probed by IF in combination with selective membrane permeabilization, as described by Hailey *et al.*[311]. Cells transfected with epitope tagged LPCAT3 were permeabilized by treatment with either Triton X-100 or digitonin. Triton X-100 permeabilizes all cellular membranes and will expose every epitope for antibody binding. Digitonin, at the concentration used, permeabilizes only the plasma membrane while leaving intracellular membranes intact. Thus, only epitopes exposed on the cytoplasmic side of intracellular membranes, but not luminal ones, will be available for antibody binding. In addition to antibodies targeting the HA epitope, cells were probed with a rabbit polyclonal that had been raised against a synthetic peptide corresponding to the C-terminus of LPCAT3.

HA epitopes inserted after amino acids 167, 218, 303, 375, and 402 showed reticular ER staining using both Triton and digitonin permeabilization, indicating that they face the cytoplasm (Figure 4-7). HA epitopes inserted at the N-terminus and after

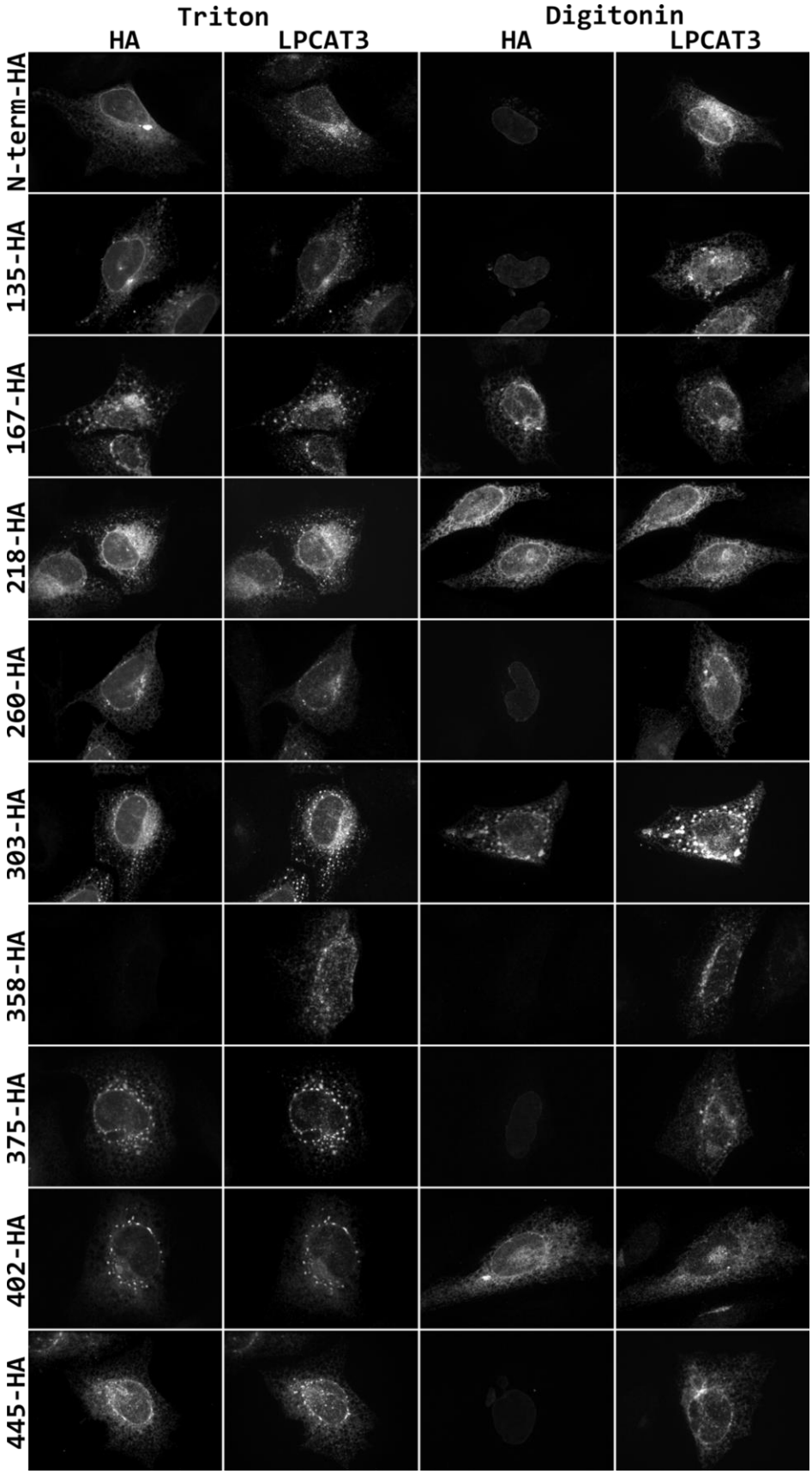
Triton
Digitonin
HA
LPCAT3
HA
LPCAT3
N-term-HA
135-HA
167-HA
218-HA
260-HA
303-HA
358-HA
375-HA
402-HA
445-HA

Figure 4-7. Selective permeabilization reveals the topological orientation of LPCAT3

The two leftmost columns show LPCAT3 IF using Triton-100 permeabilization. The two rightmost columns were cells permeabilized using digitonin. Cells were simultaneously probed by antibodies against both the HA epitope and the C-terminus of LPCAT3.

amino acids 135, 260, and 445 showed reticular ER staining using Triton permeabilization but not using digitonin permeabilization, indicating that these epitopes face the lumen. An HA epitope inserted after amino acid 358 could not be detected using either Triton or digitonin, indicating a sterically shielded local environment with inconclusive topology.

Refined model of LPCAT3 topology

A second round of topology prediction through the TOPCONS server was performed using the selective permeabilization results as restraints. With these restraints in place, the minimum reliability of prediction increased from less than 40% to greater than 75% (Figure 4-8). Based on this prediction, I proposed a topology model that included 11 transmembrane domains and a luminal active site (Figure 4-9).

Exclusion from the Golgi requires C-terminal dilysine motif

The localization of LPCAT3 to the ER is suspected to be dependent on an ER-retrieval motif, K(x)KXX, at the extreme C-terminus[310]. The K(x)KXX motif is a binding site for COPI coatomer and facilitates sorting into budding COPI vesicles[296]. Human MBOAT1, MBOAT4, and MBOAT7 contain similar C-terminal motifs that might function as ER retrieval signals, although MBOAT2 lacks this motif (Figure 4-2). To explore the importance of the K(x)KXX motif for LPCAT3 localization, the localization of three overexpression constructs was compared. These constructs were 1) a positive control with a wild-type sequence and an N-terminal HA epitope tag (HA-LPCAT3 KKME),

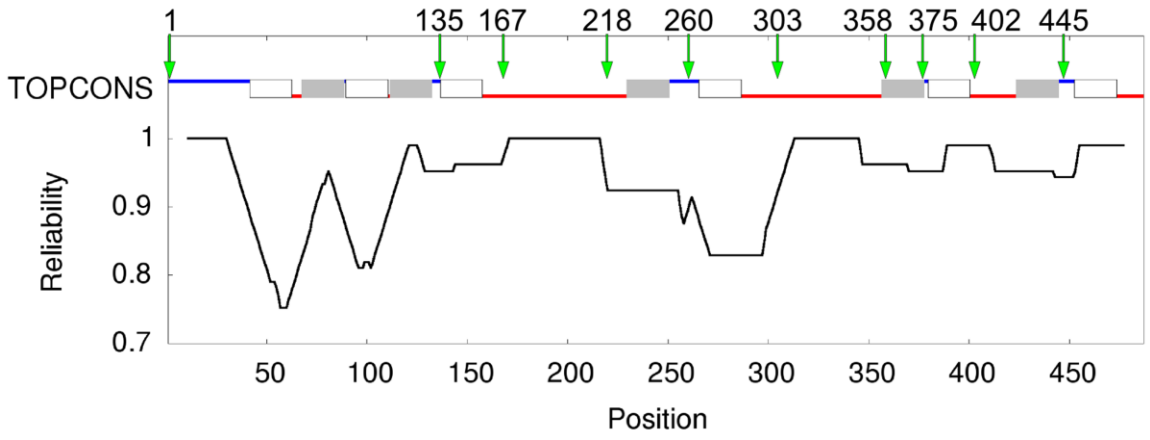

Figure 4-8. Restrained TOPCONS predicted transmembrane domains of LPCAT3

The TOPCONS algorithm was restrained as follows. Amino-terminus: lumen, amino acid (aa) 135: lumen, aa 167: cytoplasm, aa 218: cytoplasm, aa 260: lumen, aa 303: cytoplasm, aa 402: cytoplasm, aa 445: lumen, and carboxyl-terminus: cytoplasm. Green arrows indicate the approximate locations of HA epitope insertion sites. Blue: lumen, red: cytoplasm.

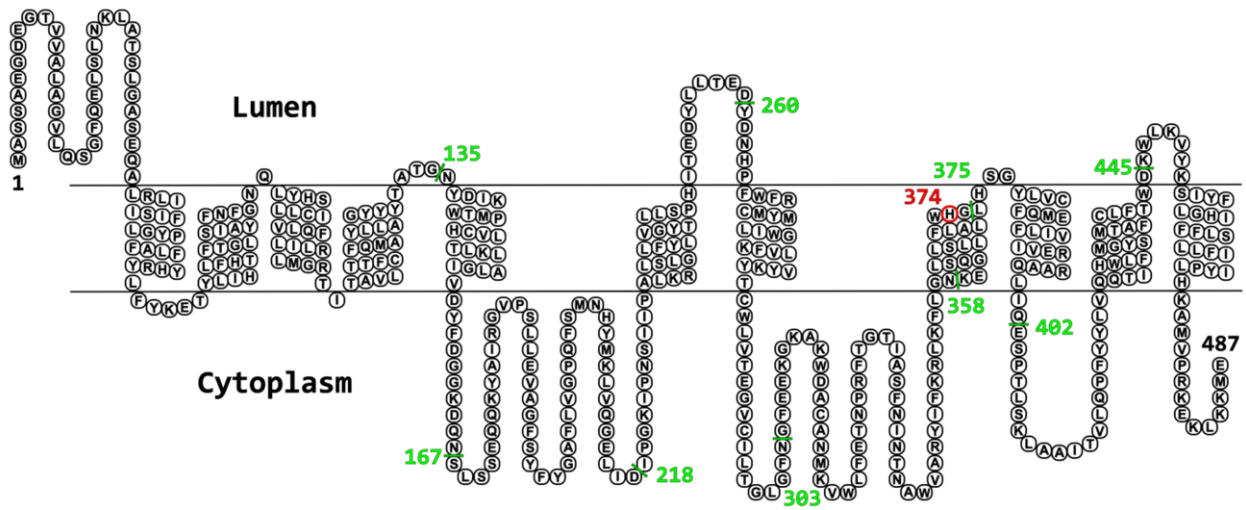

Figure 4-9. LPCAT3 transmembrane topology model

Human LPCAT3 has a luminal active site and eleven transmembrane domains. Green dashes indicate the location of HA epitope tags. The catalytic histidine is labeled in red.

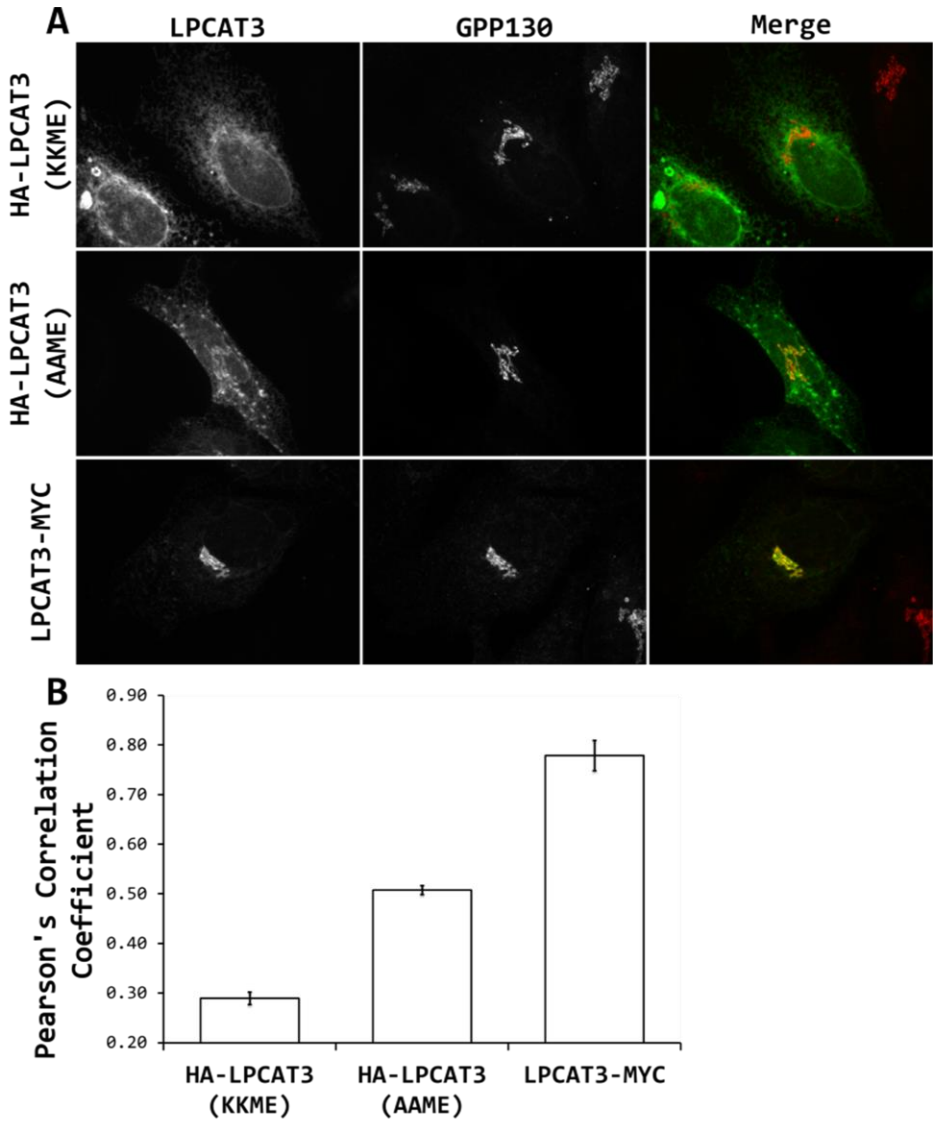

Figure 4-10. Exclusion from the Golgi requires a C-terminal K(x)KXX motif

A) IF of overexpressed LPCAT3 and endogenous GPP130 shows exclusion from the Golgi complex of wild-type N-terminally epitope tagged LPCAT3 (HA-LPCAT3 KKME), partial Golgi localization of mutated LPCAT3 (HA-LPCAT3 AAME), and strong Golgi localization of C-terminally epitope tagged LPCAT3 (LPCAT3-MYC). B) Quantitation of colocalization between LPCAT3 and GPP130 by Pearson's correlation coefficient. (n=5)

2) an alanine substituted mutant (HA-LPCAT3 AAME) with an N-terminal HA epitope tag, 3) and a wild-type sequence with a C-terminal myc epitope fusion (LPCAT3-MYC). The localization of these three constructs was examined in HeLa cells and compared to the localization of the *cis*-Golgi glycoprotein GPP130 (Figure 4-10). To quantitate differences in colocalization with GPP130, the Pearson's correlation coefficient was calculated between the fluorescent intensity of GPP130 and LPCAT3. Relative to the N-terminally tagged positive control, both C-terminally modified proteins increasingly localized to the Golgi complex.

Discussion

LPCAT3 active site topology

Reports of MBOAT transmembrane topologies have been contradictory, though most evidence points to MBOAT proteins having a luminal active site[291,293]. What is clear is that the enzyme MBOAT4 must have a luminal active site, because it acylates secreted proteins[202]. Also, Pagac *et al.* convincingly identify a luminal active site in yeast Ale1[202,294]. The evidence I have presented here also supports a model of a lumen facing active site for LPCAT3. Specifically, I showed that an HA epitope inserted after amino acid 375, adjacent to the active site histidine 374, has luminal localization. Also, the immediately adjacent loop regions were shown to be cytosolic by the mapping of HA epitopes at amino acids 303 and 402.

The topological location of an HA epitope inserted after amino acid 358 could not be determined. IF using either Triton or digitonin permeabilization did not detect the epitope. Lack of staining is likely due to a protein folding state that does not allow the

anti-HA antibody to bind the epitope and not due to a lack of protein expression or protein degradation. The protein appears to have been synthesized completely, as the C-terminus could be detected in the cytosol by immunofluorescence (Figure 4-7) and the HA epitope could be detected by Western blot (data not shown).

The topology model presented here places the active site histidine 374 at the border of a transmembrane domain and a very short luminal loop. However, it is impossible to conclusively discriminate between the localization of the active site to a luminal extra-membrane loop or to the luminal edge of a transmembrane domain. Either location necessitates that cytosolic acyl-CoA traverse the membrane to a luminal active site. Consequentially, conserved cytosolic motifs must recognize acyl-CoA and mediate membrane traversal. Intriguingly, the two largest extra-membrane loops (158-229 and 287-356) are localized to the cytoplasm and contain highly conserved residues (Figure 4-3, Figure 4-9). Shindou *et al.* reported several amino acids that are required for LPCAT3 activity, including tryptophan 313 and aspartic acid 314[298]. Additionally, asparagine 318 and asparagine 338 in the 287-356 loop and glycine 200 and proline 201 in the 158-229 loop have perfect conservation across human MBOAT LPATs and yeast Ale1.

Topological map

When interpreting the topological map in Figure 4-9, it is important to keep in mind the shortcomings of the techniques from which it was constructed. First, it should be understood that the topology of three extra-membrane loops (starting at amino acids 63, 89, and 111) has not been experimentally verified. Also, the insertion of an epitope

tag may disrupt the native structure, charge distribution, and potentially the membrane topology of LPCAT3. It is somewhat reassuring that for every epitope tag, the C-terminus of LPCAT3 localized to the cytoplasm.

Membrane re-entrant structures are regions that are hydrophobic enough to dip into the membrane, but do not fully penetrate to the other side[312]. It is possible that the insertion of an HA-epitope into a long, membrane re-entrant structure would create two new transmembrane helixes flanked by a new extra-membrane loop, which contains the epitope. Such a topology change would have no effect on the localization of the C-terminus[312]. This consideration applies most particularly to the interpretation of the two short loop regions spanning amino acids 133-136 and 378-379.

The topology prediction for the first four transmembrane helixes of LPCAT3 (42-132) has lower reliability than that of any other region. This is in part because the modeling of these transmembrane domains is constrained only by the N-terminus and an HA-epitope at amino acid 135 (Figure 4-8). Additionally, this region appears to be difficult to predict computationally. There is no agreement in this region between the predictions of the TMHMM server, the naïve TOPCONS algorithm and the restrained TOPCONS algorithm.

An O-linked glycosylation site is predicted in the luminal N-terminus of LPCAT3[308]. This glycosylation motif is conserved across mammalian LPCAT3 homologues (Figure 4-6). Cotranslational translocation during the biosynthesis of transmembrane proteins often takes place in conjunction with posttranslational modification by glycosyltransferases[87]. Topology prediction algorithms have the lowest

reliability score in the first four predicted transmembrane domains of LPCAT3, possibly indicating that this region exists on the borderline of stability. The placement of a cotranslational glycosylation site at the N-terminus of LPCAT3 could enable more efficient protein folding by stabilizing the topological orientation of the N-terminus to the lumen, constraining the topological orientation of subsequent transmembrane domains.

ER localization motif

The cytosolic C-terminal K(x)KXX ER localization motif of LPCAT3 was shown to be important for maintaining LPCAT3 localization to the ER and exclusion from the Golgi complex (Figure 4-10). This motif interacts with COPI coatomer and is responsible for recruitment to retrograde transport vesicles[295]. Mutation of the dilysine residues to alanine residues was effective at relocalizing LPCAT3 to the Golgi complex but not as effective as the fusion of an epitope tag to LPCAT3's C-terminus. It is likely that other motifs in LPCAT3's C-terminus contribute to ER localization. There are several other basic amino acid dependent mechanisms for ER localization such as those mediated by the KDEL receptor's C-terminal KKLSLPA sequence and the RXR and FLxK motifs[54,295,313].

Sequences similar to the K(x)KXX motif can be found in MBOAT1, MBOAT4, and MBOAT7. These sequences have not been investigated experimentally but likely play a role in the ER localization pattern of these proteins. Interestingly, MBOAT2 may localize to the ER by a different mechanism, as it does not have a C-terminal sequence similar to the K(x)KXX motif.

In summary, my studies have defined the membrane topology of human LPCAT3 by mapping the N- and C-termini, 11 transmembrane domains, and the likely luminal catalytic histidine residue. In addition, I have identified C-terminal motifs, including a K(x)KXX motif, that are likely required for Golgi to ER retrieval.

CHAPTER FIVE: LPCAT3 regulates retrograde trafficking from the Golgi complex

Introduction

Previous reports showed that overexpressed LPCAT3 was localized to the ER and to karmellae-like structures, which I confirmed in the studies presented in Chapter 3 and 4[261]. It prefers long-chain, unsaturated acyl-CoA donors and LPC acceptors[310,314]. Expression is ubiquitous, high in metabolically active cells, and greatest in the liver, adipose tissue, and pancreas[261]. The siRNA mediated knockdown of LPCAT3 in human hepatoma Huh7 cells nearly eliminated membrane bound LPC acyltransferase activity[310]. Adenoviral knockdown in mice attenuated hepatic LPC acyltransferase activity, increased hepatic LPC concentration, and increased hepatic triglyceride secretion[140].

Little is known about how LPCAT3 regulates membrane trafficking. In Chapter 3, I established that LPCAT3 overexpression inhibits ssHRP secretion. In this chapter, I characterize the effect of LPCAT3 overexpression and knockdown on organelle morphology and membrane trafficking.

Materials and methods

Cell Culture

HeLa cells were grown and maintained in MEM supplemented with 10% FBS and 1% penicillin/streptomycin at 37°C in a 95% humidity and 5% CO_2 environment. Cells were transfected in 35 mm^2 culture dishes using PEI from Polysciences Inc. according to the manufacturer's instructions. DNA transfection was performed using 1 µg DNA/5 µg PEI

for the 24 h prior to experiments. Knockdown was performed using Lipofectamine RNAiMAX (Life Technologies) twice prior to experiments, at 24 h and 48 h, using 25 pmoles of siRNA/3 µl RNAiMAX according to the manufacturer's instructions. Two siRNAs targeting the LPCAT3 coding sequence (Ambion siRNA 122586: CCAUUGCCUCAUUCAACAUtt and 16819: GGGAAAGAUCAGAAUUCCUtt) were tested for LPCAT3 knockdown; 16819 was most effective and subsequently used for all experiments (Figure 5-6). Ambion AM4611 siRNA was used as negative control.

IF microscopy

Rabbit anti-GPP130 (Covance), mouse anti-HA (Covance), rabbit anti-HA (Santa Cruz), mouse anti-myc (Cell Signaling), rabbit anti-LPCAT3 C-terminus (NEOBioscience, Cambridge, MA), and FITC/TRITC conjugated secondary antibodies (Jackson ImmunoResearch Laboratories and Invitrogen) were used for IF. Cells were grown on glass coverslips and fixed with 3.7% formaldehyde in PBS, washed 3 times in PBS, and permeabilized with 0.1% Triton X-100 in PBS. Cells were incubated with primary antibodies for 1 h at room temperature using the manufacturer's recommended dilution, washed 3 times, treated identically with secondary antibodies, and mounted on glass slides with VectaShield (Vector Laboratories). Cells were viewed and imaged using a Perkin-Elmer Ultraview spinning disk confocal microscope at 100X. Image analysis was performed using the ImageJ software package (NIH, Bethesda, MD) or the FIJI distribution of ImageJ[254]. Error bars are SEM. Significance determined by paired Student's t-test.

ssHRP secretion assay

To perform the HRP secretion assay, cells were washed 3 times in MEM without FBS and then incubated in MEM containing 3% FBS. After 6 h, 10 µl duplicate samples were removed to a 96-well plate and 50 µl of TMB chromogenic reagent (Pierce) was added to each. The reaction was allowed to proceed until saturation, halted by the addition of 50 µl 1 M sulfuric acid, and absorbance measured at 450 nm.

Brefeldin A induced Golgi recycling assay

To examine membrane tubule-mediated retrograde trafficking form the Golgi to the ER, I took advantage of Brefeldin A (BFA) (Endo Life Sciences or Sigma-Aldrich). Cells were washed 3 times with 37°C MEM without FBS followed by incubation with 1 µg/ml BFA at 37°C. Coverslips were fixed at 0 min, 8 min, and 20 min timepoints and prepared for IF of endogenous GPP130. Scoring for intact Golgi complexes was performed by visual inspection with wide field epifluorescence at 100X magnification. At the 8 min time point, cells were categorized as having 'ER localization' if GPP130 was partially localized to reticular ER. At the 20 min time point, cells were categorized as having 'completed recycling' if GPP130 localized to the reticular ER and an intact Golgi could not be found. Membrane tubules were counted in cells at the 8 min time point.

ERGIC-53 recycling assay

For ERGIC-53 transport assays, I used the temperature shift protocol to induce tubule-mediated retrograde transport from the ERGIC to the ER[315]. Cells were washed with bicarbonate buffered MEM containing 10% FBS, held at 15°C for 4 h, washed with 37°C MEM containing 10% FBS, and shifted to 37°C. Coverslips were fixed at 0 min, 2 min, and 5 min post-temperature shift and prepared for IF of HA-LPCAT3. Scoring for

ER localized ERGIC-53-GFP was performed by visual inspection under a mercury lamp at 100X.

VSV-G transport assay

For YFP-VSV-G-ts045 transport assays, cells were held at 40°C for 18 h and then shifted to 32°C. Cells from the 8 min time point were scored based on the presence of Golgi staining; cells at 40 min were scored based on the presence of plasma membrane staining.

Results

Localization of overexpressed LPCAT3 and organelle morphology

Overexpressed LPCAT3 localized to the ER and induced the formation of karmellae-like membrane structures (Figure 5-1). The physiological significance of karmellae is unclear, but they are not inherently detrimental to cell health and not uncommon when transmembrane proteins are overexpressed[260]. Indeed, all of the AGPAT and MBOAT family members shown in Figure 3-1 had a propensity to localize to large puncta/karmellae-like structures. When overexpressed in HeLa cells, GFP-LPCAT3 and HA-LPCAT3 could be found throughout the ER, nuclear envelope and in karmellae-like structures (Figure 5-1, Figure 5-2).

Overexpression of LPCAT3 altered the localization of some markers of the early secretory system (Figure 5-2). GFP-ERGIC-53 became less juxta-Golgi in localization and increasingly localized to juxtanuclear puncta and to the reticular ER. An ER resident (v)R-SNARE protein, Sec22, colocalized nearly perfectly with

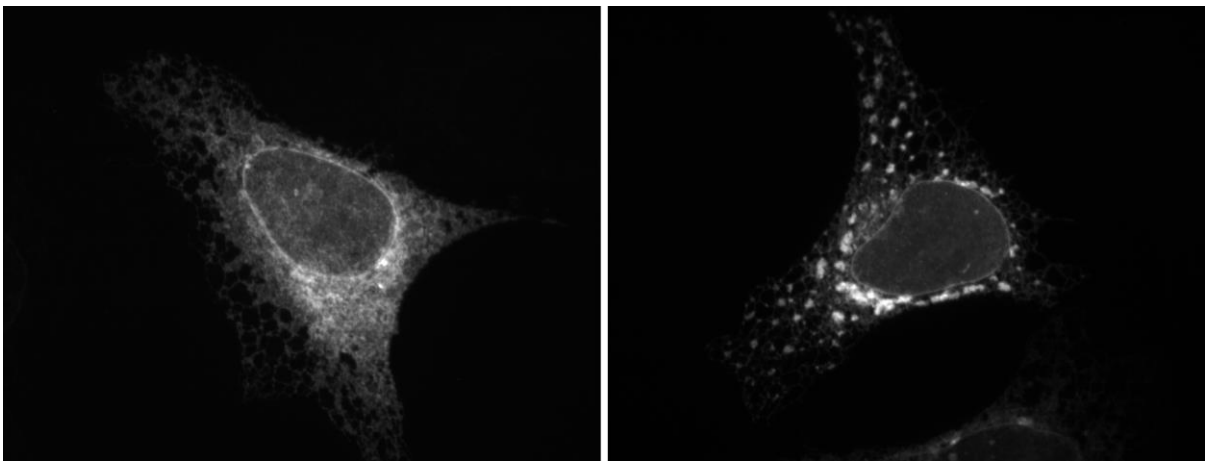

Figure 5-1. LPCAT3 localization

When overexpressed in HeLa cells, N-terminally GFP tagged human LPCAT3 localized to the ER, to the nuclear envelope, and to large puncta/karmellae-like structures.

LPCAT3, although its distribution was largely unchanged by LPCAT3 overexpression. The COPII components Sec24 and Sec31 showed a decrease in the number of disperse puncta and Sec24 showed an increase in juxta-Golgi localization. The COPI component β-COP showed a dramatic loss of peripheral puncta and greatly increased juxta-Golgi localization.

Despite the LPCAT3 overexpression induced change in the localization of markers of the early secretory system, LPCAT3 overexpression did not appear to grossly affect the morphology of the Golgi complex, TGN, AP-1 labeled vesicles, or EEA1 labeled endosomes (data not shown).

HA-LPCAT3 overexpression inhibits HRP secretion

In order to confirm the findings of the HRP secretion screen from Chapter 3, which identified GFP-LPCAT3 as an inhibitor of HRP secretion, the HRP secretion experiment was repeated with HA epitope tagged LPCAT3. In agreement with the HRP screen (Figure 3-4), secretion was dramatically reduced in cells co-overexpressing HA-LPCAT3 (Figure 5-3). HRP colocalized with LPCAT3 to karmellae-like structures, but also localized to the ER and Golgi complex.

HA-LPCAT3 overexpression had no effect on ERGIC-53 retrograde trafficking kinetics

Once a defect in HRP secretion was confirmed for cells overexpressing HA-LPCAT3, the kinetics of other membrane trafficking processes were measured. ERGIC-53 traffics between the ER, ERGIC, and *cis*-Golgi but can be held in the ERGIC by a 15°C temperature block[43]. Removal of this temperature block induces a bolus of ERGIC-53 trafficking to the ER by vesicular and tubular membrane trafficking

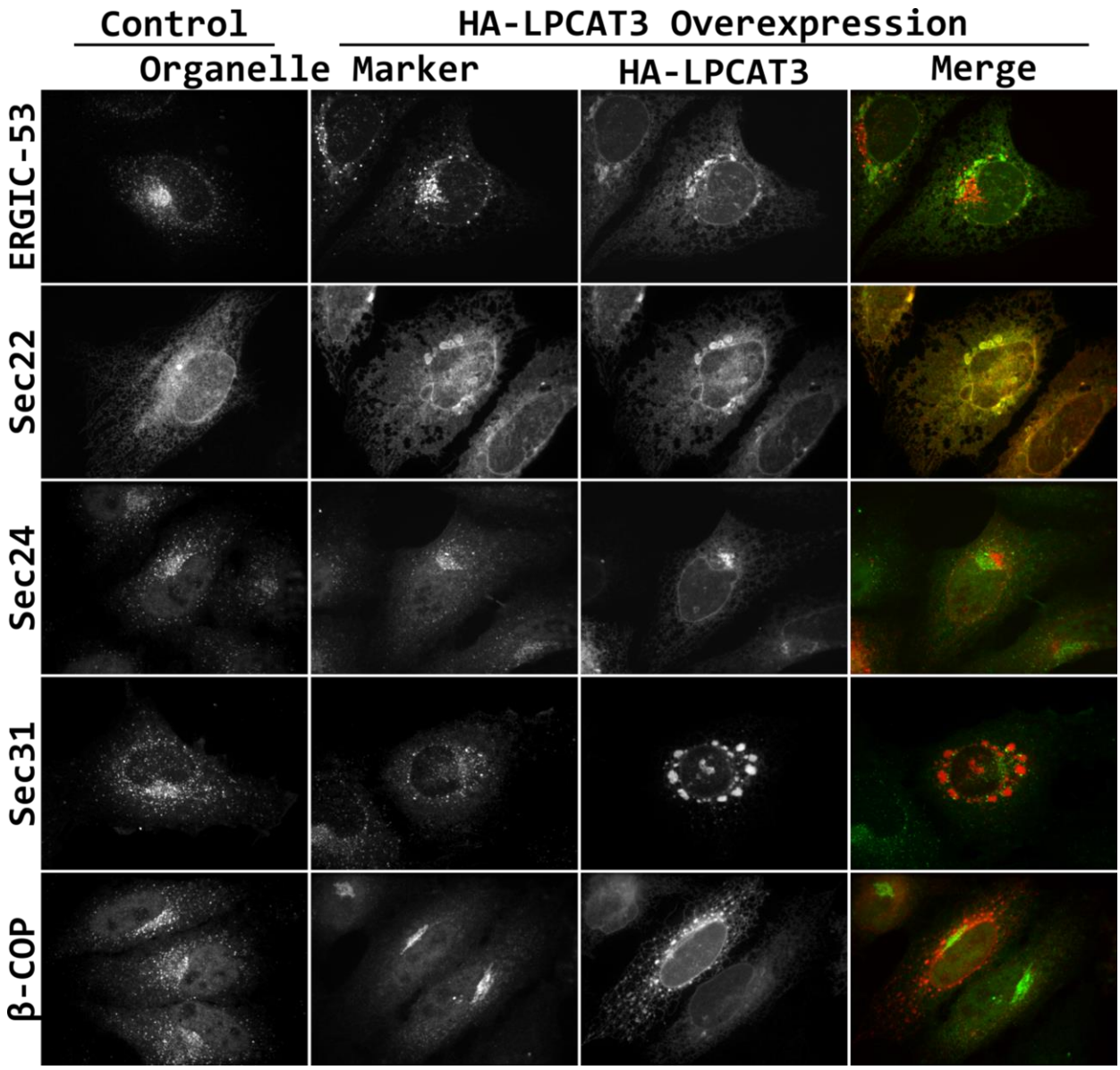

Figure 5-2. LPCAT3 overexpression disrupts the localization of early secretory system markers

The overexpression of LPCAT3 affected the localization of ERGIC-53-GFP and endogenous Sec24, Sec31, and β-COP. LPCAT3 had near perfect colocalization with Sec22-myc.

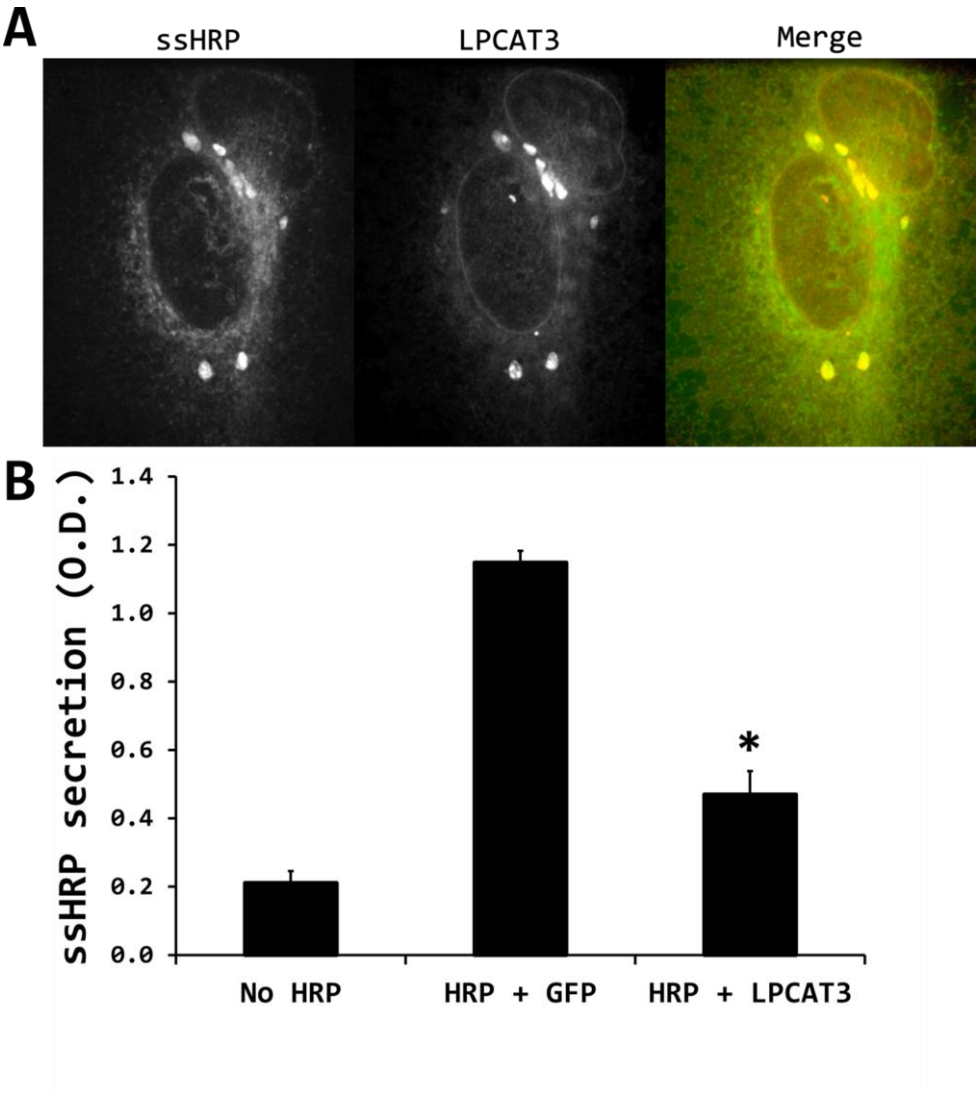

Figure 5-3. HA-LPCAT3 overexpression decreased HRP secretion

A) Colocalization of ssHRP and LPCAT3 to karmellae–like structures of the ER. B) ssHRP secretion measurements. (n=4, * $p<0.01$)

intermediates[39]. Despite the altered ERGIC morphology (Figure 5-2), the overexpression of HA-LPCAT3 had no obvious effect on the kinetics of retrograde ERGIC-53 trafficking by this assay (Figure 5-4).

HA-LPCAT3 overexpression had no effect on VSV-G secretion

There are at least three COPII mediated routes of anterograde trafficking from the ER[316]. HRP is a soluble luminal protein that is expected to be secreted by 'bulk' trafficking, whereas the integral membrane protein VSV-G has a cytoplasmic motif that coordinates its enrichment in COPII vesicles[28]. The temperature sensitive VSV-G mutant ts045 does not fold properly at the non-permissive temperature of 40°C and is retained in the ER by protein quality control machinery[86]. The involvement of LPCAT3 in VSV-G transport was assayed by shifting cells from 40°C to 32°C and measuring the trafficking kinetics of YFP-VSV-G-ts045 anterograde transport. No change in VSV-G transport kinetics, to the Golgi complex was observed (Figure 5-5).

siRNA treatment to knockdown overexpressed LPCAT3

LPCAT3 is broadly expressed in mammalian cells and its knockdown in HeLa cells decreases polyunsaturated fatty acid incorporation into PC, PS, and PE[317]. An antibody raised to the C-terminus of LPCAT3 is capable of detecting overexpressed LPCAT3 in HeLa cells; overexpressed LPCAT3 could be detected by both Western blot and IF. However, endogenous LPCAT3 could not be detected in HeLa cells, HepG2 cells, or BTRD cells (Figure 5-6, data not shown).

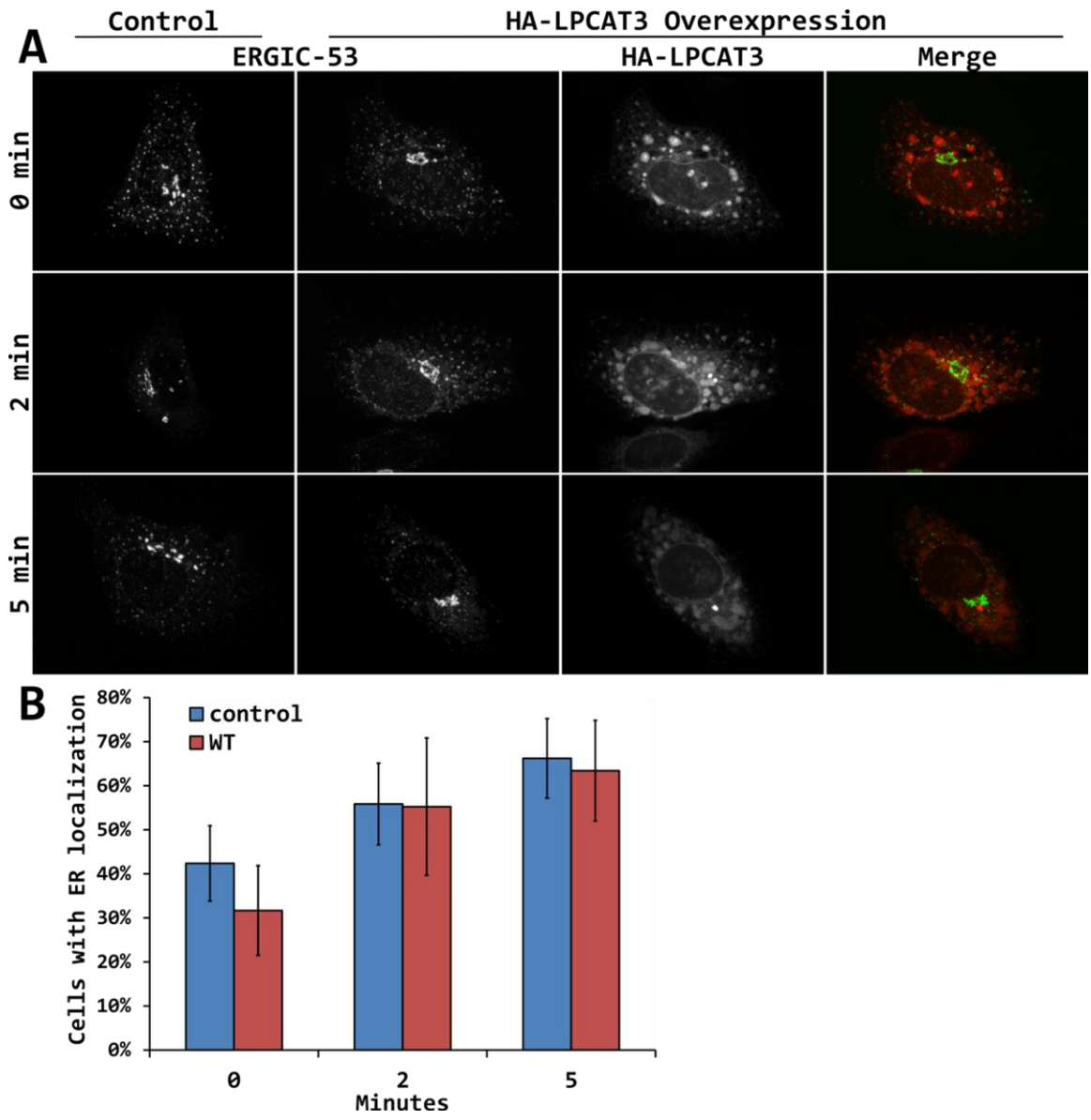

Figure 5-4. LPCAT3 overexpression did not affect the kinetics of ERGIC-53 recycling

A) HeLa cells co-overexpressing GFP-ERGIC-53 and HA-LPCAT3 were held at 15°C and then shifted to 37°C. Recycling of ERGIC-53 to the ER was unaffected by co-overexpressed HA-LPCAT3. B) Quantitation of A. (n=4)

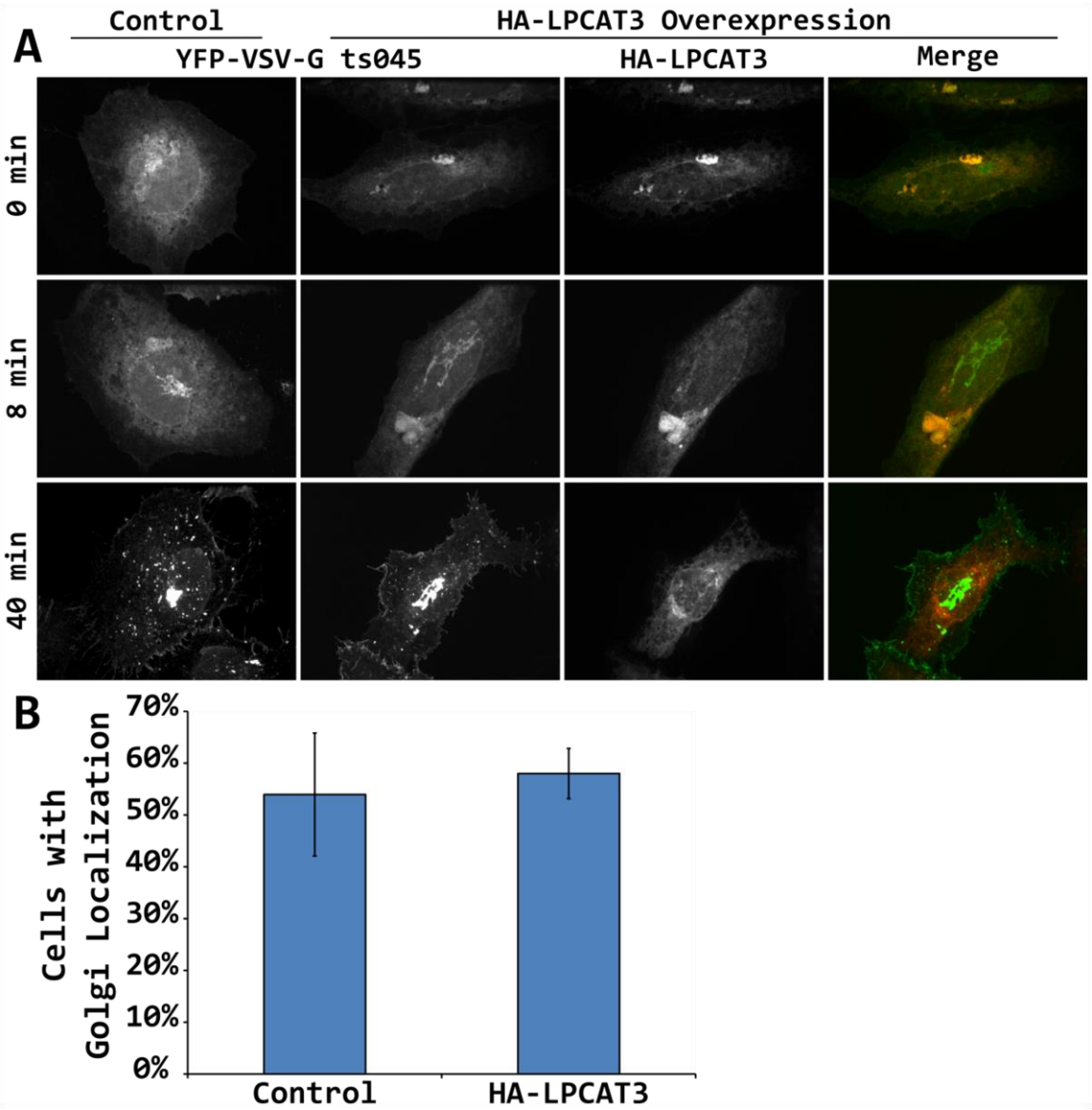

Figure 5-5. VSV-G transport was unaffected by HA-LPCAT3 co-overexpression

A) YFP-VSV-G-ts045 was expressed in HeLa cells in combination with HA-LPCAT3. Cells were held at 40°C and then shifted to 32°C. Transport of VSV-G to the Golgi and the plasma membrane was unaffected by co-overexpressed HA-LPCAT3. B) Quantitation of the 8 min time point showing localization of VSV-G to the Golgi complex. (n=3)

Ambion 16819 siRNA was demonstrated by Zhao *et al.* to knockdown LPCAT3 human hepatic Huh7 cells. I found it effective for the knockdown of overexpressed LPCAT3 and used it exclusively for the following experiments (Figure 5-6).

LCPAT3 knockdown disrupts ERGIC, COPI, and COPII markers

Changes in the morphology or localization of organelle markers indicate disruption of membrane trafficking. To detect organelle morphology changes caused by LPCAT3 knockdown, IF was performed for a variety of organelle markers. In knockdown cells, ERGIC-53-GFP, endogenous Sec24, Sec31, and β-COP exhibited decreased localization to peripheral puncta and a variable increase in juxta-Golgi and juxta-nuclear localization (Figure 5-7). β-COP localization was especially disrupted, with nearly complete depletion of peripheral puncta. These results indicate that siRNA treatment affected the morphology and steady state distribution of the early secretory system.

However, it appears that the alteration of membrane trafficking in LPCAT3 knockdown cells has limited scope. Despite the disruptions of early secretory markers that are seen in LPCAT3 knockdown cells, the localization of the ER marker Sec22-myc and the endogenous *cis*-Golgi protein GPP130 was not altered (Figure 5-8). Additionally, the localization of TGN markers, AP-1, and EEA1 labeled endosomes was likewise unaffected (data not shown). Given these findings, it is likely that only the early secretory system was disrupted in siRNA treated cells.

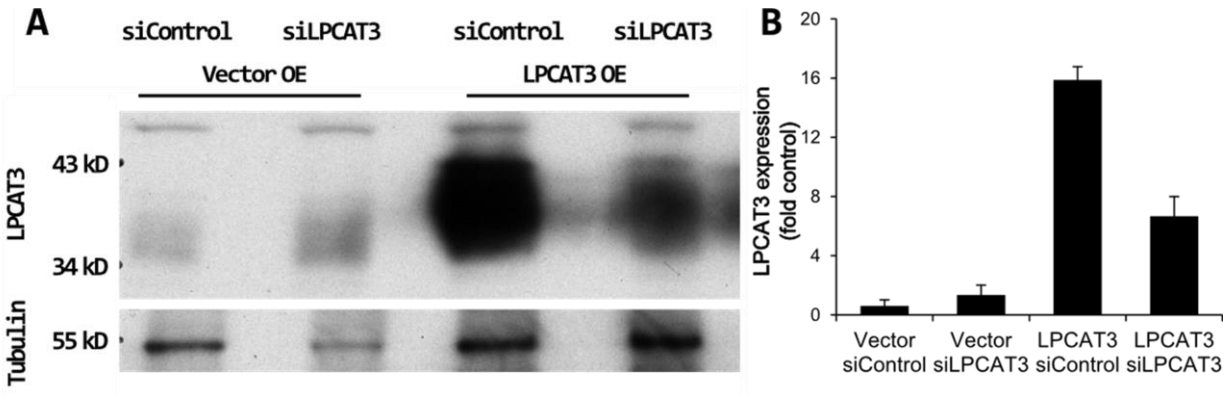

Figure 5-6. Knockdown of LPCAT3

A) Representative Western blot using a custom anti-LPCAT3 C-terminus polyclonal antibody to detect knockdown of overexpressed HA-LPCAT3. B) Quantitation of tubulin normalized LPCAT3 overexpression relative to vector overexpressing, siControl treated cells. n=3

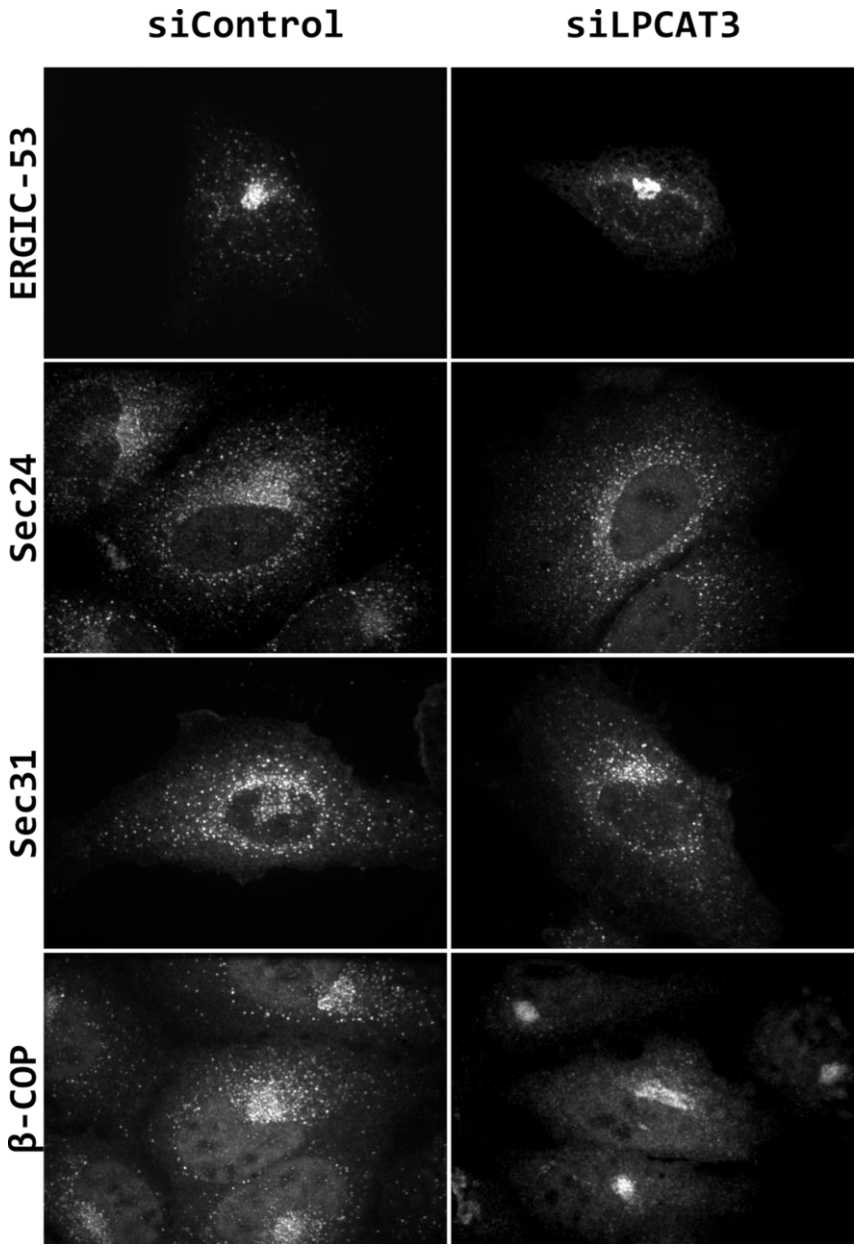

Figure 5-7. LPCAT3 Knockdown disrupts markers of the early secretory system

Treatment with LPCAT3 siRNA disrupted GFP-ERGIC-53, Sec24, Sec31, and β-COP localization. All disrupted markers showed decreased peripheral puncta and variably increased juxta-Golgi and juxta-nuclear localization.

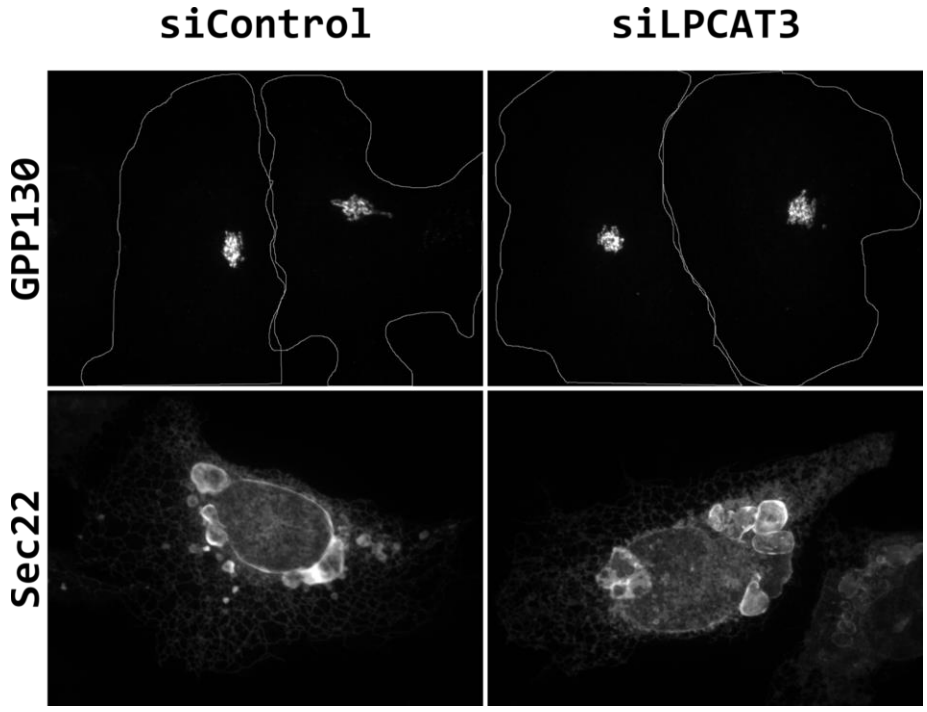

Figure 5-8. Knockdown of LPCAT3 does not affect the localization of GPP130 or Sec22

Knockdown of LPCAT3 in HeLa cells does not disrupt the localization of endogenous GPP130 or transiently transfected Sec22-myc.

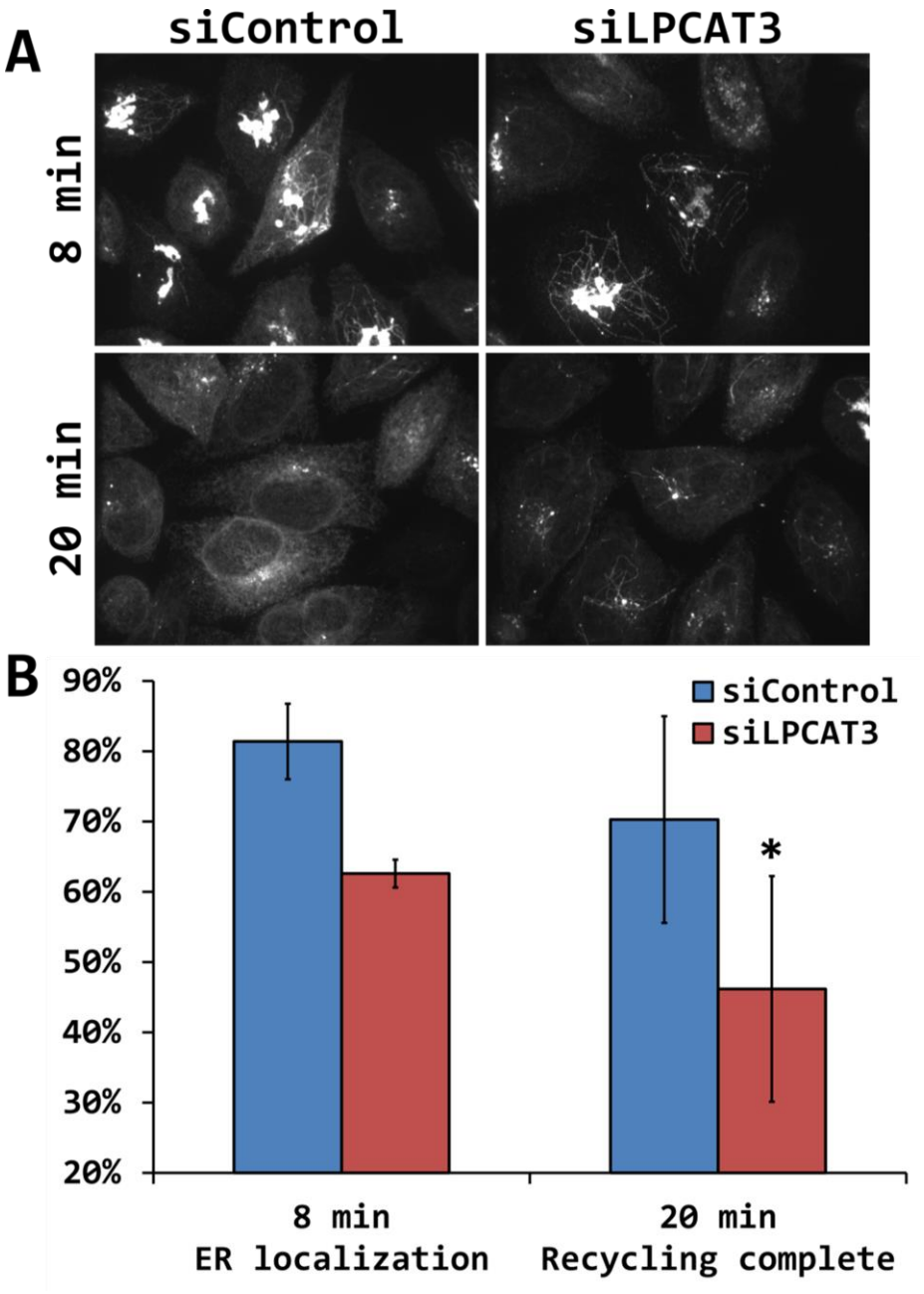

Figure 5-9. Knockdown delays BFA induced Golgi recycling to the ER

A) Golgi morphology as shown by GPP130 staining in RNAi treated HeLa cells at 8 min and 20 min post-BFA treatment. B) Quantitation of A. (n=3, * $p<0.01$)

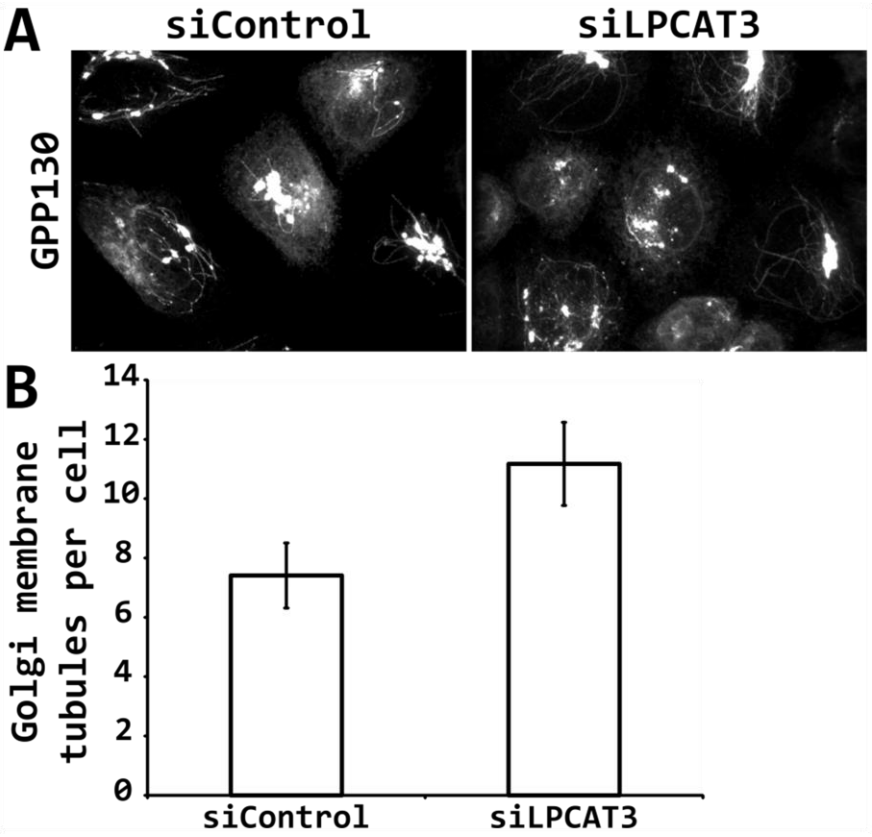

Figure 5-10. LPCAT3 siRNA treatment enhances BFA stimulated Golgi tubulation

siRNA treated HeLa cells were examined 8 min after treatment with BFA. A) Representative images of GPP130 labeled tubules. B) Quantitation of tubulation. (n=4)

Knockdown slows BFA mediated Golgi recycling to the ER

In response to BFA, the Golgi apparatus undergoes massive tubulation and subsequent trafficking to, fusion with, and absorption by the ER. It has been previously shown that BFA mediated recycling and membrane tubulation is influenced by other LPATs[181,245,318]. In order to determine if LPCAT3 activity plays a role in this process, BFA stimulated recycling of GPP130 was measured at 8 min and 20 min timepoints in knockdown cells. At each timepoint, Golgi recycling to the ER was slower in siLPCAT3 cells than in siControl cells (Figure 5-9).

LPCAT3 knockdown increased Golgi membrane tubulation in response to BFA treatment

The retrograde trafficking of the Golgi complex to the ER in response to BFA treatment is characterized by extensive Golgi membrane tubulation. Quantitation of the extent of tubulation revealed, surprisingly, that siLPCAT3 treated cells had increased tubulation at the 8 min time point (Figure 5-10).

LPCAT3 Knockdown inhibited ERGIC-53 retrograde trafficking

Treatment with siLPCAT3 was shown to disrupt the localization of ERGIC-53, inducing a more juxta-Golgi and juxta-nuclear localization (Figure 5-7). This result indicated that LPCAT3 activity may be necessary for regulating ERGIC-53 retrograde trafficking. To confirm this hypothesis, the kinetics of membrane tubule-mediated retrograde trafficking of ERGIC-53 in response to 15°C to 37°C temperature shift was measured. Similar to the BFA results, siLPCAT3 treated cells exhibited slowed retrograde trafficking, but ERGIC-53 membrane tubulation actually increased.

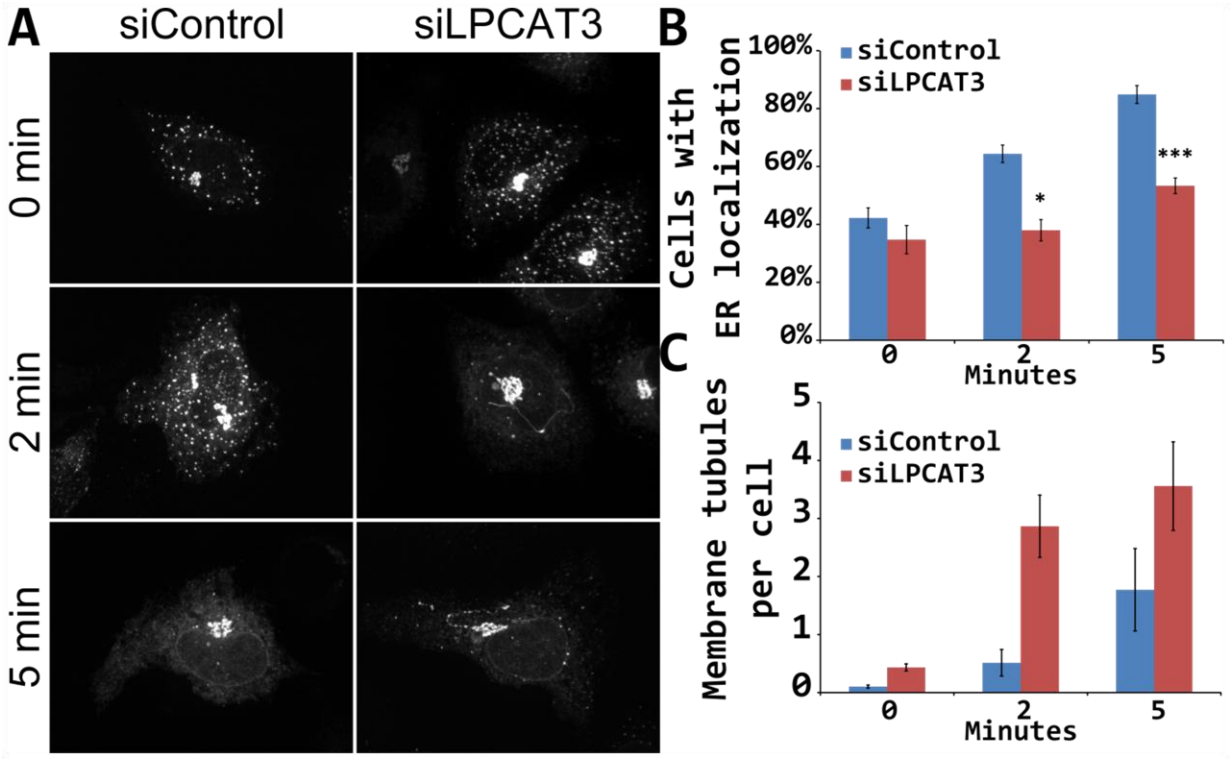

Figure 5-11. Knockdown of LPCAT3 inhibits retrograde trafficking and promotes tubulation of ERGIC-53

Treatment of HeLa cells with LPCAT3 siRNA slows the trafficking of ERGIC-53-GFP to the ER following 15°C to 37°C temperature shift. A) Time points following temperature shift. Note the long membrane tubules in knockdown cells at the 2 and 5 min time points. B) Quantitation of ERGIC trafficking. (n=7, * $p < 0.01$, *** $p < 0.0001$) C) Quantitation of ERGIC tubulation. (n=3)

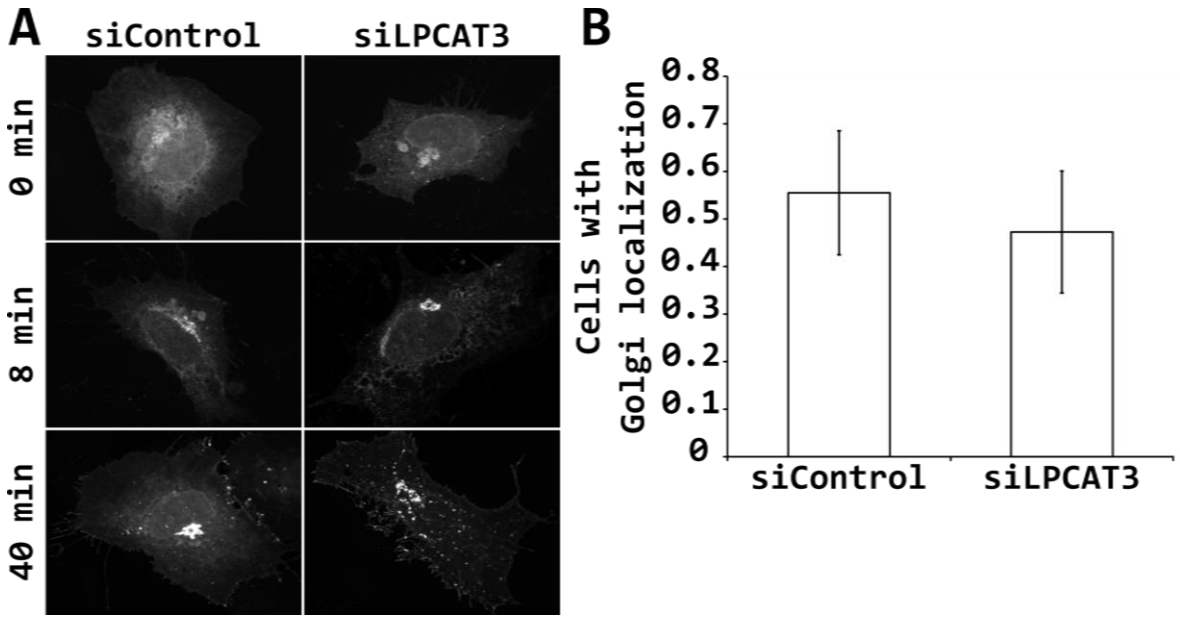

Figure 5-12. Knockdown does not affect anterograde trafficking of VSV-G

VSV-G-YFPts045 was held in the ER by 40°C temperature block and shifted to 30°C to initiate trafficking. Trafficking to the Golgi at 8 min and the PM at 40 min was unaffected. A) Representative images of VSV-G-YFPts045. B) Quantitation of Golgi localization at 8 min. (n=3)

LPCAT3 knockdown did not affect transport of VSV-G through the secretory pathway

The secretory system requires a balanced flow of anterograde and retrograde trafficking between compartments to maintain organelle integrity. Slowed retrograde trafficking from the Golgi to the ER may be accompanied by slowed anterograde trafficking of either VSV-G or ssHRP. To determine if this was the case, the kinetics of secretion were measured. Treatment of HeLa cells with LPCAT3 siRNA did not affect the kinetics of VSV-G transport from ER to Golgi complex (Figure 5-12). Likewise, cells treated with LPCAT3 siRNA did not have any defects in HRP secretion (data not shown).

Discussion

The major findings in this chapter are that changing the levels of LPCAT3 expression can have a significant effect on intracellular membrane trafficking, although not always in a predictable way. For example, overexpression and knockdown of LPCAT3 do not necessarily produce opposite effects on membrane trafficking. Perhaps the most robust trafficking defect was the inhibition of retrograde trafficking from the Golgi complex to the ER, as observed by two independent measures. Both of these retrograde pathways are mediated by the formation of membrane tubules. Surprisingly, however, knockdown of LPCAT3, although inhibiting retrograde trafficking, actually resulted in the formation of increased numbers of membrane tubules. At first glance, these results appear counter-intuitive; however, they can be explained by a simple model by which LPCAT3 knockdown results in the prolonged persistence of membrane tubules and the

decreased retrograde trafficking. I will expand below on the possible mechanistic explanations for these results.

Disruption of lipid remodeling by LPCAT3 overexpression

LPCAT3 overexpression induces the formation of ER karmellae, inhibits HRP secretion, and disrupts the localization of ERGIC-53 and markers of COPII and COPI vesicles. In Chapter 3, the mechanisms by which LPAT overexpression could inhibit HRP secretion were discussed. Briefly, these mechanisms were the induction of the UPR, disruption of COPII trafficking, and disruption of lipid remodeling. Further investigation is required to determine precisely how LPCAT3 overexpression affected membrane trafficking, however the most relevant mechanisms related to lipid remodeling are discussed below.

Phospholipids produced *de novo* by the Kennedy pathway have a high degree of saturation at the *sn*-1 and *sn*-2 position[177]. LPCAT3 enzymatic activity increases unsaturation at the *sn*-2 position creating asymmetry between the *sn*-1 and *sn*-2 position[261]. In comparison to symmetric, fully saturated phospholipids, asymmetric phospholipids induce negative membrane curvature, increase membrane fluidity, prefer liquid-disordered (L_d) phase states, and induce phase separation[269]. Also, they are preferred by some lipid remodeling enzymes and membrane binding domains[319].

While LPCAT3 activity produces asymmetric acyl chain saturation at the *sn*-1 and *sn*-2 positions, LPCAT3 activity is not expected to create phospholipid asymmetry across the ER membrane bilayer. In the ER, phospholipid flippases transport phospholipids across the membrane, equalizing their concentration on each side of the

bilayer[320]. During the course of anterograde trafficking, however, the action of cytosolic lipases may establish a phospholipid gradient across the bilayer.

LPCAT3 activity has been shown to reduce the concentration of free unsaturated fatty acids[321]. This reduction is likely to disrupt the activity of other enzymes that depend on free unsaturated fatty acids and potentially disrupt membrane trafficking. PI synthesis by MBOAT7 has a strict requirement for polyunsaturated fatty acids[200,281]. PI is phosphorylated to form phosphatidylinositol 4-phosphate (PI4P) at ERES where it is critically important for COPII function and ER export[322].

Knockdown of LPCAT3

Knockdown of LPCAT3 disrupted the localization of ERGIC-53 and markers for COPII and COPI vesicles. Most dramatically, peripheral localization of β-COP was nearly eliminated in knockdown cells. Knockdown also slowed retrograde trafficking of ERGIC-53 in response to 15°C to 37°C temperature shift and retrograde trafficking of GPP130 from the Golgi complex in response to BFA treatment. Slowed retrograde trafficking was accompanied by increased membrane tubulation. Taken together, these findings suggest that LPCAT3 knockdown promotes membrane tubulation by inhibiting COPI-mediated scission, thus tubules would persist longer and fusion with the ER would be inhibited.

LPCAT3 is an ER localized protein, but LPCAT3 knockdown most severely disrupts ERGIC and Golgi retrograde trafficking. This suggests that the substrates and/or products of LPCAT3's enzymatic activity regulate membrane trafficking, and not directly through interactions of LPCAT3 with trafficking machinery. Knockdown is

thought to increase LPC, increase polyunsaturated acyl-CoA, and decrease polyunsaturated PC concentrations (Figure 5-13). Membrane tubulation and COPI vesiculation is influenced by each of these changes.

Following LPCAT3 knockdown, the expression levels of other LPC specific LPATs such as LPCAT1 and LPCAT4 did not increase in a compensatory manner. This was shown by Li *et al.* using murine adenoviral knockdown; they found that saturated PC of liver tissue did not increase in response to LPCAT3 knockdown[140]. Ishibashi *et al*. came to a similar conclusion using siRNA treated macrophages[321]. Consequentially, LPC concentrations rise in response to LPCAT3 knockdown; Li *et al.* observed a 39% increase[140]. The positive spontaneous curvature of LPC aids in the formation of membrane tubules and prevents fusion[264,323]. The 'stalk' and 'hemifusion' intermediates of early membrane fusion have high negative curvature and are energetically unfavorable for LPC containing membranes[324]. Thus, increased LPC concentrations would increase the capacity of the ERGIC and Golgi to form membrane tubules and prevent their fusion with the ER.

LPCAT3 knockdown increases the concentration of free AA (and other polyunsaturated fatty acids) in the cell, which can then be used by other AA specific acyltransferases[321]. There is evidence that the activity of at least MBOAT7 and DGAT1 increases in response to elevated AA concentrations. In the *C. elegans* model system, knockdown of the LPCAT3 orthologue increases polyunsaturated fatty acid incorporation into PI, an activity thought to be dependent on MBOAT7[317]. The evidence for increased DGAT1 activity comes from LPCAT3 siRNA treated macrophages and

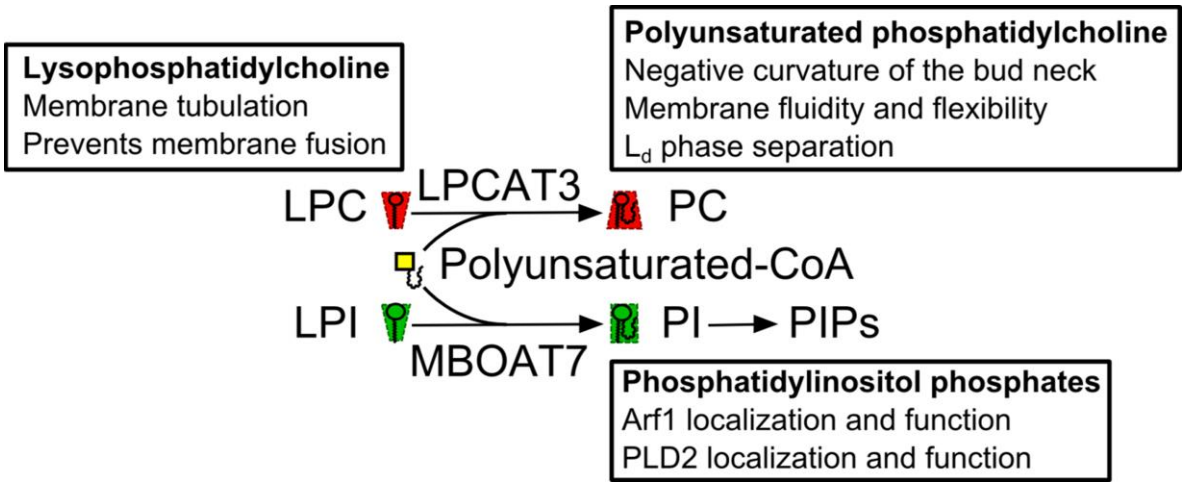

Figure 5-13. LPCAT3 related phospholipid remodeling and membrane trafficking

LPCAT3 and MBOAT7 acylate lysophospholipids with polyunsaturated acyl-CoA. Knockdown of LCPAT3 decreases the concentration of polyunsaturated PC and increases the concentration of LPC, polyunsaturated acyl-CoA, and PI. LPC, polyunsaturated PC, and PI/PIPs have important effects on membrane curvature and membrane trafficking.

murine hepatic knockdown model systems, both of which showed elevated triglyceride synthesis[140,321]. Altered triglyceride synthesis is not expected to affect retrograde membrane trafficking from the ERGIC and Golgi, but increased PI synthesis could have profound effects.

PI derived PIPs have an integral role in retrograde membrane trafficking due to their direct interaction and regulation of Arf1 and PLD[325,326]. Increased PIP concentrations may overcome the activity of PIP phosphatases that maintain their precise localization and steep concentration gradients. This would cause Arf1 and PLD to more diffusely localize to the Golgi. This was what was observed for the Arf1 dependent localization of β-COP in LPCAT3 knockdown cells. β-COP lost peripheral cytoplasmic localization and Golgi localization became stronger and less punctate. Mislocalization of Arf1, COPI coatomer, and PLD would be expected to decrease the efficiency of COPI vesiculation leading to enhanced membrane tubulation.

Arf1 cycling is critical for the loading of cargo proteins into retrograde transport carriers[64]. Mislocalization or decreased efficiency of COPI components would result in the depletion of SNAREs that are required for fusion of retrograde carriers with the ER[327,328]. In this way, retrograde membrane tubules would be prevented from fusing with the ER in LPCAT3 knockdown cells.

As was discussed above in the context of LPCAT3 overexpression, the polyunsaturated PC produced by LPCAT3 activity contributes to negative membrane curvature, increased fluidity, L_d phase separation, and is preferred by some phospholipid remodeling and membrane binding proteins[269]. Of these mechanisms, L_d

phase separation is of particular importance to COPI mediated retrograde transport from the Golgi. COPI vesicles are depleted of highly ordered lipid raft species such as cholesterol and sphingolipids, an effect that is partially mediated by Arf1 binding, exclusively, to L_d domains[329,330]. Phase separation is also critically important for the fission of *in vitro* generated membrane tubules[331]. Decreased concentrations of unsaturated PC at the Golgi complex would therefore inhibit COPI efficiency and promote long-lived membrane tubules.

As AGPAT3 is the only other mammalian LPAT that has been extensively studied in the context of membrane trafficking, it is useful to compare its activities to that of LPCAT3[245]. Both enzymes acylate lysophospholipids using unsaturated acyl chain donors and their knockdown promotes Golgi membrane tubulation. However, knockdown has strikingly different effects on the kinetics of tubule mediated retrograde trafficking. AGPAT3 knockdown accelerates BFA stimulated Golgi recycling, ERGIC-53 recycling, and CI-976 stimulated Golgi recycling[73,245]. LPCAT3 knockdown slows retrograde trafficking. AGPAT3 knockdown is thought to promote tubulation by decreasing the concentration of PA and consequentially, the efficiency of COPI budding. I discussed how LPCAT3 knockdown could promote tubulation by decreasing COPI budding efficiency; however, LPCAT3 knockdown also inhibits the fusion of membrane tubules with the ER. I propose that, it is this defect in membrane fusion that accounts for slowed retrograde trafficking in LPCAT3 knockdown cells.

In summary, I have shown that LPCAT3 knockdown inhibits COPI vesiculation and promotes the formation of membrane tubules with increased stability. Decreased

vesiculation and increased tubule stability contributed to slowed retrograde trafficking from the Golgi and ERGIC. I have argued that the ER localization of LPCAT3 necessitates a mechanistic model based on changes in membrane lipid composition. As reduction of LPCAT3 activity has been previously shown to change the concentration of LPC, PI, and polyunsaturated PC, I propose that these were the primary mediators of knockdown effects. In support of this argument, I have discussed previous reports in which changes in the concentration of these lipids has disrupted: Golgi membrane dynamics; the localization and activity of Arf1, COPI coatomer, and PLD; and L_d phase separation in retrograde transport carriers.

CHAPTER SIX: Conclusions

The underlying focus of my research was to better understand the relationship between lipid modeling and membrane trafficking. These studies began as a series of experiments looking at the interplay between phospholipase activity and acyltransferase activity. My experiments then shifted to the role of acyltransferase activity in regulating protein secretion and the relative importance of individual LPAT enzymes in regulating secretion. LPCAT3 was then selected for in depth study of its role in regulating membrane trafficking.

The experiments described in Chapter 2, were designed to ascertain if synergistic or antagonist relationship between LPAT and phospholipase activity regulate membrane trafficking and Golgi morphology. Using cells co-overexpressing AGPAT3 and one of three phospholipases, Golgi morphology, Golgi reformation, and Golgi recycling was investigated. The results suggested an antagonistic relationship between AGPAT3 and $cPLA_2\alpha$ activity during Golgi reformation and CI-976 induced Golgi recycling. A weak synergistic relationship between AGPAT3 and $iPLA_1\gamma$ during the process of Golgi reformation was also detected.

To determine the LPAT enzyme isoforms that have important roles in membrane trafficking, a screening experiment measuring ssHRP secretion was performed. Chapter 3 presented the results of this screen in the testing of LPAT overexpressing cells for alterations in secretory trafficking. Ten LPAT enzymes were screened and a broad range of phenotypes were observed. MBOAT7 was the most effective inhibitor of HRP secretion, reducing extracellular HRP to 7% of control. AGPAT5 was the most effect stimulator of HRP secretion, increasing extracellular HRP to 276% of control.

LPCAT3 was selected for further study due to its strong secretion defect (reducing extracellular HRP to 22% of control), putative K(x)KXX motif, and unique role in maintaining the asymmetry of saturated and unsaturated acyl chains between the *sn*-1 and *sn*-2 positions of phospholipids[261].

In the process of characterizing LPCAT3's effect on membrane trafficking, I became aware of a controversy in the field of MBOAT protein topology. Also, no attempts had yet been made to develop a whole protein topological map for any MBOAT family LPAT enzyme. In order to resolve these questions, the transmembrane topological orientation of LPCAT3 was mapped by epitope tag insertion and selective membrane permeabilization. This mapping was combined with a computational topology prediction algorithm to produce a high confidence model of LPCAT3 transmembrane topology containing 11 transmembrane domains and a luminal active site. The LPCAT3 topology model and supporting experiments were discussed in Chapter 4.

In Chapter 5, the characterization of human LPCAT3 as it affected membrane trafficking was reported. LPCAT3 activity was important for regulating efficient retrograde trafficking to the ER, membrane tubulation, and COPI function. These activities were unlike those of any other characterized LPAT enzyme and have important implications for the regulation of COPI trafficking and lipoprotein secretion. Several mechanisms were proposed by which LPCAT3 could affect retrograde trafficking through changes in lipid shape, protein recruitment, and lipid remodeling pathways.

Future experiments

I have proposed mechanisms for LPCAT3 knockdown mediated inhibition of COPI, promotion of membrane tubulation, and inhibition of fusion between retrograde membrane tubules and the ER. Verification of these mechanisms will require additional studies. An excellent place to start would be with *in vitro* assays and immuno-EM to more clearly describe how COPI vesiculation and membrane tubulation are effected by LPCAT3 knockdown. Increased PIP concentrations at the Golgi could be confirmed through the use of PIP binding domains. PIP binding domains can detect aberrantly high concentrations of PIPs at the Golgi. It may also be possible to restore normal PIP concentration in LPCAT3 knockdown cells by the overexpression of DGAT1, which would convert excess polyunsaturated fatty acids into inert triglycerides and prevent their utilization by MBOAT7. The mechanism of L_d phase separation is very difficult to study in cells, but its consequences may be measurable by analyzing the lipid and protein composition of retrograde transport carriers. If retrograde carriers in knockdown cells contain higher than normal concentrations of GPI-anchored proteins, cholesterol, or sphingolipids, this would indicate decreased L_d phase separation.

These exciting findings that LPCAT3, an ER localized protein, regulates Golgi membrane trafficking should be encouraging to investigators of lipid remodeling and LPAT enzymes. Of the many mammalian LPAT enzymes, LPCAT3 is only the second to be studied in the context of membrane trafficking. Other LPAT enzymes will unquestionably prove of equal importance to the regulation of membrane trafficking and membrane tubulation. I have also, reported the first experimentally supported full length transmembrane topology of a MBOAT family LPAT enzyme and characterized the C-

terminal motifs necessary for ER-retrieval of LPCAT3. While further research is needed to confirm, refute, or expand these models, the findings of this dissertation provide new insights into one of biology's most complex systems.

REFERENCES

1. Michaelis, L. & Menten, M. Die Kinetik der Inwertin Wirkung. *Biochem.* 333–369 (1913).
2. Ashburner, M. *et al.* Gene Ontology: tool for the unification of biology. *Nat Genet* **25,** 25–29 (2000).
3. Farquhar, M. G. A Man for All Seasons: Reflections on the Life and Legacy of George Palade. *Annual Review of Cell and Developmental Biology* **28,** 1–28 (2012).
4. Hegde, R. S. & Lingappa, V. R. Membrane Protein Biogenesis: Regulated Complexity at the Endoplasmic Reticulum. *Cell* **91,** 575–582 (1997).
5. Pfeffer, S. R. & Rothman, J. E. Biosynthetic Protein Transport and Sorting by the Endoplasmic Reticulum and Golgi. *Annual Review of Biochemistry* **56,** 829–852 (1987).
6. Barlowe, C. COPII-dependent transport from the endoplasmic reticulum. *Current Opinion in Cell Biology* **14,** 417–422 (2002).
7. Glick, B. S. & Luini, A. Models for Golgi traffic: a critical assessment. *Cold Spring Harb Perspect Biol* **3,** a005215 (2011).
8. Jahn, R. & Fasshauer, D. Molecular machines governing exocytosis of synaptic vesicles. *Nature* **490,** 201–207 (2012).
9. Bonifacino, J. S. & Lippincott-Schwartz, J. Coat proteins: shaping membrane transport. *Nature Reviews Molecular Cell Biology* **4,** 409–414 (2003).
10. Polishchuk, E. V., Pentima, A. D., Luini, A. & Polishchuk, R. S. Mechanism of Constitutive Export from the Golgi: Bulk Flow via the Formation, Protrusion, and En

Bloc Cleavage of large trans-Golgi Network Tubular Domains. *Mol. Biol. Cell* **14,** 4470–4485 (2003).

11. Matsuura, S., Masuda, R., Sakai, O. & Tashiro, Y. Immunoelectron Microscopy of the Outer Membrane of Rat Hepatocyte Nuclear Envelopes in Relation to the Rough Endoplasmic Reticulum. *Cell Structure and Function* **8,** 1–9 (1983).

12. Lakkaraju, A. K. K., Mary, C., Scherrer, A., Johnson, A. E. & Strub, K. SRP Keeps Polypeptides Translocation-Competent by Slowing Translation to Match Limiting ER-Targeting Sites. *Cell* **133,** 440–451 (2008).

13. Meusser, B., Hirsch, C., Jarosch, E. & Sommer, T. ERAD: the long road to destruction. *Nat Cell Biol* **7,** 766–772 (2005).

14. Fagone, P. & Jackowski, S. Membrane phospholipid synthesis and endoplasmic reticulum function. *The Journal of Lipid Research* **50,** S311–S316 (2008).

15. Li, Z. & Vance, D. E. Thematic Review Series: Glycerolipids. Phosphatidylcholine and choline homeostasis. *J. Lipid Res.* **49,** 1187–1194 (2008).

16. Vance, J. E. Thematic Review Series: Glycerolipids. Phosphatidylserine and phosphatidylethanolamine in mammalian cells: two metabolically related aminophospholipids. *J. Lipid Res.* **49,** 1377–1387 (2008).

17. Antonsson, B. Phosphatidylinositol synthase from mammalian tissues. *Biochimica et Biophysica Acta (BBA) - Lipids and Lipid Metabolism* **1348,** 179–186 (1997).

18. Presley, J. F. *et al.* ER-to-Golgi transport visualized in living cells. *Nature* **389,** 81–85 (1997).

19. Antonny, B. & Schekman, R. ER export: public transportation by the COPII coach. *Current Opinion in Cell Biology* **13,** 438–443 (2001).

20. Stagg, S. M. *et al.* Structure of the Sec13/31 COPII coat cage. *Nature* **439,** 234–238 (2006).

21. Weissman, J. T., Plutner, H. & Balch, W. E. The Mammalian Guanine Nucleotide Exchange Factor mSec12 is Essential for Activation of the Sar1 GTPase Directing Endoplasmic Reticulum Export. *Traffic* **2,** 465–475 (2001).

22. Yoshihisa, T., Barlowe, C. & Schekman, R. Requirement for a GTPase-Activating Protein in Vesicle Budding from the Endoplasmic Reticulum. *Science* **259,** 1466–1468 (1993).

23. Aridor, M., Weissman, J., Bannykh, S., Nuoffer, C. & Balch, W. E. Cargo Selection by the COPII Budding Machinery during Export from the ER. *J Cell Biol* **141,** 61–70 (1998).

24. Antonny, B., Madden, D., Hamamoto, S., Orci, L. & Schekman, R. Dynamics of the COPII coat with GTP and stable analogues. *Nat Cell Biol* **3,** 531–537 (2001).

25. Mahmood Hussain, M. A proposed model for the assembly of chylomicrons. *Atherosclerosis* **148,** 1–15 (2000).

26. Siddiqi, S. A., Gorelick, F. S., Mahan, J. T. & Mansbach, C. M. COPII proteins are required for Golgi fusion but not for endoplasmic reticulum budding of the pre-chylomicron transport vesicle. *J Cell Sci* **116,** 415–427 (2003).

27. Springer, S. & Schekman, R. Nucleation of COPII Vesicular Coat Complex by Endoplasmic Reticulum to Golgi Vesicle SNAREs. *Science* **281,** 698–700 (1998).

28. Nishimura, N. & Balch, W. E. A Di-Acidic Signal Required for Selective Export from the Endoplasmic Reticulum. *Science* **277,** 556–558 (1997).

29. Appenzeller, C., Andersson, H., Kappeler, F. & Hauri, H.-P. The lectin ERGIC-53 is a cargo transport receptor for glycoproteins. *Nat Cell Biol* **1,** 330–334 (1999).

30. Kelly, R. B. Pathways of Protein Secretion in Eukaryotes. *Science* **230,** 25–32 (1985).

31. Wiest, D. L. *et al.* Membrane biogenesis during B cell differentiation: most endoplasmic reticulum proteins are expressed coordinately. *J Cell Biol* **110,** 1501–1511 (1990).

32. Yoshida, H. ER stress response, peroxisome proliferation, mitochondrial unfolded protein response and Golgi stress response. *IUBMB Life* **61,** 871–879 (2009).

33. Harding, H. P., Zhang, Y., Bertolotti, A., Zeng, H. & Ron, D. Perk Is Essential for Translational Regulation and Cell Survival during the Unfolded Protein Response. *Molecular Cell* **5,** 897–904 (2000).

34. Yoshida, H., Haze, K., Yanagi, H., Yura, T. & Mori, K. Identification of the cis-Acting Endoplasmic Reticulum Stress Response Element Responsible for Transcriptional Induction of Mammalian Glucose-regulated Proteins INVOLVEMENT OF BASIC LEUCINE ZIPPER TRANSCRIPTION FACTORS. *J. Biol. Chem.* **273,** 33741–33749 (1998).

35. Iwawaki, T. *et al.* Translational control by the ER transmembrane kinase/ribonuclease IRE1 under ER stress. *Nat Cell Biol* **3,** 158–164 (2001).

36. Yoshida, H. *et al.* A Time-Dependent Phase Shift in the Mammalian Unfolded Protein Response. *Developmental Cell* **4,** 265–271 (2003).

37. Puthalakath, H. *et al.* ER Stress Triggers Apoptosis by Activating BH3-Only Protein Bim. *Cell* **129,** 1337–1349 (2007).

38. Horstmann, H., Ng, C. P., Tang, B. L. & Hong, W. Ultrastructural characterization of endoplasmic reticulum — Golgi transport containers (EGTC). *J Cell Sci* **115,** 4263–4273 (2002).

39. Ben-Tekaya, H., Miura, K., Pepperkok, R. & Hauri, H.-P. Live imaging of bidirectional traffic from the ERGIC. *J. Cell. Sci.* **118,** 357–367 (2005).

40. Appenzeller-Herzog, C. & Hauri, H. P. The ER-Golgi intermediate compartment (ERGIC): in search of its identity and function. *Journal of cell science* **119,** 2173 (2006).

41. Schweizer, A., Fransen, J. A., Bachi, T., Ginsel, L. & Hauri, H. P. Identification, by a monoclonal antibody, of a 53-kD protein associated with a tubulo-vesicular compartment at the cis-side of the Golgi apparatus. *J Cell Biol* **107,** 1643–1653 (1988).

42. Kappeler, F., Klopfenstein, D. R. C., Foguet, M., Paccaud, J.-P. & Hauri, H.-P. The Recycling of ERGIC-53 in the Early Secretory Pathway ERGIC-53 CARRIES A CYTOSOLIC ENDOPLASMIC RETICULUM-EXIT DETERMINANT INTERACTING WITH COPII. *J. Biol. Chem.* **272,** 31801–31808 (1997).

43. Itin, C., Schindler, R. & Hauri, H. P. Targeting of protein ERGIC-53 to the ER/ERGIC/cis-Golgi recycling pathway. *J Cell Biol* **131,** 57–67 (1995).

44. Tisdale, E. J., Plutner, H., Matteson, J. & Balch, W. E. p53/58 Binds COPI and Is Required for Selective Transport through the Early Secretory Pathway. *J Cell Biol* **137,** 581–593 (1997).

45. Malhotra, Vivek, Serafini, Tito, Orci, Lelio, Shepherd, James C. & Rothman, James E. Purification of a novel class of coated vesicles mediating biosynthetic protein transport through the Golgi stack. *Cell* **58,** 329–336 (1989).

46. Casanova, J. E. Regulation of Arf Activation: the Sec7 Family of Guanine Nucleotide Exchange Factors. *Traffic* **8,** 1476–1485 (2007).

47. Gommel, D. U. *et al.* Recruitment to Golgi membranes of ADP-ribosylation factor 1 is mediated by the cytoplasmic domain of p23. *EMBO J* **20,** 6751–6760 (2001).

48. Franco, M., Chardin, P., Chabre, M. & Paris, S. Myristoylation-facilitated Binding of the G Protein ARF1 to Membrane Phospholipids Is Required for Its Activation by a Soluble Nucleotide Exchange Factor. *J. Biol. Chem.* **271,** 1573–1578 (1996).

49. Antonny, B., Beraud-Dufour, S., Chardin, P. & Chabre, M. N-Terminal Hydrophobic Residues of the G-Protein ADP-Ribosylation Factor-1 Insert into Membrane Phospholipids upon GDP to GTP Exchange†. *Biochemistry* **36,** 4675–4684 (1997).

50. Lowe, M. & Kreis, T. E. In Vitro Assembly and Disassembly of Coatomer. *J. Biol. Chem.* **270,** 31364–31371 (1995).

51. Fiedler, K., Rothman, J. E., Stamnes, M. A. & Veit, M. Bimodal interaction of coatomer with the p24 family of putative cargo receptors. *Science* **273,** 1396+ (1996).

52. Pavel, J., Harter, C. & Wieland, F. T. Reversible dissociation of coatomer: Functional characterization of a β/δ-coat protein subcomplex. *PNAS* **95,** 2140–2145 (1998).

53. Sohn, K. *et al.* A major transmembrane protein of Golgi-derived COPI-coated vesicles involved in coatomer binding. *J Cell Biol* **135,** 1239–1248 (1996).

54. Cabrera, M. *et al.* The Retrieval Function of the KDEL Receptor Requires PKA Phosphorylation of Its C-Terminus. *Mol. Biol. Cell* **14,** 4114–4125 (2003).

55. Pelham, H. R. B. Recycling of proteins between the endoplasmic reticulum and Golgi complex. *Current Opinion in Cell Biology* **3,** 585–591 (1991).

56. Majoul, I. *et al.* KDEL Receptor (Erd2p)-mediated Retrograde Transport of the Cholera Toxin A Subunit from the Golgi Involves COPI, p23, and the COOH Terminus of Erd2p. *J Cell Biol* **143,** 601–612 (1998).

57. Zerangue, N. *et al.* Analysis of endoplasmic reticulum trafficking signals by combinatorial screening in mammalian cells. *PNAS* **98,** 2431–2436 (2001).

58. Eugster, A., Frigerio, G., Dale, M. & Duden, R. The α- and β′-COP WD40 Domains Mediate Cargo-selective Interactions with Distinct Di-lysine Motifs. *Mol. Biol. Cell* **15,** 1011–1023 (2004).

59. Serafini, T. *et al.* ADP-Ribosylation factor is a subunit of the coat of Golgi-derived COP-coated vesicles: A novel role for a GTP-binding protein. *Cell* **67,** 239–253 (1981).

60. Tanigawa, G. *et al.* Hydrolysis of bound GTP by ARF protein triggers uncoating of Golgi-derived COP-coated vesicles. *J Cell Biol* **123,** 1365–1371 (1993).

61. Nickel, W. *et al.* Uptake by COPI-coated vesicles of both anterograde and retrograde cargo is inhibited by GTPgammaS in vitro. *J Cell Sci* **111,** 3081–3090 (1998).

62. Malsam, J., Gommel, D., Wieland, F. T. & Nickel, W. A role for ADP ribosylation factor in the control of cargo uptake during COPI-coated vesicle biogenesis. *FEBS Letters* **462,** 267–272 (1999).

63. Lanoix, J. *et al.* GTP hydrolysis by arf-1 mediates sorting and concentration of Golgi resident enzymes into functional COP I vesicles. *EMBO J* **18,** 4935–4948 (1999).

64. Pepperkok, R., Whitney, J. A., Gomez, M. & Kreis, T. E. COPI vesicles accumulating in the presence of a GTP restricted arf1 mutant are depleted of anterograde and retrograde cargo. *J Cell Sci* **113,** 135–144 (2000).

65. Goldberg, J. Decoding of Sorting Signals by Coatomer through a GTPase Switch in the COPI Coat Complex. *Cell* **100,** 671–679 (2000).

66. Lanoix, J. *et al.* Sorting of Golgi resident proteins into different subpopulations of COPI vesicles a role for ArfGAP1. *J Cell Biol* **155,** 1199–1212 (2001).

67. Spang, A., Matsuoka, K., Hamamoto, S., Schekman, R. & Orci, L. Coatomer, Arf1p, and nucleotide are required to bud coat protein complex I-coated vesicles from large synthetic liposomes. *PNAS* **95,** 11199–11204 (1998).

68. Beck, R. *et al.* Membrane curvature induced by Arf1-GTP is essential for vesicle formation. *PNAS* **105,** 11731–11736 (2008).

69. Krauss, M. *et al.* Arf1-GTP-induced Tubule Formation Suggests a Function of Arf Family Proteins in Curvature Acquisition at Sites of Vesicle Budding. *J. Biol. Chem.* **283,** 27717–27723 (2008).

70. Yang, J.-S. *et al.* ARFGAP1 promotes the formation of COPI vesicles, suggesting function as a component of the coat. *J Cell Biol* **159,** 69–78 (2002).

71. Yang, J.-S. *et al.* A role for BARS at the fission step of COPI vesicle formation from Golgi membrane. *EMBO J* **24,** 4133–4143 (2005).

72. Yang, J.-S. *et al.* Key components of the fission machinery are interchangeable. *Nature Cell Biology* **8,** 1376–1382 (2006).

73. Yang, J.-S. *et al.* COPI acts in both vesicular and tubular transport. *Nature Cell Biology* **13,** 996–1003 (2011).

74. Aoe, T. *et al.* The KDEL receptor, ERD2, regulates intracellular traffic by recruiting a GTPase-activating protein for ARF1. *EMBO J* **16,** 7305–7316 (1997).

75. Aoe, T., Lee, A. J., Donselaar, E. van, Peters, P. J. & Hsu, V. W. Modulation of intracellular transport by transported proteins: Insight from regulation of COPI-mediated transport. *PNAS* **95,** 1624–1629 (1998).

76. Bigay, J., Gounon, P., Robineau, S. & Antonny, B. Lipid packing sensed by ArfGAP1 couples COPI coat disassembly to membrane bilayer curvature. *Nature* **426,** 563–566 (2003).

77. Tisdale, E. J. Rab2 Interacts Directly with Atypical Protein Kinase C (aPKC) ı/λ and Inhibits aPKCı/λ-dependent Glyceraldehyde-3-phosphate Dehydrogenase Phosphorylation. *J. Biol. Chem.* **278,** 52524–52530 (2003).

78. Volpicelli-Daley, L. A., Li, Y., Zhang, C.-J. & Kahn, R. A. Isoform-selective Effects of the Depletion of ADP-Ribosylation Factors 1–5 on Membrane Traffic. *Molecular Biology of the Cell* **16,** 4495–4508 (2005).

79. Allan, B. B., Moyer, B. D. & Balch, W. E. Rab1 Recruitment of p115 into a cis-SNARE Complex: Programming Budding COPII Vesicles for Fusion. *Science* **289,** 444–448 (2000).

80. Cao, X., Ballew, N. & Barlowe, C. Initial docking of ER-derived vesicles requires Uso1p and Ypt1p but is independent of SNARE proteins. *EMBO J* **17,** 2156–2165 (1998).

81. Moyer, B. D., Allan, B. B. & Balch, W. E. Rab1 Interaction with a GM130 Effector Complex Regulates COPII Vesicle cis-Golgi Tethering. *Traffic* **2,** 268–276 (2001).

82. Malsam, J., Satoh, A., Pelletier, L. & Warren, G. Golgin Tethers Define Subpopulations of COPI Vesicles. *Science* **307,** 1095–1098 (2005).

83. Wegmann, D., Hess, P., Baier, C., Wieland, F. T. & Reinhard, C. Novel Isotypic γ/ζ Subunits Reveal Three Coatomer Complexes in Mammals. *Mol. Cell. Biol.* **24,** 1070–1080 (2004).

84. Mellman, I. & Warren, G. The Road Taken: Past and Future Foundations of Membrane Traffic. *Cell* **100,** 99–112 (2000).

85. Farquhar, M. G. Progress in Unraveling Pathways of Golgi Traffic. *Annual Review of Cell Biology* **1,** 447–488 (1985).

86. Bergmann, J. E. & Singer, S. J. Immunoelectron microscopic studies of the intracellular transport of the membrane glycoprotein (G) of vesicular stomatitis virus in infected Chinese hamster ovary cells. *J Cell Biol* **97,** 1777–1787 (1983).

87. Kleene, R. & Berger, E. G. The molecular and cell biology of glycosyltransferases. *Biochimica et Biophysica Acta (BBA) - Reviews on Biomembranes* **1154,** 283–325 (1993).

88. Dunphy, W. G. & Rothman, J. E. Compartmental organization of the Golgi stack. *Cell* **42,** 13–21 (1985).

89. Dahan, S., Ahluwalia, J. P., Wong, L., Posner, B. I. & Bergeron, J. J. Concentration of intracellular hepatic apolipoprotein E in Golgi apparatus saccular distensions and endosomes. *J Cell Biol* **127,** 1859–1869 (1994).

90. Martínez-Menárguez, J. A. *et al.* Peri-Golgi vesicles contain retrograde but not anterograde proteins consistent with the cisternal progression model of intra-Golgi transport. *J Cell Biol* **155,** 1213–1224 (2001).

91. Melkonian, M., Becker, B. & Becker, D. Scale formation in algae. *Journal of Electron Microscopy Technique* **17,** 165–178 (1991).

92. Bonfanti, L. *et al.* Procollagen Traverses the Golgi Stack without Leaving the Lumen of Cisternae: Evidence for Cisternal Maturation. *Cell* **95,** 993–1003 (1998).

93. Losev, E. *et al.* Golgi maturation visualized in living yeast. *Nature* **441,** 1002–1006 (2006).

94. Matsuura-Tokita, K., Takeuchi, M., Ichihara, A., Mikuriya, K. & Nakano, A. Live imaging of yeast Golgi cisternal maturation. *Nature* **441,** 1007–1010 (2006).

95. Patterson, G. H. *et al.* Transport through the Golgi Apparatus by Rapid Partitioning within a Two-Phase Membrane System. *Cell* **133,** 1055–1067 (2008).

96. Lavieu, G., Zheng, H. & Rothman, J. E. Stapled Golgi cisternae remain in place as cargo passes through the stack. *eLife* **2,** (2013).

97. Rizzo, R. *et al.* The dynamics of engineered resident proteins in the mammalian Golgi complex relies on cisternal maturation. *J Cell Biol* **201,** 1027–1036 (2013).

98. Rambourg, A. & Clermont, Y. Three-dimensional electron microscopy: structure of the Golgi apparatus. *Eur. J. Cell Biol.* **51,** 189–200 (1990).

99. Mellman, I. & Simons, K. The Golgi complex: in vitro veritas? *Cell* **68,** 829–840 (1992).

100. Marsh, B. J., Mastronarde, D. N., Buttle, K. F., Howell, K. E. & McIntosh, J. R. Organellar relationships in the Golgi region of the pancreatic beta cell line, HIT-T15, visualized by high resolution electron tomography. *Proc Natl Acad Sci U S A* **98,** 2399–2406 (2001).

101. Pietro, E. S. *et al.* Group IV Phospholipase A2α Controls the Formation of Inter-Cisternal Continuities Involved in Intra-Golgi Transport. *PLoS Biology* **7,** e1000194 (2009).

102. Tomás, M., Martínez-Alonso, E., Ballesta, J. & Martínez-Menárguez, J. A. Regulation of ER–Golgi Intermediate Compartment Tubulation and Mobility by COPI Coats, Motor Proteins and Microtubules. *Traffic* **11,** 616–625 (2010).

103. Polishchuk, R. S. *et al.* Correlative Light-Electron Microscopy Reveals the Tubular-Saccular Ultrastructure of Carriers Operating between Golgi Apparatus and Plasma Membrane. *J Cell Biol* **148,** 45–58 (2000).

104. Donaldson, J. G., Finazzi, D. & Klausner, R. D. Brefeldin A inhibits Golgi membrane-catalysed exchange of guanine nucleotide onto ARF protein. *Nature* **360,** 350–352 (1992).

105. Peyroche, A. *et al.* Brefeldin A Acts to Stabilize an Abortive ARF–GDP–Sec7 Domain Protein Complex. *Molecular Cell* **3,** 275–285 (1999).

106. Peyroche, A. & Jackson, C. L. Functional analysis of ADP-ribosylation factor (ARF) guanine nucleotide exchange factors Gea1p and Gea2p in yeast. *Meth. Enzymol.* **329,** 290–300 (2001).

107. Szul, T. *et al.* Dissecting the role of the ARF guanine nucleotide exchange factor GBF1 in Golgi biogenesis and protein trafficking. *Journal of Cell Science* **120,** 3929–3940 (2007).

108. Puertollano, R. *et al.* Morphology and Dynamics of Clathrin/GGA1-coated Carriers Budding from the Trans-Golgi Network. *Mol. Biol. Cell* **14,** 1545–1557 (2003).

109. Caplan, S. *et al.* A tubular EHD1-containing compartment involved in the recycling of major histocompatibility complex class I molecules to the plasma membrane. *EMBO J* **21,** 2557–2567 (2002).

110. Bechler, M. E. *et al.* The phospholipase complex PAFAH Ib regulates the functional organization of the Golgi complex. *J. Cell Biol.* **190,** 45–53 (2010).

111. Bechler, M. E. *et al.* The phospholipase A_2 enzyme complex PAFAH Ib mediates endosomal membrane tubule formation and trafficking. *Mol. Biol. Cell* **22,** 2348–2359 (2011).

112. Skjeldal, F. M. *et al.* The fusion of early endosomes induces molecular-motor-driven tubule formation and fission. *J Cell Sci* **125,** 1910–1919 (2012).

113. Lippincott-Schwartz, J. *et al.* Microtubule-dependent retrograde transport of proteins into the ER in the presence of brefeldin A suggests an ER recycling pathway. *Cell* **60,** 821–836 (1990).

114. Beck, R., Adolf, F., Weimer, C., Bruegger, B. & Wieland, F. T. ArfGAP1 Activity and COPI Vesicle Biogenesis. *Traffic* **10,** 307–315 (2009).

115. Huang, F., Nesterov, A., Carter, R. E. & Sorkin, A. Trafficking of yellow-fluorescent-protein-tagged mu1 subunit of clathrin adaptor AP-1 complex in living cells. *Traffic* **2,** 345–357 (2001).

116. Kametaka, S. & Waguri, S. Visualization of TGN-endosome trafficking in mammalian and Drosophila cells. *Meth. Enzymol.* **504,** 255–271 (2012).

117. Aridor, M., Bannykh, S. I., Rowe, T. & Balch, W. E. Sequential coupling between COPII and COPI vesicle coats in endoplasmic reticulum to Golgi transport. *J. Cell Biol.* **131,** 875–893 (1995).

118. Baumgart, T., Hess, S. T. & Webb, W. W. Imaging coexisting fluid domains in biomembrane models coupling curvature and line tension. *Nature* **425,** 821–824 (2003).

119. Bacia, K., Schwille, P. & Kurzchalia, T. Sterol structure determines the separation of phases and the curvature of the liquid-ordered phase in model membranes. *Proc. Natl. Acad. Sci. U.S.A.* **102,** 3272–3277 (2005).

120. Stowell, M. H., Marks, B., Wigge, P. & McMahon, H. T. Nucleotide-dependent conformational changes in dynamin: evidence for a mechanochemical molecular spring. *Nat. Cell Biol.* **1,** 27–32 (1999).

121. Presley, J. F. *et al.* Dissection of COPI and Arf1 dynamics in vivo and role in Golgi membrane transport. *Nature* **417,** 187–193 (2002).

122. Hirschberg, K. *et al.* Kinetic Analysis of Secretory Protein Traffic and Characterization of Golgi to Plasma Membrane Transport Intermediates in Living Cells. *J Cell Biol* **143,** 1485–1503 (1998).

123. Bigay, J., Casella, J.-F., Drin, G., Mesmin, B. & Antonny, B. ArfGAP1 responds to membrane curvature through the folding of a lipid packing sensor motif. *EMBO J.* **24,** 2244–2253 (2005).

124. Sheetz, M. P. & Singer, S. J. Biological Membranes as Bilayer Couples. A Molecular Mechanism of Drug-Erythrocyte Interactions. *PNAS* **71,** 4457–4461 (1974).

125. Zimmerberg, J. & Kozlov, M. M. How proteins produce cellular membrane curvature. *Nat Rev Mol Cell Biol* **7,** 9–19 (2006).

126. Peter, B. J. *et al.* BAR domains as sensors of membrane curvature: the amphiphysin BAR structure. *Science* **303,** 495–499 (2004).

127. Takei, K., Slepnev, V. I., Haucke, V. & De Camilli, P. Functional partnership between amphiphysin and dynamin in clathrin-mediated endocytosis. *Nat. Cell Biol.* **1,** 33–39 (1999).

128. Farsad, K. *et al.* Generation of high curvature membranes mediated by direct endophilin bilayer interactions. *J. Cell Biol.* **155,** 193–200 (2001).

129. Razzaq, A. *et al.* Amphiphysin is necessary for organization of the excitation-contraction coupling machinery of muscles, but not for synaptic vesicle endocytosis in Drosophila. *Genes Dev.* **15,** 2967–2979 (2001).

130. Kooijman, E. E. *et al.* Spontaneous curvature of phosphatidic acid and lysophosphatidic acid. *Biochemistry* **44,** 2097–2102 (2005).

131. Kooijman, E. E., Chupin, V., de Kruijff, B. & Burger, K. N. J. Modulation of membrane curvature by phosphatidic acid and lysophosphatidic acid. *Traffic* **4,** 162–174 (2003).

132. Fuller, N., Benatti, C. R. & Rand, R. P. Curvature and bending constants for phosphatidylserine-containing membranes. *Biophys. J.* **85,** 1667–1674 (2003).

133. Ford, M. G. J. *et al.* Curvature of clathrin-coated pits driven by epsin. *Nature* **419,** 361–366 (2002).

134. Stahelin, R. V. *et al.* Contrasting membrane interaction mechanisms of AP180 N-terminal homology (ANTH) and epsin N-terminal homology (ENTH) domains. *J. Biol. Chem.* **278,** 28993–28999 (2003).

135. Burke, J. E. & Dennis, E. A. Phospholipase A2 structure/function, mechanism, and signaling. *The Journal of Lipid Research* **50,** S237–S242 (2008).

136. Shindou, H. *et al.* A Single Enzyme Catalyzes Both Platelet-activating Factor Production and Membrane Biogenesis of Inflammatory Cells. *Journal of Biological Chemistry* **282,** 6532–6539 (2007).

137. Harayama, T., Shindou, H., Ogasawara, R., Suwabe, A. & Shimizu, T. Identification of a Novel Noninflammatory Biosynthetic Pathway of Platelet-activating Factor. *J. Biol. Chem.* **283,** 11097–11106 (2008).

138. McIntyre, T. M., Prescott, S. M. & Stafforini, D. M. The emerging roles of PAF acetylhydrolase. *The Journal of Lipid Research* **50,** S255–S259 (2008).

139. Ayciriex, S. *et al.* YPR139c/LOA1 encodes a novel lysophosphatidic acid acyltransferase associated with lipid droplets and involved in TAG homeostasis. *Molecular Biology of the Cell* (2011). doi:10.1091/mbc.E11-07-0650

140. Li, Z. *et al.* Lysophosphatidylcholine Acyltransferase 3 Knockdown-mediated Liver Lysophosphatidylcholine Accumulation Promotes Very Low Density Lipoprotein Production by Enhancing Microsomal Triglyceride Transfer Protein Expression. *J. Biol. Chem.* **287,** 20122–20131 (2012).

141. Das, S., Castillo, C. & Stevens, T. Phospholipid remodeling/generation in Giardia: the role of the Lands cycle. *Trends in Parasitology* **17,** 316–319 (2001).

142. Merkel, O. *et al.* Characterization and Function in Vivo of Two Novel Phospholipases B/Lysophospholipases fromSaccharomyces cerevisiae. *J. Biol. Chem.* **274,** 28121–28127 (1999).

143. McDermott, M., Wakelam, M. J. . & Morris, A. J. Phospholipase D. *Biochemistry and Cell Biology* **82,** 225–253 (2004).

144. Vernon, L. P. & Bell, J. D. Membrane structure, toxins and phospholipase A2 activity. *Pharmacology & therapeutics* **54,** 269–295 (1992).

145. Flick, J. S. & Thorner, J. Genetic and biochemical characterization of a phosphatidylinositol-specific phospholipase C in Saccharomyces cerevisiae. *Molecular and cellular biology* **13,** 5861 (1993).

146. Wilson, P. A., Gardner, S. D., Lambie, N. M., Commans, S. A. & Crowther, D. J. Characterization of the human patatin-like phospholipase family. *Journal of Lipid Research* **47,** 1940 –1949 (2006).

147. Darios, F., Connell, E. & Davletov, B. Phospholipases and fatty acid signalling in exocytosis. *The Journal of Physiology* **585,** 699 –704 (2007).

148. Bechler, M. E., de Figueiredo, P. & Brown, W. J. A PLA1-2 punch regulates the Golgi complex. *Trends in Cell Biology* **22,** 116–124 (2012).

149. Aloulou, A. *et al.* Exploring the specific features of interfacial enzymology based on lipase studies. *Biochimica et Biophysica Acta (BBA) - Molecular and Cell Biology of Lipids* **1761,** 995–1013 (2006).

150. Balsinde, J., Winstead, M. V. & Dennis, E. A. Phospholipase A2 regulation of arachidonic acid mobilization. *FEBS Letters* **531,** 2–6 (2002).

151. Burke, J. E. & Dennis, E. A. Phospholipase A2 Biochemistry. *Cardiovascular Drugs and Therapy* **23,** 49–59 (2008).

152. Murakami, M. *et al.* Recent progress in phospholipase A_2 research: from cells to animals to humans. *Prog. Lipid Res.* **50,** 152–192 (2011).

153. Yedgar, S., Cohen, Y. & Shoseyov, D. Control of phospholipase A2 activities for the treatment of inflammatory conditions. *Biochimica et Biophysica Acta (BBA) - Molecular and Cell Biology of Lipids* **1761,** 1373–1382 (2006).

154. Evans, J. H., Spencer, D. M., Zweifach, A. & Leslie, C. C. Intracellular Calcium Signals Regulating Cytosolic Phospholipase A2 Translocation to Internal Membranes ,. *J. Biol. Chem.* **276,** 30150–30160 (2001).

155. Regan-Klapisz, E. *et al.* Golgi-associated cPLA2α Regulates Endothelial Cell–Cell Junction Integrity by Controlling the Trafficking of Transmembrane Junction Proteins. *Molecular Biology of the Cell* **20,** 4225 –4234 (2009).

156. Herbert, S. P., Odell, A. F., Ponnambalam, S. & Walker, J. H. Activation of Cytosolic Phospholipase A2- as a Novel Mechanism Regulating Endothelial Cell Cycle Progression and Angiogenesis. *Journal of Biological Chemistry* **284,** 5784–5796 (2008).

157. Bonventre, J. V. *et al.* Reduced fertility and postischaemic brain injury in mice deficient in cytosolic phospholipase A2. *Nature* **390,** 622–625 (1997).

158. Adler, D. H. *et al.* Inherited human cPLA2α deficiency is associated with impaired eicosanoid biosynthesis, small intestinal ulceration, and platelet dysfunction. *J Clin Invest* **118,** 2121–2131 (2008).

159. Reed, K. A. *et al.* Functional Characterization of Mutations in Inherited Human cPLA2 Deficiency. *Biochemistry* **50,** 1731–1738 (2011).

160. Hattori, M., Adachi, H., Tsujimoto, M., Arai, H. & Inoue, K. The catalytic subunit of bovine brain platelet-activating factor acetylhydrolase is a novel type of serine esterase. *J. Biol. Chem.* **269,** 23150–23155 (1994).

161. Hattori, M., Arai, H. & Inoue, K. Purification and characterization of bovine brain platelet-activating factor acetylhydrolase. *J. Biol. Chem.* **268,** 18748–18753 (1993).

162. Ho, Y. S. *et al.* Probing the substrate specificity of the intracellular brain platelet-activating factor acetylhydrolase. *Protein Eng.* **12,** 693–700 (1999).

163. Ho, Y. S. *et al.* Brain acetylhydrolase that inactivates platelet-activating factor is a G-protein-like trimer. *Nature* **385,** 89–93 (1997).

164. Tarricone, C. *et al.* Coupling PAF signaling to dynein regulation: structure of LIS1 in complex with PAF-acetylhydrolase. *Neuron* **44,** 809–821 (2004).

165. Banta, M., Polizotto, R. S., Wood, S. A., de Figueiredo, P. & Brown, W. J. Characterization of a cytosolic activity that induces the formation of Golgi membrane tubules in a cell-free reconstitution system. *Biochemistry* **34,** 13359–13366 (1995).

166. Ben-Tekaya, H., Kahn, R. A. & Hauri, H.-P. ADP Ribosylation Factors 1 and 4 and Group VIA Phospholipase A2 Regulate Morphology and Intraorganellar Traffic in the Endoplasmic Reticulum–Golgi Intermediate Compartment. *Mol. Biol. Cell* **21,** 4130–4140 (2010).

167. Nakajima, K. -i. A Novel Phospholipase A1 with Sequence Homology to a Mammalian Sec23p-interacting Protein, p125. *Journal of Biological Chemistry* **277,** 11329–11335 (2002).

168. Morikawa, R. K. *et al.* Intracellular Phospholipase A1 (iPLA1) Is a Novel Factor Involved in Coat Protein Complex I- and Rab6-independent Retrograde Transport between the Endoplasmic Reticulum and the Golgi Complex. *Journal of Biological Chemistry* **284,** 26620–26630 (2009).

169. Sato, S., Inoue, H., Kogure, T., Tagaya, M. & Tani, K. Golgi-localized KIAA0725p regulates membrane trafficking from the Golgi apparatus to the plasma membrane in mammalian cells. *FEBS letters* **584,** 4389–4395 (2010).

170. Gelb, M. H., Jain, M. K. & Berg, O. G. Inhibition of phospholipase A2. *FASEB J* **8,** 916–924 (1994).

171. De Figueiredo, P., Drecktrah, D., Katzenellenbogen, J. A., Strang, M. & Brown, W. J. Evidence that phospholipase A2 activity is required for Golgi complex and trans Golgi network membrane tubulation. *Proceedings of the National Academy of Sciences* **95,** 8642 –8647 (1998).

172. Lands, W. E. M. Metabolism of Glycerolipides: A Comparison of Lecithin and Triglyceride Synthesis. *Journal of Biological Chemistry* **231,** 883 –888 (1958).

173. Kennedy, E. P. The Synthesis of Cytidine Diphosphate Choline, Cytidine Diphosphate Ethanolamine, and Related Compounds. *Journal of Biological Chemistry* **222,** 185 –191 (1956).

174. Kennedy, E. P. & Weiss, S. B. The Function of Cytidine Coenzymes in the Biosynthesis of Phospholipides. *Journal of Biological Chemistry* **222,** 193 –214 (1956).

175. Carman, G. M. & Zeimetz, G. M. Regulation of Phospholipid Biosynthesis in the Yeast Saccharomyces cerevisiae. *Journal of Biological Chemistry* **271,** 13293 – 13296 (1996).

176. Lands, W. E. Stories about acyl chains. *Biochim. Biophys. Acta* **1483,** 1–14 (2000).

177. Gibellini, F. & Smith, T. K. The Kennedy pathway—De novo synthesis of phosphatidylethanolamine and phosphatidylcholine. *IUBMB Life* **62,** 414–428 (2010).

178. Chilton, F. H., Fonteh, A. N., Surette, M. E., Triggiani, M. & Winkler, J. D. Control of arachidonate levels within inflammatory cells. *Biochimica et Biophysica Acta (BBA) - Lipids and Lipid Metabolism* **1299,** 1–15 (1996).

179. Shaw, D. I., Hall, W. L., Jeffs, N. R. & Williams, C. M. Comparative effects of fatty acids on endothelial inflammatory gene expression. *European Journal of Nutrition* **46,** 321–328 (2007).

180. Bocan, T. M., Mueller, S. B., Uhlendorf, P. D., Newton, R. S. & Krause, B. R. Comparison of CI-976, an ACAT inhibitor, and selected lipid-lowering agents for

antiatherosclerotic activity in iliac-femoral and thoracic aortic lesions. A biochemical, morphological, and morphometric evaluation. *Arterioscler Thromb Vasc Biol* **11,** 1830–1843 (1991).

181. Drecktrah, D. *et al.* Inhibition of a Golgi Complex Lysophospholipid Acyltransferase Induces Membrane Tubule Formation and Retrograde Trafficking. *Molecular Biology of the Cell* **14,** 3459 –3469 (2003).

182. Brown, W. J., Chambers, K. & Doody, A. Phospholipase A2 (PLA2) enzymes in membrane trafficking: mediators of membrane shape and function. *Traffic* **4,** 214–221 (2003).

183. Brown, W. J., Plutner, H., Drecktrah, D., Judson, B. L. & Balch, W. E. The lysophospholipid acyltransferase antagonist CI-976 inhibits a late step in COPII vesicle budding. *Traffic* **9,** 786–797 (2008).

184. Chambers, K., Judson, B. & Brown, W. J. A unique lysophospholipid acyltransferase (LPAT) antagonist, CI-976, affects secretory and endocytic membrane trafficking pathways. *Journal of cell science* **118,** 3061 (2005).

185. Shindou, H. & Shimizu, T. Acyl-CoA:Lysophospholipid Acyltransferases. *Journal of Biological Chemistry* **284,** 1–5 (2008).

186. Yen, C.-L. E., Stone, S. J., Koliwad, S., Harris, C. & Farese, R. V. Thematic Review Series: Glycerolipids. DGAT enzymes and triacylglycerol biosynthesis. *Journal of Lipid Research* **49,** 2283 –2301 (2008).

187. Stone, S. J., Levin, M. C. & Farese, R. V. Membrane Topology and Identification of Key Functional Amino Acid Residues of Murine Acyl-CoA:Diacylglycerol Acyltransferase-2. *J. Biol. Chem.* **281,** 40273–40282 (2006).

188. Stone, S. J. *et al.* Lipopenia and Skin Barrier Abnormalities in DGAT2-deficient Mice. *J. Biol. Chem.* **279,** 11767–11776 (2004).

189. Man, W. C., Miyazaki, M., Chu, K. & Ntambi, J. Colocalization of SCD1 and DGAT2: implying preference for endogenous monounsaturated fatty acids in triglyceride synthesis. *J. Lipid Res.* **47,** 1928–1939 (2006).

190. Cao, J. *et al.* A Predominant Role of Acyl-CoA:monoacylglycerol Acyltransferase-2 in Dietary Fat Absorption Implicated by Tissue Distribution, Subcellular Localization, and Up-regulation by High Fat Diet. *J. Biol. Chem.* **279,** 18878–18886 (2004).

191. Yen, C.-L. E., Stone, S. J., Cases, S., Zhou, P. & Farese, R. V. Identification of a gene encoding MGAT1, a monoacylglycerol acyltransferase. *Proc Natl Acad Sci U S A* **99,** 8512–8517 (2002).

192. Turkish, A. R. *et al.* Identification of Two Novel Human Acyl-CoA Wax Alcohol Acyltransferases MEMBERS OF THE DIACYLGLYCEROL ACYLTRANSFERASE 2 (DGAT2) GENE SUPERFAMILY. *J. Biol. Chem.* **280,** 14755–14764 (2005).

193. Buhman, K. F., Accad, M. & Farese, R. V. Mammalian acyl-CoA:cholesterol acyltransferases. *Biochim. Biophys. Acta* **1529,** 142–154 (2000).

194. An, S. *et al.* A critical role for the histidine residues in the catalytic function of acyl-CoA:cholesterol acyltransferase catalysis: Evidence for catalytic difference between ACAT1 and ACAT2. *FEBS Letters* **580,** 2741–2749 (2006).

195. Wurie, H. R., Buckett, L. & Zammit, V. A. Evidence That Diacylglycerol Acyltransferase 1 (DGAT1) Has Dual Membrane Topology in the Endoplasmic Reticulum of HepG2 Cells. *Journal of Biological Chemistry* **286,** 36238–36247 (2011).

196. Wurie, H. R., Buckett, L. & Zammit, V. A. Diacylglycerol acyltransferase 2 acts upstream of diacylglycerol acyltransferase 1 and utilizes nascent diglycerides and de novo synthesized fatty acids in HepG2 cells. *FEBS Journal* **279,** 3033–3047 (2012).

197. Turchetto-Zolet, A. C. *et al.* Evolutionary view of acyl-CoA diacylglycerol acyltransferase (DGAT), a key enzyme in neutral lipid biosynthesis. *BMC Evol Biol* **11,** 263 (2011).

198. Qi, J. *et al.* The use of stable isotope-labeled glycerol and oleic acid to differentiate the hepatic functions of DGAT1 and -2. *J. Lipid Res.* **53,** 1106–1116 (2012).

199. Gijon, M. A., Riekhof, W. R., Zarini, S., Murphy, R. C. & Voelker, D. R. Lysophospholipid Acyltransferases and Arachidonate Recycling in Human Neutrophils. *Journal of Biological Chemistry* **283,** 30235–30245 (2008).

200. Lee, H.-C. *et al.* LPIAT1 regulates arachidonic acid content in phosphatidylinositol and is required for cortical lamination in mice. *Mol. Biol. Cell* **23,** 4689–4700 (2012).

201. Anderson, K. E. *et al.* Lysophosphatidylinositol-Acyltransferase-1 (LPIAT1) Is Required to Maintain Physiological Levels of PtdIns and PtdInsP2 in the Mouse. *PLoS ONE* **8,** e58425 (2013).

202. Gutierrez, J. A. *et al.* Ghrelin octanoylation mediated by an orphan lipid transferase. *Proc. Natl. Acad. Sci. U.S.A.* **105,** 6320–6325 (2008).

203. Covey, T. M. *et al.* PORCN Moonlights in a Wnt-Independent Pathway That Regulates Cancer Cell Proliferation. *PLoS One* **7,** (2012).

204. Coleman, J. Characterization of the Escherichia coli gene for 1-acyl-sn-glycerol-3-phosphate acyltransferase (plsC). *Mol. Gen. Genet.* **232,** 295–303 (1992).

205. Coleman, J. Characterization of Escherichia coli cells deficient in 1-acyl-sn-glycerol-3- phosphate acyltransferase activity. *J. Biol. Chem.* **265,** 17215–17221 (1990).

206. Lewin, T. M., Wang, P. & Coleman, R. A. Analysis of Amino Acid Motifs Diagnostic for the sn-Glycerol-3-phosphate Acyltransferase Reaction†. *Biochemistry* **38,** 5764–5771 (1999).

207. Yamashita, A. *et al.* Topology of acyltransferase motifs and substrate specificity and accessibility in 1-acyl-sn-glycero-3-phosphate acyltransferase 1. *Biochimica et Biophysica Acta (BBA) - Molecular and Cell Biology of Lipids* **1771,** 1202–1215 (2007).

208. Schmidt, J. A., Yvone, G. M. & Brown, W. J. Membrane topology of human AGPAT3 (LPAAT3). *Biochem Biophys Res Commun* **397,** 661–667 (2010).

209. Turnbull, A. P. *et al.* Analysis of the Structure, Substrate Specificity, and Mechanism of Squash Glycerol-3-Phosphate (1)-Acyltransferase. *Structure* **9,** 347–353 (2001).

210. Tamada, T. *et al.* Substrate recognition and selectivity of plant glycerol-3-phosphate acyltransferases (GPATs) from Cucurbita moscata and Spinacea oleracea. *Acta Crystallographica Section D Biological Crystallography* **60,** 13–21 (2003).

211. Gimeno, R. E. & Cao, J. Thematic Review Series: Glycerolipids. Mammalian glycerol-3-phosphate acyltransferases: new genes for an old activity. *J. Lipid Res.* **49,** 2079–2088 (2008).

212. Igal, R. A., Wang, S., Gonzalez-Baró, M. & Coleman, R. A. Mitochondrial Glycerol Phosphate Acyltransferase Directs the Incorporation of Exogenous Fatty Acids into Triacylglycerol. *J. Biol. Chem.* **276,** 42205–42212 (2001).

213. Harada, N., Fujimoto, E., Okuyama, M., Sakaue, H. & Nakaya, Y. Identification and functional characterization of human glycerol-3-phosphate acyltransferase 1 gene promoters. *Biochemical and Biophysical Research Communications* **423,** 128–133 (2012).

214. Wang, S. *et al.* Cloning and functional characterization of a novel mitochondrialN-ethylmaleimide-sensitive glycerol-3-phosphate acyltransferase (GPAT2). *Arch Biochem Biophys* **465,** 347–358 (2007).

215. Lewin, T. M., Schwerbrock, N. M. J., Lee, D. P. & Coleman, R. A. Identification of a New Glycerol-3-phosphate Acyltransferase Isoenzyme, mtGPAT2, in Mitochondria. *J. Biol. Chem.* **279,** 13488–13495 (2004).

216. Tang, W. *et al.* Identification of a novel human lysophosphatidic acid acyltransferase, LPAAT-theta, which activates mTOR pathway. *J. Biochem. Mol. Biol.* **39,** 626–635 (2006).

217. Cao, J., Li, J.-L., Li, D., Tobin, J. F. & Gimeno, R. E. Molecular identification of microsomal acyl-CoA:glycerol-3-phosphate acyltransferase, a key enzyme in de novo triacylglycerol synthesis. *Proc Natl Acad Sci U S A* **103,** 19695–19700 (2006).

218. Shan, D. *et al.* GPAT3 and GPAT4 are regulated by insulin-stimulated phosphorylation and play distinct roles in adipogenesis. *J Lipid Res* **51,** 1971–1981 (2010).

219. Vergnes, L. *et al.* Agpat6 deficiency causes subdermal lipodystrophy and resistance to obesity. *J. Lipid Res.* **47,** 745–754 (2006).

220. Chen, Y. Q. *et al.* AGPAT6 Is a Novel Microsomal Glycerol-3-phosphate Acyltransferase. *J. Biol. Chem.* **283,** 10048–10057 (2008).

221. Li, D. *et al.* Cloning and identification of the human LPAAT-zeta gene, a novel member of the lysophosphatidic acid acyltransferase family. *J Hum Genet* **48,** 438–442 (2003).

222. TAN, X.-J. *et al.* Molecular Cloning and Preliminary Function Study of a Novel Human Gene, TSARG7, Related to Spermatogenesis. *Acta Genetica Sinica* **33,** 294–303 (2006).

223. Aguado, B. & Campbell, R. D. Characterization of a Human Lysophosphatidic Acid Acyltransferase That Is Encoded by a Gene Located in the Class III Region of the Human Major Histocompatibility Complex. *J. Biol. Chem.* **273,** 4096–4105 (1998).

224. Subauste, A. R. *et al.* Alterations in Lipid Signaling Underlie Lipodystrophy Secondary to AGPAT2 Mutations. *Diabetes* **61,** 2922–2931 (2012).

225. Haghighi, A. *et al.* Identification of a novel nonsense mutation and a missense substitution in the AGPAT2 gene causing congenital generalized lipodystrophy type 1. *Eur J Med Genet* **55,** 620–624 (2012).

226. Agarwal, A. K. *et al.* Human 1-Acylglycerol-3-phosphate O-Acyltransferase Isoforms 1 and 2. *J Biol Chem* **286,** 37676–37691 (2011).

227. Cao, J. *et al.* Molecular Identification of a Novel Mammalian Brain Isoform of Acyl-CoA:Lysophospholipid Acyltransferase with Prominent Ethanolamine Lysophospholipid Acylating Activity, LPEAT2. *J. Biol. Chem.* **283,** 19049–19057 (2008).

228. Moessinger, C., Kuerschner, L., Spandl, J., Shevchenko, A. & Thiele, C. Human Lysophosphatidylcholine Acyltransferases 1 and 2 Are Located in Lipid Droplets Where They Catalyze the Formation of Phosphatidylcholine. *J. Biol. Chem.* **286,** 21330–21339 (2011).

229. Nakanishi, H. *et al.* Cloning and Characterization of Mouse Lung-type Acyl-CoA:Lysophosphatidylcholine Acyltransferase 1 (LPCAT1) EXPRESSION IN ALVEOLAR TYPE II CELLS AND POSSIBLE INVOLVEMENT IN SURFACTANT PRODUCTION. *J. Biol. Chem.* **281,** 20140–20147 (2006).

230. Chen, X., Hyatt, B. A., Mucenski, M. L., Mason, R. J. & Shannon, J. M. Identification and characterization of a lysophosphatidylcholine acyltransferase in alveolar type II cells. *Proceedings of the National Academy of Sciences* **103,** 11724 – 11729 (2006).

231. Mansilla, F. *et al.* Lysophosphatidylcholine acyltransferase 1 (LPCAT1) overexpression in human colorectal cancer. *J Mol Med (Berl)* **87,** 85–97 (2009).

232. Harayama, T., Shindou, H. & Shimizu, T. Biosynthesis of phosphatidylcholine by human lysophosphatidylcholine acyltransferase 1. *The Journal of Lipid Research* **50,** 1824–1831 (2009).

233. Bridges, J. P. *et al.* LPCAT1 regulates surfactant phospholipid synthesis and is required for transitioning to air breathing in mice. *J Clin Invest* **120,** 1736–1748 (2010).

234. Zhao, Y., Chen, Y.-Q., Li, S., Konrad, R. J. & Cao, G. The microsomal cardiolipin remodeling enzyme acyl-CoA lysocardiolipin acyltransferase is an acyltransferase of multiple anionic lysophospholipids. *J. Lipid Res.* **50,** 945–956 (2009).

235. Wang, C. *et al.* Mouse lysocardiolipin acyltransferase controls the development of hematopoietic and endothelial lineages during in vitro embryonic stem-cell differentiation. *Blood* **110,** 3601–3609 (2007).

236. Cao, J., Liu, Y., Lockwood, J., Burn, P. & Shi, Y. A Novel Cardiolipin-remodeling Pathway Revealed by a Gene Encoding an Endoplasmic Reticulum-associated Acyl-CoA:Lysocardiolipin Acyltransferase (ALCAT1) in Mouse. *J. Biol. Chem.* **279,** 31727–31734 (2004).

237. Agarwal, A. K., Barnes, R. I. & Garg, A. Functional characterization of human 1-acylglycerol-3-phosphate acyltransferase isoform 8: Cloning, tissue distribution, gene structure, and enzymatic activity. *Archives of Biochemistry and Biophysics* **449,** 64–76 (2006).

238. Lu, B. *et al.* Cloning and characterization of murine 1-acyl-sn-glycerol 3-phosphate acyltransferases and their regulation by PPARa in murine heart. *Biochem J* **385,** 469–477 (2005).

239. Prasad, S. S., Garg, A. & Agarwal, A. K. Enzymatic activities of the human AGPAT isoform 3 and isoform 5: localization of AGPAT5 to mitochondria. *J Lipid Res* **52,** 451–462 (2011).

240. Eto, M., Shindou, H. & Shimizu, T. A novel lysophosphatidic acid acyltransferase enzyme (LPAAT4) with a possible role for incorporating docosahexaenoic acid into brain glycerophospholipids. *Biochemical and Biophysical Research Communications* **443,** 718–724 (2014).

241. Yang, Y., Cao, J. & Shi, Y. Identification and Characterization of a Gene Encoding Human LPGAT1, an Endoplasmic Reticulum-associated Lysophosphatidylglycerol Acyltransferase. *J. Biol. Chem.* **279,** 55866–55874 (2004).

242. Phoon, C. K. L. *et al.* Tafazzin knockdown in mice leads to a developmental cardiomyopathy with early diastolic dysfunction preceding myocardial noncompaction. *J Am Heart Assoc* **1,** (2012).

243. Schlame, M. Cardiolipin remodeling and the function of tafazzin. *Biochimica et Biophysica Acta (BBA) - Molecular and Cell Biology of Lipids* **1831,** 582–588 (2013).

244. Gawrisch, K. Tafazzin senses curvature. *Nat. Chem. Biol.* **8,** 811–812 (2012).

245. Schmidt, J. A. & Brown, W. J. Lysophosphatidic acid acyltransferase 3 regulates Golgi complex structure and function. *The Journal of Cell Biology* **186,** 211 –218 (2009).

246. Yuki, K., Shindou, H., Hishikawa, D. & Shimizu, T. Characterization of mouse lysophosphatidic acid acyltransferase 3: an enzyme with dual functions in the testis. *The Journal of Lipid Research* **50,** 860–869 (2008).

247. Henneberry, A. L., Wright, M. M. & McMaster, C. R. The Major Sites of Cellular Phospholipid Synthesis and Molecular Determinants of Fatty Acid and Lipid Head Group Specificity. *Mol Biol Cell* **13,** 3148–3161 (2002).

248. Ha, K. D., Clarke, B. A. & Brown, W. J. Regulation of the Golgi complex by phospholipid remodeling enzymes. *Biochimica et Biophysica Acta (BBA) - Molecular and Cell Biology of Lipids* **1821,** 1078–1088 (2012).

249. De Figueiredo, P., Polizotto, R. S., Drecktrah, D. & Brown, W. J. Membrane Tubule-mediated Reassembly and Maintenance of the Golgi Complex Is Disrupted by Phospholipase A2 Antagonists. *Molecular Biology of the Cell* **10,** 1763 –1782 (1999).

250. De Figueiredo, P. *et al.* Phospholipase A2 Antagonists Inhibit Constitutive Retrograde Membrane Traffic to the Endoplasmic Reticulum. *Traffic* **1,** 504–511 (2000).

251. Leslie, C. C., Gangelhoff, T. A. & Gelb, M. H. Localization and function of cytosolic phospholipase A2α at the Golgi. *Biochimie* **92,** 620–626 (2010).

252. Trucco, A. *et al.* Secretory traffic triggers the formation of tubular continuities across Golgi sub-compartments. *Nat Cell Biol* **6,** 1071–1081 (2004).

253. Choukroun, G. J. *et al.* Cytosolic phospholipase A~ 2 regulates Golgi structure and modulates intracellular trafficking of membrane proteins. *Journal of Clinical Investigation* **106,** 983–1030 (2000).

254. Schindelin, J. *et al.* Fiji: an open-source platform for biological-image analysis. *Nat Meth* **9,** 676–682 (2012).

255. Brown, W. J. & Schmidt, J. A. Use of acyltransferase inhibitors to block vesicular traffic between the ER and Golgi complex. *Methods in enzymology* **404,** 115–125 (2005).

256. Pruitt, K. D. *et al.* The consensus coding sequence (CCDS) project: Identifying a common protein-coding gene set for the human and mouse genomes. *Genome Res.* **19,** 1316–1323 (2009).

257. Sievers, F. *et al.* Fast, scalable generation of high-quality protein multiple sequence alignments using Clustal Omega. *Mol Syst Biol* **7,** (2011).

258. Felsenstein, J. *PHYLIP: phylogenetic inference package, version 3.5c.* (Department of Genetics, University of Washington, 1993).

259. Satoh, M., Shimada, A., Kashiwai, A., Saga, S. & Hosokawa, M. Differential cooperative enzymatic activities of protein disulfide isomerase family in protein folding. *Cell Stress Chaperones* **10,** 211–220 (2005).

260. Profant, D. A., Roberts, C. J. & Wright, R. L. Mutational analysis of the karmellae-inducing signal in Hmg1p, a yeast HMG–CoA reductase isozyme. *Yeast* **16,** 811–827 (2000).

261. Hishikawa, D. *et al.* Discovery of a lysophospholipid acyltransferase family essential for membrane asymmetry and diversity. *Proceedings of the National Academy of Sciences* **105,** 2830 –2835 (2008).

262. Siddhanta, A. & Shields, D. Secretory Vesicle Budding from the Trans-Golgi Network Is Mediated by Phosphatidic Acid Levels. *J. Biol. Chem.* **273,** 17995–17998 (1998).

263. Weigert, R. *et al.* CtBP/BARS induces fission of Golgi membranes by acylating lysophosphatidic acid. *Nature* **402,** 429–433 (1999).

264. Choi, S.-Y. *et al.* A common lipid links Mfn-mediated mitochondrial fusion and SNARE-regulated exocytosis. *Nat Cell Biol* **8,** 1255–1262 (2006).

265. Yang, J.-S. *et al.* COPI vesicle fission: a role for phosphatidic acid and insight into Golgi maintenance. *Nat Cell Biol* **10,** 1146–1153 (2008).

266. Nakanishi, H., de los Santos, P. & Neiman, A. M. Positive and Negative Regulation of a SNARE Protein by Control of Intracellular Localization. *Mol Biol Cell* **15,** 1802–1815 (2004).

267. Manifava, M. *et al.* Differential Binding of Traffic-related Proteins to Phosphatidic Acid- or Phosphatidylinositol (4,5)- Bisphosphate-coupled Affinity Reagents. *J. Biol. Chem.* **276,** 8987–8994 (2001).

268. Huang, H. *et al.* piRNA-Associated Germline Nuage Formation and Spermatogenesis Require MitoPLD Profusogenic Mitochondrial-Surface Lipid Signaling. *Developmental Cell* **20,** 376–387 (2011).

269. Van Meer, G., Voelker, D. R. & Feigenson, G. W. Membrane lipids: where they are and how they behave. *Nat Rev Mol Cell Biol* **9,** 112–124 (2008).

270. Heacock, A. M. & Agranoff, B. W. CDP-diacylglycerol synthase from mammalian tissues. *Biochimica et Biophysica Acta (BBA) - Lipids and Lipid Metabolism* **1348,** 166–172 (1997).

271. Fleischer, S., Rouser, G., Fleischer, B., Casu, A. & Kritchevsky, G. Lipid composition of mitochondria from bovine heart, liver, and kidney. *J. Lipid Res.* **8,** 170–180 (1967).

272. Arikketh, D., Nelson, R. & Vance, J. E. Defining the Importance of Phosphatidylserine Synthase-1 (PSS1) Unexpected Viability of PSS1-Deficient Mice. *J. Biol. Chem.* **283,** 12888–12897 (2008).

273. Emoto, K., Toyama-Sorimachi, N., Karasuyama, H., Inoue, K. & Umeda, M. Exposure of Phosphatidylethanolamine on the Surface of Apoptotic Cells. *Experimental Cell Research* **232,** 430–434 (1997).

274. Fairn, G. D. *et al.* High-resolution mapping reveals topologically distinct cellular pools of phosphatidylserine. *J Cell Biol* **194,** 257–275 (2011).

275. Yeung, T. *et al.* Contribution of phosphatidylserine to membrane surface charge and protein targeting during phagosome maturation. *J Cell Biol* **185,** 917–928 (2009).

276. Fairn, G. D., Hermansson, M., Somerharju, P. & Grinstein, S. Phosphatidylserine is polarized and required for proper Cdc42 localization and for development of cell polarity. *Nat Cell Biol* **13,** 1424–1430 (2011).

277. Uchida, Y. *et al.* Intracellular phosphatidylserine is essential for retrograde membrane traffic through endosomes. *Proc Natl Acad Sci U S A* **108,** 15846–15851 (2011).

278. Leventis, P. A. & Grinstein, S. The Distribution and Function of Phosphatidylserine in Cellular Membranes. *Annual Review of Biophysics* **39,** 407–427 (2010).

279. Li, Z. *et al.* The ratio of phosphatidylcholine to phosphatidylethanolamine influences membrane integrity and steatohepatitis. *Cell Metabolism* **3,** 321–331 (2006).

280. Fukunaga-Johnson, N., Lee, S. W., Liebert, M. & Grossman, H. B. Molecular analysis of a gene, BB1, overexpressed in bladder and breast carcinoma. *Anticancer Res.* **16,** 1085–1090 (1996).

281. Lee, H. C. *et al.* Caenorhabditis elegans mboa-7, a member of the MBOAT family, is required for selective incorporation of polyunsaturated fatty acids into phosphatidylinositol. *Molecular biology of the cell* **19,** 1174–1184 (2008).

282. D'Souza, K. & Epand, R. M. Enrichment of phosphatidylinositols with specific acyl chains. *Biochimica et Biophysica Acta (BBA) - Biomembranes* doi:10.1016/j.bbamem.2013.10.003

283. Powell, K. S. & Latterich, M. The Making and Breaking of the Endoplasmic Reticulum. *Traffic* **1,** 689–694 (2000).

284. Walter, P. & Ron, D. The Unfolded Protein Response: From Stress Pathway to Homeostatic Regulation. *Science* **334,** 1081–1086 (2011).

285. Hetz, C. The unfolded protein response: controlling cell fate decisions under ER stress and beyond. *Nat Rev Mol Cell Biol* **13,** 89–102 (2012).

286. Zhang, K. *et al.* The unfolded protein response transducer IRE1[alpha] prevents ER stress-induced hepatic steatosis. *EMBO J* **30,** 1357–1375 (2011).

287. Ariyama, H., Kono, N., Matsuda, S., Inoue, T. & Arai, H. Decrease in Membrane Phospholipid Unsaturation Induces Unfolded Protein Response. *Journal of Biological Chemistry* **285,** 22027–22035 (2010).

288. Marchler-Bauer, A. *et al.* CDD: conserved domains and protein three-dimensional structure. *Nucleic Acids Res.* **41,** D348–352 (2013).

289. Lin, S., Cheng, D., Liu, M.-S., Chen, J. & Chang, T.-Y. Human Acyl-CoA:Cholesterol Acyltransferase-1 in the Endoplasmic Reticulum Contains Seven Transmembrane Domains. *Journal of Biological Chemistry* **274,** 23276 –23285 (1999).

290. Lin, S., Lu, X., Chang, C. C. Y. & Chang, T.-Y. Human Acyl-Coenzyme A:Cholesterol Acyltransferase Expressed in Chinese Hamster Ovary Cells: Membrane Topology and Active Site Location. *Molecular Biology of the Cell* **14,** 2447 –2460 (2003).

291. Joyce, C. W. *et al.* ACAT1 and ACAT2 Membrane Topology Segregates a Serine Residue Essential for Activity to Opposite Sides of the Endoplasmic Reticulum Membrane. *Molecular Biology of the Cell* **11,** 3675 –3687 (2000).

292. Guo, Z.-Y., Chang, C. C. Y. & Chang, T.-Y. Functionality of the Seventh and Eighth Transmembrane Domains of Acyl-Coenzyme A:Cholesterol Acyltransferase 1 †. *Biochemistry* **46,** 10063–10071 (2007).

293. Wurie, H. R., Buckett, L. & Zammit, V. A. Evidence That Diacylglycerol Acyltransferase 1 (DGAT1) Has Dual Membrane Topology in the Endoplasmic Reticulum of HepG2 Cells. *Journal of Biological Chemistry* **286,** 36238–36247 (2011).

294. Pagac, M. *et al.* Topology of 1-Acyl-sn-glycerol-3-phosphate Acyltransferases SLC1 and ALE1 and Related Membrane-bound O-Acyltransferases (MBOATs) of Saccharomyces cerevisiae. *Journal of Biological Chemistry* **286,** 36438–36447 (2011).

295. Shikano, S. & Li, M. Membrane receptor trafficking: Evidence of proximal and distal zones conferred by two independent endoplasmic reticulum localization signals. *PNAS* **100,** 5783–5788 (2003).

296. Ma, W. & Goldberg, J. Rules for the recognition of dilysine retrieval motifs by coatomer. *EMBO J* **32,** 926–937 (2013).

297. Hardt, B. & Bause, E. Lysine Can Be Replaced by Histidine but Not by Arginine as the ER Retrieval Motif for Type I Membrane Proteins. *Biochemical and Biophysical Research Communications* **291,** 751–757 (2002).

298. Shindou, H., Eto, M., Morimoto, R. & Shimizu, T. Identification of membrane O-acyltransferase family motifs. *Biochemical and Biophysical Research Communications* **383,** 320–325 (2009).

299. Yang, J., Brown, M. S., Liang, G., Grishin, N. V. & Goldstein, J. L. Identification of the Acyltransferase that Octanoylates Ghrelin, an Appetite-Stimulating Peptide Hormone. *Cell* **132,** 387–396 (2008).

300. Bosson, R., Jaquenoud, M. & Conzelmann, A. GUP1 of Saccharomyces cerevisiae Encodes an O-Acyltransferase Involved in Remodeling of the GPI Anchor. *Mol. Biol. Cell* **17,** 2636–2645 (2006).

301. Guo, Z.-Y., Lin, S., Heinen, J. A., Chang, C. C. Y. & Chang, T.-Y. The Active Site His-460 of Human Acyl-coenzyme A:Cholesterol Acyltransferase 1 Resides in a Hitherto Undisclosed Transmembrane Domain. *J. Biol. Chem.* **280,** 37814–37826 (2005).

302. McFie, P. J., Stone, S. L., Banman, S. L. & Stone, S. J. Topological Orientation of Acyl-CoA:Diacylglycerol Acyltransferase-1 (DGAT1) and Identification of a Putative Active Site Histidine and the Role of the N Terminus in Dimer/Tetramer Formation. *J. Biol. Chem.* **285,** 37377–37387 (2010).

303. Hofmann, K. A superfamily of membrane-bound O-acyltransferases with implications for Wnt signaling. *Trends in Biochemical Sciences* **25,** 111–112 (2000).

304. Krogh, A., Larsson, B., von Heijne, G. & Sonnhammer, E. L. . Predicting transmembrane protein topology with a hidden markov model: application to complete genomes. *Journal of Molecular Biology* **305,** 567–580 (2001).

305. Bernsel, A., Viklund, H., Hennerdal, A. & Elofsson, A. TOPCONS: consensus prediction of membrane protein topology. *Nucl. Acids Res.* **37,** W465–W468 (2009).

306. Gupta, R., Jung, E. & Brunak, S. Prediction of N-glycosylation sites in human proteins. *http://www. cbs. dtu. dk/services* (2004).

307. Steentoft, C. *et al.* Precision mapping of the human O-GalNAc glycoproteome through SimpleCell technology. *EMBO J.* **32,** 1478–1488 (2013).

308. Wilson, I., Gavel, Y. & Von Heijne, G. Amino acid distributions around O-linked glycosylation sites. *Biochem. J* **275,** 529–534 (1991).

309. Akhavan, A. N- and O-linked glycosylation coordinate cell-surface localization of a cardiac potassium channel. *J Physiol* **589,** 4647–4648 (2011).

310. Zhao, Y. *et al.* Identification and Characterization of a Major Liver Lysophosphatidylcholine Acyltransferase. *Journal of Biological Chemistry* **283,** 8258–8265 (2008).

311. Hailey, D. W., Lippincott-Schwartz, J. & Lorenz, H. Fluorescence protease protection of GFP chimeras to reveal protein topology and subcellular localization. *Nature Methods* **3,** 205+ (2006).

312. Viklund, H., Granseth, E. & Elofsson, A. Structural Classification and Prediction of Reentrant Regions in α-Helical Transmembrane Proteins: Application to Complete Genomes. *Journal of Molecular Biology* **361,** 591–603 (2006).

313. Quiroga, R., Trenchi, A., Montoro, A. G., Taubas, J. V. & Maccioni, H. J. F. Short length transmembrane domains having voluminous exoplasmic halves determine retention of Type II membrane proteins in the Golgi complex. *J Cell Sci* jcs.130658 (2013). doi:10.1242/jcs.130658

314. Kazachkov, M., Chen, Q., Wang, L. & Zou, J. Substrate Preferences of a Lysophosphatidylcholine Acyltransferase Highlight Its Role in Phospholipid Remodeling. *Lipids* **43,** 895–902 (2008).

315. Klumperman, J. *et al.* The recycling pathway of protein ERGIC-53 and dynamics of the ER-Golgi intermediate compartment. *J Cell Sci* **111,** 3411–3425 (1998).

316. Castillon, G. A., Watanabe, R., Taylor, M., Schwabe, T. M. E. & Riezman, H. Concentration of GPI-Anchored Proteins upon ER Exit in Yeast. *Traffic* **10,** 186–200 (2009).

317. Matsuda, S. *et al.* Member of the membrane-bound O-acyltransferase (MBOAT) family encodes a lysophospholipid acyltransferase with broad substrate specificity. *Genes to Cells* **13,** 879–888 (2008).

318. Klausner, R. D., Donaldson, J. G. & Lippincott-Schwartz, J. Brefeldin A: insights into the control of membrane traffic and organelle structure. *The Journal of cell biology* **116,** 1071–1080 (1992).

319. Colón-González, F. & Kazanietz, M. G. C1 domains exposed: from diacylglycerol binding to protein-protein interactions. *Biochimica et Biophysica Acta (BBA)-Molecular and Cell Biology of Lipids* **1761,** 827–837 (2006).

320. Daleke, D. L. Phospholipid Flippases. *J. Biol. Chem.* **282,** 821–825 (2007).

321. Ishibashi, M. *et al.* Liver x receptor regulates arachidonic acid distribution and eicosanoid release in human macrophages: a key role for lysophosphatidylcholine acyltransferase 3. *Arterioscler. Thromb. Vasc. Biol.* **33,** 1171–1179 (2013).

322. Blumental-Perry, A. *et al.* Phosphatidylinositol 4-Phosphate Formation at ER Exit Sites Regulates ER Export. *Developmental Cell* **11,** 671–682 (2006).

323. Mayorga, L. S. *et al.* Inhibition of endosome fusion by phospholipase A2 (PLA2) inhibitors points to a role for PLA2 in endocytosis. *Proceedings of the National Academy of Sciences* **90,** 10255 (1993).

324. Chernomordik, L., Chanturiya, A., Green, J. & Zimmerberg, J. The hemifusion intermediate and its conversion to complete fusion: regulation by membrane composition. *Biophysical Journal* **69,** 922–929 (1995).

325. Jones, D. H. *et al.* Type I Phosphatidylinositol 4-Phosphate 5-Kinase Directly Interacts with ADP-ribosylation Factor 1 and Is Responsible for Phosphatidylinositol 4,5-Bisphosphate Synthesis in the Golgi Compartment. *J. Biol. Chem.* **275,** 13962–13966 (2000).

326. Hodgkin, M. N. *et al.* Phospholipase D regulation and localisation is dependent upon a phosphatidylinositol 4,5-bisphosphate-specific PH domain. *Current Biology* **10,** 43–46 (2000).

327. Honda, A., Al-Awar, O. S., Hay, J. C. & Donaldson, J. G. Targeting of Arf-1 to the early Golgi by membrin, an ER-Golgi SNARE. *J Cell Biol* **168,** 1039–1051 (2005).

328. Rein, U., Andag, U., Duden, R., Schmitt, H. D. & Spang, A. ARF-GAP–mediated interaction between the ER-Golgi v-SNAREs and the COPI coat. *J Cell Biol* **157,** 395–404 (2002).

329. Manneville, J. B. *et al.* COPI coat assembly occurs on liquid-disordered domains and the associated membrane deformations are limited by membrane tension. *Proceedings of the National Academy of Sciences* **105,** 16946 (2008).

330. Brügger, B. *et al.* Evidence for Segregation of Sphingomyelin and Cholesterol during Formation of Copi-Coated Vesicles. *J Cell Biol* **151,** 507–518 (2000).

331. Roux, A. *et al.* Role of curvature and phase transition in lipid sorting and fission of membrane tubules. *EMBO J* **24,** 1537–1545 (2005).